March 2015

Layer-by-Layer Antimicrobial N-Halamine Polymer Coatings for Food Contact Materials

Luis J. Bastarrachea Gutierrez
University of Massachusetts Amherst

LAYER-by-LAYER ANTIMICROBIAL N-HALAMINE POLYMER COATINGS FOR FOOD CONTACT MATERIALS

A Dissertation Presented

By

LUIS JAVIER BASTARRACHEA GUTIÉRREZ

Submitted to the Graduate School of the
University of Massachusetts Amherst in partial fulfillment
of the requirements of the degree of

DOCTOR OF PHILOSOPHY

February 2015

Food Science

LAYER-by-LAYER ANTIMICROBIAL N-HALAMINE POLYMER COATINGS FOR FOOD CONTACT MATERIALS

A Dissertation Presented

By

LUIS JAVIER BASTARRACHEA GUTIÉRREZ

Approved as to style and content by:

_____

Julie M. Goddard, Chair

_____

Lynne A. McLandsborough, Member

_____

Micha Peleg, Member

_____

Vincent Rotello, Member

_____

Eric A. Decker, Department Head

Food Science

DEDICATION

To my parents Jorge A. Bastarrachea and Noemí E. Gutiérrez, and my grandparents †Roberto Bastarrachea, †María L. Sabido, †Carlos E. Gutiérrez, and María de los Ángeles Vargas. And to all those who have been a source of motivation and inspiration in my life.

To my middle school teachers Rita Morales, Mario Anzúrez, Esteban Pérez, María G. Villalpando, Aurelio Mendoza, Alberto Avendaño and Javier Mendoza, whom I feel fortunate to have met and from whom I had the privilege to have as living examples of a number of human virtues at an early age.

To my high school teachers María O. Murad, Susana Limón, María Guerrero, Héctor González, Leopoldo Cendejas, Alberto Flandes and Roberto Hernández, who are also living examples of human virtues, dedication, talent, passion and professionalism.

To my doctor, Jorge A. González Barranco, a renowned expert in Nutrition whose guidance and advice were part of a life-changing experience.

To my neighbor in Mexico, Alberto Arouesty, an extraordinary architect and artist who shared countless hours of his vast and delightful talent with me.

And last but not least, to my closest friends †David Romo, Alonso Velázquez, Abraham Mendoza, José L. Moreno, Jorge Yúdico, Octavio Benítez, José A. Gómez, Dunque Martínez, Amir Gol Mohamadi, Yahya Al-Wahaibi, Cynthia L. López Peña, and Tiphaine Mérian. Thank you for your friendship and all the good memories.

"The secret of achievement is to hold a picture of a successful outcome in the mind."
– Henry David Thoreau (polymath philosopher from Massachusetts)

"Your beliefs become your thoughts, your thoughts become your words, your words become your actions, your actions become your habits, your habits become your values, your values become your destiny."
– Mahatma Gandhi

ACKNOWLEDGEMENTS

Firstly, I would like to express my deepest gratitude to my advisor, Prof. Julie M. Goddard, for giving me the privilege to work in her group, as well as providing me with her support, advice and guidance throughout my doctoral studies. My most sincere acknowledgement also to my committee members; to Prof. Lynne A. McLandsborough, for her valuable support and guidance in the microbiology-related parts of this research; to Prof. Micha Peleg, for sharing his vast knowledge in microbial inactivation; and to Prof. Vincent Rotello, for his helpful guidance and innovative ideas in chemistry.

My special thanks to my labmates Tiphaine Mérian, Joey Talbert, Jeffrey Barish, Fang Tian, Dana Wong, Maxine Roman, Anna Denis-Rohr, Stephanie Andler, Kang Huang, Cynthia Kane, Jason Lin, Chanelle Adams, John Cotter, Imelda Tirtajaya, Yuhua Chang and Kyle Landry for their support and help throughout these years.

I would also like to thank Prof. D. Julian McClements for allowing me to use his facilities, and Prof. Thomas J. McCarthy, Jacob Hirsch and Dr. Sekar T. Dhanasekaran from the department of Polymer Science and Engineering for their assistance in surface characterization techniques.

And last but not least, I would like to express my infinite gratitude to my family, for their continous support and encouragement.

This research work was supported by the National Institute of Food and Agriculture, US Department of Agriculture under project number 2011–65210–20059 and in part by the Center for Hierarchical Manufacturing at UMass Amherst, and the National Science Foundation under NSF grant No. CMMI-0531171.

ABSTRACT

LAYER-by-LAYER ANTIMICROBIAL N-HALAMINE POLYMER COATINGS FOR FOOD CONTACT MATERIALS

FEBRUARY 2015

LUIS JAVIER BASTARRACHEA GUTIÉRREZ, B.S., INSTITUTO TECNOLÓGICO Y DE ESTUDIOS SUPERIORES DE MONTERREY

M.S., WASHINGTON STATE UNIVERSITY PULLMAN

Ph.D., UNIVERSITY OF MASSACHUSETTS AMHERST

Directed by Prof. Julie M. Goddard

Cross contamination during food processing represents a risk for public health and financial burden. Surface modification of food contact materials to render them antimicrobial can be an effective tool to minimize such risk and improve higyene throughout the food chain. The objective of the present work was to develop antimicrobial coatings with the potential to be applied in a variety of food contact materials. The polymer coatings developed achieved their antimicrobial character by incorporation of a unique type of chlorinated compounds called N-halamines, which are capable of regenerating their antimicrobial activity enabling many cycles of disinfection.

Two layer-by-layer (LbL) assembly surface modification procedures were followed. In the first procedure, multiple bilayers of branched polyethyleneimine (PEI) and poly(acrylic acid) (PAA) were applied onto stainless steel and polyethylene (PE). As

the number of bilayers applied increased, so did the number of antimicrobial N-halamines the coatings were able to harbor. Similarly, increasing the number of bilayers also translated into greater antimicrobial efficacy against the pathogen *Listeria monocytogenes*. The maximum level of inactivation achieved was > 99.999%, which was comparable to the equivalent concentration of free chlorine in solution. The kinetics of inactivation was also studied. Coatings gave inactivation kinetics with a sigmoidal behavior, showing a substantially slower biocidal effect as compared to free chlorine in solution. The PEI-PAA coating was also challenged against multiple cycles of regeneration of N-halamines (rechlorinations) and washing under different levels of pH, and exhibited stability and ability to be regenerated.

Although robust and effective, the preparation of the PEI-PAA coating was time consuming and required the use of expensive crosslinkers. As an alternative method for N-halamine surface modification, two bilayers of PEI and styrene maleic anhydride copolymer (SMA) were coated onto polypropylene (PP). The coating exhibited intrinsic antimicrobial properties against *L. monocytogenes* due to its cationic nature, being able to achieve approximately 3 logarithmic cycles (~ 99.9%) in reduction as prepared, and more than 5 logarithmic cycles (> 99.999%) when chlorinated in the form of N-halamines. This method showed to be more advantageous than the previous one involving PEI and PAA given the fact that no carbodiimide crosslinkers were needed. In addition, the coating didn't result in a significant change in surface energy ($P > 0.05$) as compared to PP. The coating was also challenged against multiple rechlorinations, and the results showed that it has the potential to be reused.

The results of the present research suggest that the surface modification methods studied possess the potential to be applied on a variety of materials used in food processing to avoid microbial contamination. Future research will focus on developing N-halamine antimicrobial coatings with improved stability and more efficient preparation, and in the development of new antimicrobial N-halamine materials.

Keywords: Antimicrobial coatings, N-halamines, surface modification, microbial inactivation, food safety.

TABLE OF CONTENTS

Page

LIST OF TABLES

Table **Page**

LIST OF FIGURES

Figure **Page**

LIST OF ABBREVIATIONS

AFM: Atomic Force Microscopy.

AM: Antimicrobial.

AO7: Acid orange 7.

ATR-FTIR: Attenuated Total Reflectance Fourier Transform Infrared Spectroscopy.

CDC: Centers for Disease Control and Prevention.

CVD: Chemical Vapor Deposition.

DI: Deionized.

DPD: N,N-diethyl-p-phenylenediamine.

EDC-HCl: 1-(3-Dimethylaminopropyl)-3-ethylcarbodiimide hydrochloride.

EEDQ: 2-ethoxy-1-ethoxycarbonyl-1,2-dihydroquioline.

FDA: Food and Drug Administration.

FTIR: Fourier Transform Infrared Spectroscopy.

GOPTS: 1-(3-Dimethylaminopropyl)-3-ethylcarbodiimide hydrochloride.

LbL: Layer-by-layer.

LDPE: Low Density Polyethylene.

iCVP: initiated Chemical Vapor Deposition.

MES: 2-(*N*-morpholino)ethanesulfonic acid.

NB: Neutralizing Buffer.

NHS: N-hydrosuccinimide.

PAA: Poly(acrylic acid).

PE: Polyethylene.

PEI: Branched polyethyleneimine.

PP: Polypropylene.

QAC: Quaternary Ammonium Compounds.

SAMs: Self Assembled Monolayers.

SD: Standard deviation.

SEM: Scanning Electron Microscopy.

SMA: Styrene maleic anhydride copolymer

TSA: Tryptic Soy Agar.

TSB: Tryptic Soy Broth.

UV: Ultraviolet.

UV-O_3: Ultraviolet-ozone.

XPS: X-Ray Photoelectron Spectroscopy.

CHAPTER 1

INTRODUCTION

Every year in The United States of America about 48 million people get sick from foodborne diseases. From that number, 128,000 are hospitalized, 3,000 of which die (Centers for Disease Control and Prevention 2013). Microbial contamination of surfaces in utensils and food processing equipment is among the top risk factors that can provoke foodborne outbreaks (Food and Drug Administration 2000). In the food processing environment, food contact surfaces are capable of harboring and potentially transferring microorganisms into finished food products. The transmission of such microorganisms is a significant risk to food safety and spoilage. One of the most important factors involved in the retention of microorganisms relates to the intrinsic contact surface's characteristics, like topography, charge, chemistry, hydrophobicity, etc. (Brooks and Flint 2008; Verran and others 2008; Araújo and others 2010). To avoid retention of microorganisms, industry employs chemical and physical methods. Chemical methods involve cleaning with detergents to remove residual organic matter generated during the processing operations, followed by disinfection with different types of substances that include oxidizing agents, chlorine based compounds, hydrogen peroxide, etc. Physical methods involve the application of heat, ultrasound, irradiation, etc. (Van Houdt and Michiels 2010). However, research has shown that the mentioned methods can be insufficient to control surface microbial cross contamination (Brooks and Flint 2008).

One strategy to minimize microbial contamination of food contact surfaces has been to modify the surface of food contact materials, by coating or other surface modification techniques. Stainless steel is one of the most used materials for construction of equipment commonly found in food processing facilities. Its mechanical, chemical and thermal properties make it ideal to resist the conditions given by the unit operations involved in food processing, as well as the repeated cleaning and washing cycles that are necessary (Brooks and Flint 2008; Verran and others 2008). Plastic surfaces are also widely used in food processing facilities, but they represent some disadvantages in terms of durability and easiness to be cleaned. In addition, scratches and abrasion that occurs during their use and cleaning make them more prone to microbial contamination (Verran and others 2008). For these reasons, there is an increased interest for the development of new materials and coatings that can help improve hygiene and prevent microbial cross-contamination (Møretrø and Langsrud 2011). Surface modification is a technique in which the surface chemistry of different materials is altered by the addition or chemical attachment of molecules (e.g. nanoparticles, monomers, polymers), resulting in the application of a layer ranging in thickness from a few nm to several μm. Such change in surface chemistry is expected to be small enough to retain the bulk properties of the modified material (mainly thermal and mechanical properties) (Ratner 1995). The types of changes that can be applied on contact surfaces include those that involve increase/decrease in hydrophobicity, an increase in mechanical strength, those that impart steric hindrance (blocking of unwanted reactions within a system), the attachment of bioactive substances like enzymes, and the addition of antimicrobial properties (Brooks and Flint 2008; Verran and others 2008; Araújo and others 2010)).

Due to safety concerns and limited standard methods to prove efficacy, the development and extensive use of this type of antimicrobial technology have been slow (Kenawy and others 2007). There are two main methods to provide a surface with antimicrobial properties. The first one consists of applying a coating on to the treated surface, from which the corresponding antimicrobial substance will be released over time. The second approach involves immobilization through covalent bonds between the antimicrobial substance and the treated material. The first migratory method exhibits the advantage of a fast antimicrobial effect and facile application, which may be increased as temperature rises since that is a temperature-dependent phenomenon, and that also results advantageous given the fact that microorganisms proliferate at higher rates as temperature increases. However, the risk given by residual toxicity, eventual loss of activity and development of resistance against the corresponding antimicrobial is the main limitation of the first method. The second non-migratory method exhibits as an advantage the reduced risk for developing resistance as the antimicrobials are immobilized on the modified material's surface, but the antimicrobial effect is limited to direct contact with the microorganisms and the modified material's surface (Kenawy and others 2007; Bastarrachea and others 2011).

In the present work, the surface of materials commonly used in the food industry has been modified through LbL assembly of multiple layers of polyethyleneimine (PEI) alternating with poly(acrylic acid) (PAA) or styrene maleic anhydride copolymer (SMA) in order to render them antimicrobial. Antimicrobial character was imparted by introduction of N-halamine moieties, a type of antimicrobial which can regenerate antimicrobial activity with each exposure to a halogen source, such as bleach. The main

approach followed was the surface functionalization of food contact materials like stainless steel, polyethylene and polypropylene followed by the application of polyelectrolites that would harbor N-halamines (Figure 1.1). These modified materials were successfully challenged against *L. monocytogenes*, showing biocidal effect. When PEI and PAA were used and the coatings were fully chlorinated, more than 5 logarithmic cycles in reduction were possible to achieve. The PEI-SMA coatings exhibited cationic antimicrobial properties able to reduce *L. monocytogenes* in approximately 3 logarithmic cycles, and in more than 5 logarithmic cycles when fully chlorinated. The kinetics of microbial inactivation exhibited a sigmoidal behavior when the modified surfaces were chlorinated, and a Weibullian behavior when not chlorinated in the form of cationic PEI-SMA. The changes in surface chemistry were also assessed through different techniques like ATR-FTIR, FTIR, XPS, SEM, AFM, etc. The durability and reusability of N-halamine surface modified PE towards simulated washing cycles and continuous rechlorination were also evaluated, showing stability of the coating consisting of PEI and PAA. Rechlorination was also studied when PP was coated with PEI and SMA, and the results showed potential of the material to be reused.

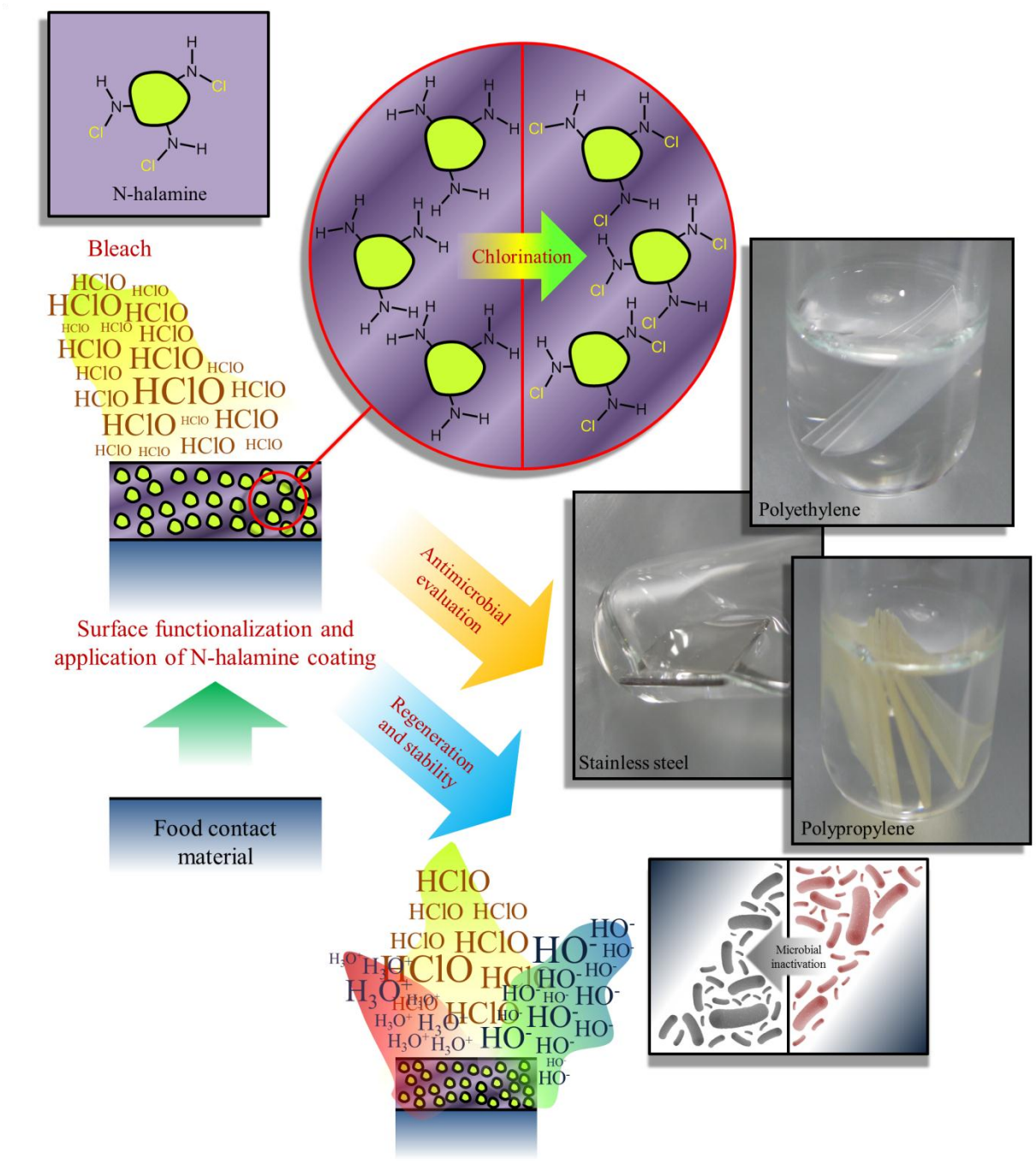

Figure 1.1 Scheme showing the functioning of surface-modified materials with N-halamines and a summary of the present research work.

CHAPTER 2

ANTIMICROBIAL FOOD EQUIPMENT COATINGS: APPLICATIONS AND CHALLENGES[1]

2.1 Introduction

During the food processing operations, food products are under constant risk of becoming contaminated with microorganisms. The large surface areas found within the food production facilities can be prone to microbial proliferation (e.g., surfaces of gaskets, converyor belts, work tables, etc.) (Cools and others 2005; Vorst and others 2006; Wilks and others 2006; Rodriguez and others 2007). These surfaces can be cleaned and sanitized constantly to prevent accumulation of harmful microorganisms and the consequent transfer to the foods. However, these operations do not eliminate the risk of microbial cross contamination (Brooks and Flint 2008).

Materials surface and bulk modification represents a promising tool to diminish the risk of microbial cross-contamination during food processing. However, implementing this type of technology in such environment is still a challenge, given the conditions found during the food processing operations (extreme levels of pH, high temperatures, mechanical stress, cleaning, etc.), which may eliminate in the middle or long term their effectiveness. In this chapter, the most frequently applied methods for surface modification are reviewed, as well as the types of antimicrobial compounds most commonly chosen for antimicrobial surface modification reported in the literature, which leads to concluding remarks with perspectives about challenges and opportunities.

[1] Submitted to Annual Review of Food Science and Technology.

2.2 Coating technologies

A wide range of surface modification technologies have been studied to render a variety of materials antimicrobial. The reported techniques possess diversity in terms of easiness to be applied, cost, durability, etc. Figure 2.1 shows a graphic summary of some of the most extensively evaluated approaches. Some techniques are explained below.

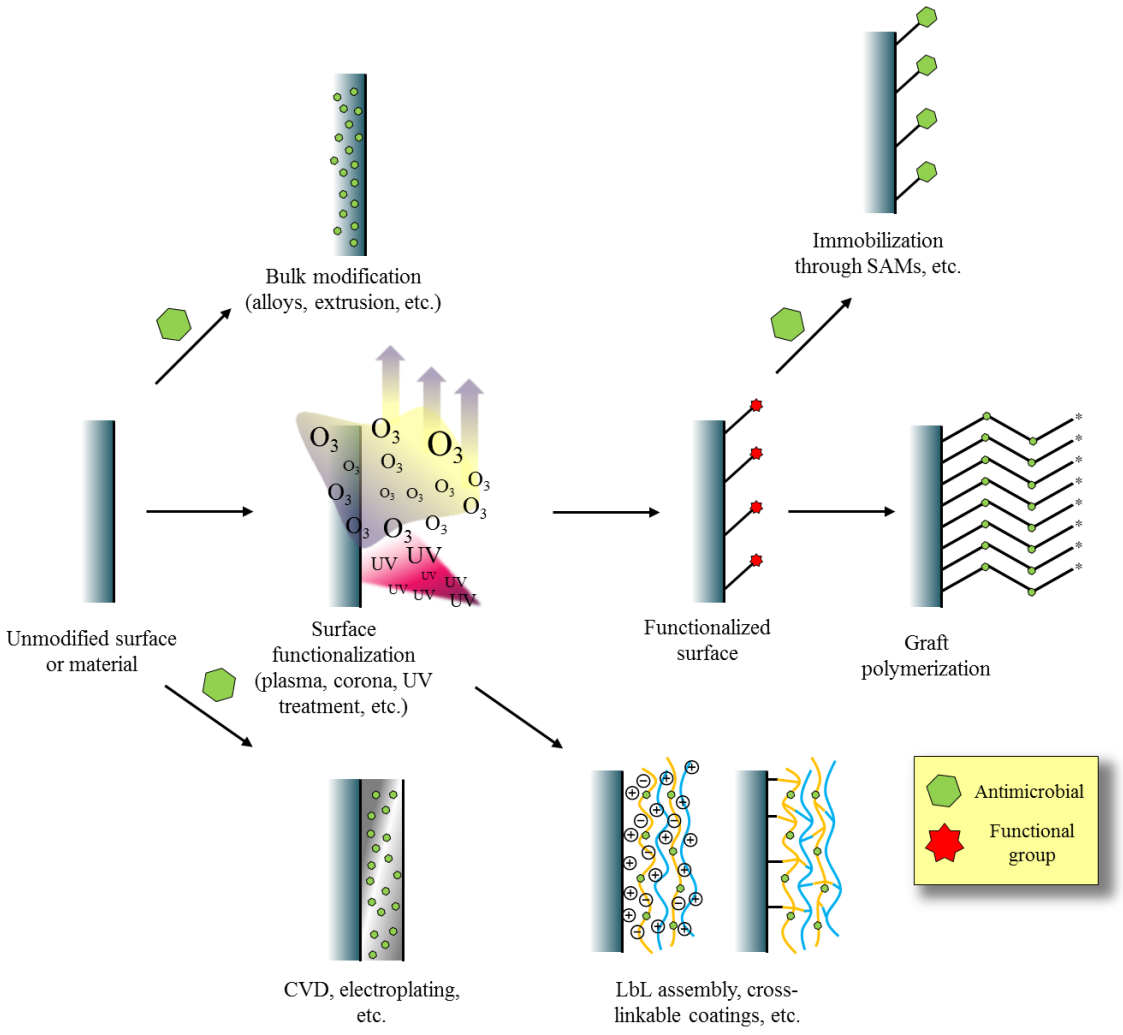

Figure 2.1 Schematic summary of the studied coating technologies.

In graft polymerization, materials of organic and inorganic nature can be functionalized (often by gamma, UV, and electron beam irradiation, or by plasma, corona and ozone treatments) in order to promote growth of polymer chains from their surface, with diverse characteristics and functions (Cleland and others 1992; Chan 1993; Yang and Lin 2002; Dargaville and others 2003; Ratner 2004; Zhao and others 2005; Murata and others 2007; Roman and others 2014). In most of the studies the approach followed involves growth of the polymer chains from the surface of the modified materials ("grafting from"), although it has been possible to first build the polymer chains of a predetermined length to later bind them to the corresponding substrate ("grafting to") (Zhao and Brittain 2000).

In another technique called cross-linkable coatings, polymers are commonly applied onto the surface of a substrate along with a crosslinker that can create covalent bonds within their matrix. This bond formation can be promoted through exposure to heat (curing) or irradiation. Cross-linking can take place in the form of free radical or condensation reactions (Goldschmidt and Streitberger 2003). Different antimicrobials have been tested using this approach, like N-halamines (Bhattacharya and others 2009; Ahmed and others 2011) and chitosan (Periolatto and others 2012). Due to its simplicity, this method offers the advantage of easiness of application at a large scale.

In the method of self-assembled monolayers (SAMs), molecules form bonds with reactive groups on the surface of a previously functionalized substrate creating ordered layers with a thickness usually measured in several nanometers. Some examples include reaction of silanes with hydroxyl groups in a surface, thiol groups with gold, etc. (Raynor and others 2009). Antimicrobial peptides like Magainin I have been studied using this

surface modification technique, showing antimicrobial effectiveness and durability (Humblot and others 2009). In a different approach called Langmuir-Blodgett films, the molecules are deposited through physisorption rather than through covalent bonds, which makes them less stable. However, the deposited molecules can later be crosslinked through covalent bonds (Zasadzinski and others 1994; Ratner 2004).

Layer-by-layer (LbL) assembly is probably the most studied surface modification technique. It has been used to provide antimicrobial activity to materials and for a variety of other purposes. In this technique, polyelectrolytes of opposite charge are alternatively deposited onto the surface of a material to which a charge has been previously created. An indefinite number of polymer layers may be applied, with the corresponding rinsing steps between each application in order to remove not strongly bound chains. The polyelectrolytes may have intrinsic antimicrobial nature, or antimicrobial compounds may be incorporated within the layers throughout the deposition process (Decher and others 1998; Ratner 2004). The polymer chains can be applied through dip coating or spray coating (Izquierdo and others 2005). Different antimicrobials have been tested using this approach, like silver nanoparticles (Grunlan and others 2005; Dubas and others 2006), N-halamines (Cerkez and others 2011; Bastarrachea and others 2013), quaternary ammonium compounds (QAC) (Grunlan and others 2005; Dvoracek and others 2009), and chitosan (Gomes and others 2013). The main advantage of this technique is its easiness to be applied and its versatility in terms of the types of substrates in which it can be tested (organic and inorganic). However, as it will be explained later, some coatings applied using this approach can also exhibit pure durability.

In chemical vapor deposition (CVD) a thin film is applied from a gaseous phase onto a solid support by means of heat, plasma or photons. By varying temperature and pressure, uniform coatings can be applied on irregular surfaces (Pierson 1999). However, this technique is not suitable to apply polymers, and possesses the risk of residual toxicity and physical and chemical hazards from the by-products of the process (Park and Sudarshan 2001; Irikura and others 2003; Alf and others 2010). In a subcategory of this technique called initiated chemical vapor deposition (iCVD), lower temperatures may be used. Few antimicrobial materials haven been developed using this method. In a research work, a coating of poly(dimethylaminomethyl styrene) applied through iCVD was effective against *Escherichia coli*, reducing it in more than 6 logarithmic cycles (Martin and others 2007).

In electroplating, an electric current enhances the deposition of a metal on the surface of another metal in solution. In contrast, in electroless plating, a reducing agent promotes the deposition of the metal without the need to apply an electric current (Mallory and Hajdu 1990). During the deposition process, particles present in the solution can be incorporated along with the metals on the surface to be modified (Barish and Goddard 2013). This can include particles with antimicrobial activity such as copper and silver (Zhao and others 1998; Ghodssi and Lin 2011). In a study that involved modification of carbon fibers through electroplating with silver and copper it was possible to inactivate in more than 2 lolarithmic cycles *Staphyloccocus aureus* and *Klebsciella pneumonia* (Kim and Park 2008). Bacteriostatic activity has also been given to polyurethane by silver coating (Gray and others 2003). The main advantage of this approach is the availability of large-scale equipments for surface modification

(Ghodssi and Lin 2011). However, research is needed in terms of stability against deteriorating agents like extreme levels of pH, cleaning agents, etc.

2.3 Antimicrobials

A range of antimicrobial agents have been explored for use in preparation of antimicrobial coatings by the technologies described above. In addition to antimicrobial effectiveness, factors such as mechanism of activity, efficacy for long-term repeated use, and stability against pH/temperature extremes and cleaning/sanitization regiments, must be considered in selecting an antimicrobial agent. Below we describe the major classes of antimicrobial agents used in antimicrobial materials and coatings and discuss their advantages and limitations in adoption by food processing equipment manufacturers. Figure 2 shows a schematic summary of the effects the studied antimicrobials have on microbial cells.

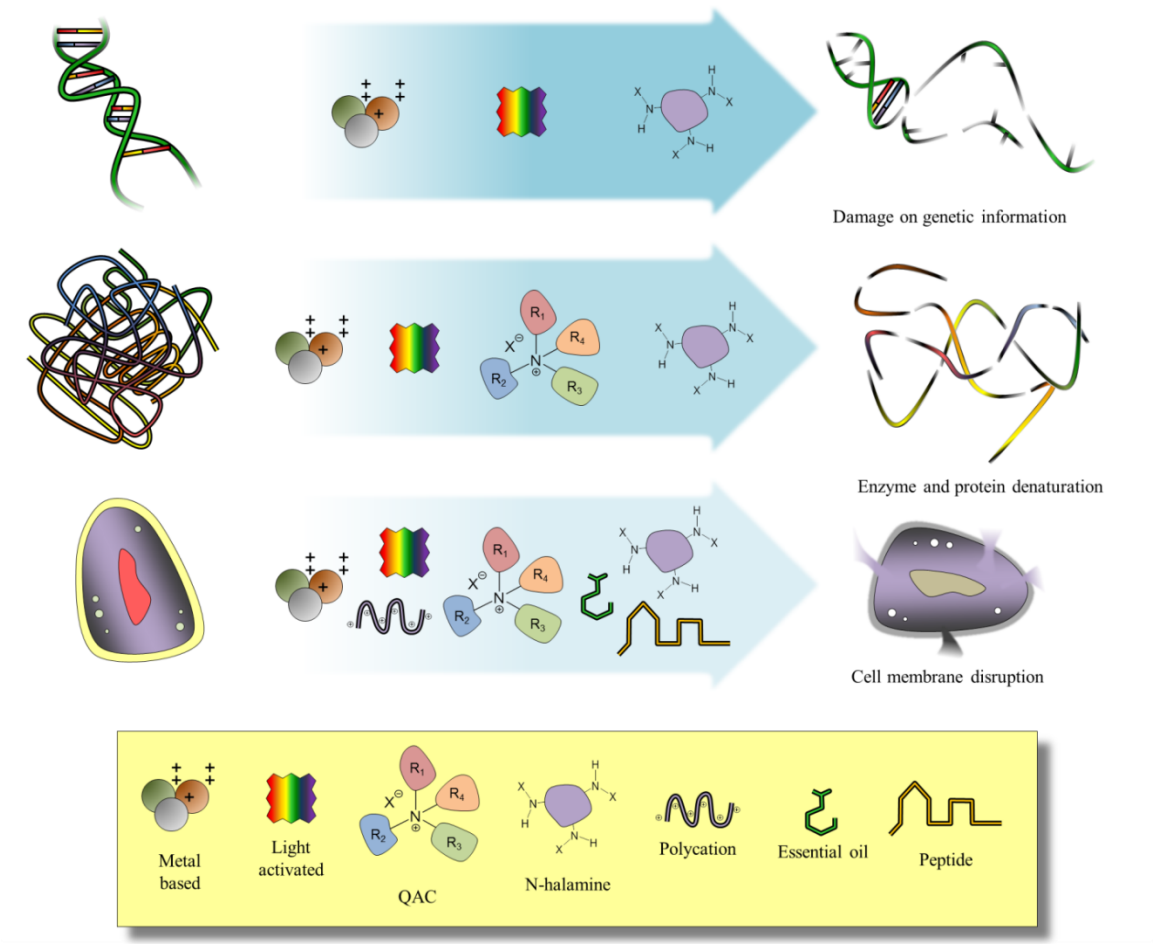

Figure 2.2 Summary of the main effects given by the studied antimicrobials on microbial cells.

2.3.1 Metal based

Metals have been used to impart broad spectrum antimicrobial activity to materials for thousands of years, yet their exact mechanism is still not unanimously agreed upon. Most interpretations explain that penetration of cells by metal ions can affect microbial membrane integrity, generate free radicals, denature vital proteins, disrupt cell reproduction and multiplication through DNA chemical deterioration, and

interfere with the generation of energy through the leakage of protons from the cell membrane by ionic interchange (Llorens and others 2012; Lemire and others 2013). Antimicrobial effectiveness is therefore dependent on migration of the metal ion or particle from a coating. Among the metals that have been studied for antimicrobial applications are silver (Marambio-Jones and Hoek 2010; Yun and others 2013; Maillard and Hartemann 2013), copper (Chen and others 2013; Wang and others 2013; Stranak and others 2014), titanium (Chen and others 2013; Yu and others 2013; Stranak and others 2014) and zinc (Llorens and others 2012).

Metal-based antimicrobial materials have been prepared as bulk alloys (Noyce and others 2006), incorporated as nanoparticles in coatings (Mauter and others 2011; Liu and others 2012), and embedded in the matrix of different carriers (like polymers, zeolites and resins) for subsequent coating (He and Chan 2010; Lee and others 2011; Vignesh and others 2012). Metal nanoparticles have been explored for preparation of metal based antimicrobial surfaces, with enhanced activity resulting from both their small size (enabling direct penetration of cell membranes) and improved surface area to volume ratio (increasing the amount of released metal ions) (Marambio-Jones and Hoek 2010; Lemire and others 2013). Nanoparticles of metals like silver and copper can be prepared by chemical reduction of their corresponding salts resulting in nanometric aggregates of the metal ions followed by subsequent surface modification or incorporation into different media to prevent aggregation (Llorens and others 2012; Lemire and others 2013). Antimicrobial metal nanoparticles and ions can also be loaded into zeolites, nanoporous materials prepared from alkaline earth metallic compounds and aluminosilicate (Rai and others 2009; Marambio-Jones and Hoek 2010).

The effectiveness of antimicrobial metal based surfaces has been demonstrated against Gram positive and Gram negative bacteria, as well as yeasts and fungi. Materials are typically challenged by direct contact with microbial suspensions followed by quantification of the number of surviving microorganisms or zone of inhibition assays. In one study, plasma functionalized rubber and stainless steel substrates were coated by thin layers of silver nanoparticles by reduction of Tollen's reagent, resulting in a 5 log reduction in *Listeria monocytogenes* populations after 5 hours exposure (Jiang and others 2004). In other work, up to 7 log reductions in *Escherichia coli* 0157:H7 was demonstrated by copper alloys depending on percentage of copper in the alloy, temperature, and presence of organic matter (Noyce and others 2006).

Silver and silver zeolite based antimicrobial materials and coatings have been commercially manufactured, mainly in consumer goods, healthcare, and cutlery. Applications in food contact materials are somewhat more limited, largely due to public health and environmental concerns about 'nanosilver', given their necessary migration for activity (Rai and others 2009; Marambio-Jones and Hoek 2010; Llorens and others 2012; Lemire and others 2013). Some applications of silver based coatings are currently listed in the "Inventory of Effective Food Contact Substance (FCS) Notifications" by the Food and Drug Administration (FDA) (Food and Drug Administration 2014), however consumers are increasingly demanding stronger federal regulation on nano-based materials, particularly in food applications. Indeed, the recent order issued by the U.S. Environmental Protection Agency (EPA) for a U.S. manufacturer to stop sale of nanosilver-based storage containers suggests that commercial production of silver-based antimicrobial materails is likely to see increased regulatory scrutiny (Environmental

Protection Agency 2014). In addition to toxicity and regulatory concerns, the effectiveness of this type of antimicrobials can be reduced in the presence of organic matter, which can react with metallic ions (Noyce and others 2006). Finally, no extensive stability studies have been reported on metal based antimicrobial materials. Because the metal ions must migrate from the materials to be effective, in addition to toxicity concerns, such coating may not retain effectiveness after frequent washings as seen by food processing surfaces.

2.3.2 Quaternary ammonium compounds

Quaternary ammonium compounds (QAC) are salts of quaternary ammonium cations that possess a protonated nitrogen atom with an anion (a halogen). The rest of the bonds the nitrogen atom shares are with alkyl groups normally. Biocidal activity relates to chain length of the alkyl groups bound to the nitrogen ($R_1R_2R_3R_4N^+X^-$). At least one of the substituents must be alkyl, between 5 and 17 carbons in length, to be biocidal (Gilbert and Moore 2005; Buffet-Bataillon and others 2012), with chain length requirements different for Gram positive and Gram negative bacteria due to differences in wall structure (Gilbert and Moore 2005; Kenawy and others 2007). QAC may inactivate microorganisms by disrupting the cell membrane and the cytoplasmic membrane through hydrophobic interactions, causing release and/or denaturation of vital biomolecules (Ikeda and others 1986; Murata and others 2007; Møretrø and Langsrud 2011; Buffet-Bataillon and others 2012). Another commonly reported interpretation explains that QAC promote an ionic exchange in which cations that are electrostatically bound to negatively charged phospholipids in the cell membrane are displaced by the positive charges QAC

contain, which subsequently affects cell integrity and microbial viability (Kugler and others 2005; Murata and others 2007). The exact antimicrobial mechanism of QACs likely varies based on QAC chemistry, microbial membrane structure, and mode of application (in solution vs. in a coating). Membrane disruption due to QAC induced ionic exchange is likely the mechanism by which QACs bound to or impregnated into surfaces exert their antimicrobial efficacy, although the exact mechanism of immobilized QACs remains unclear (Asri and others 2014).

QAC have been prepared from a very diverse group of compounds, generally organic, which can be low molecular weight structures or polymers. The preparation of QAC typically involves nucleophilic substitution of a nitrogenous compound (general formula $R_1R_2R_3N$) with a halogenoalkane (R_4X) to form the QAC $R_1R_2R_3R_4N^+X^-$. The resulting compound can be modified from any of the alkyl groups R for subsequent crosslinking onto a solid support or a polymer. QAC can also be incorporated into coatings by ionic exchange (Khalil 2013). It may therefore be possible to prepare 'rechargeable' antimicrobial coatings in which QACs electrostatically adsorb onto an anionic solid support and can be refreshed with subsequent exposure to QAC based sanitizers.

Antimicrobial activity of QACs has been tested by a range of methods including zone of inhibition or incubation with microbial suspension followed by quantification of number of survivors. QAC have been demonstrated to be biocidal towards Gram positive and Gram negative bacteria, as well as yeasts and fungi. In a recent study (Khalil 2013) QAC used in food processing facilities were incorporated into montmorillonite through ionic exchange. The modified clay was challenged against *Escherichia coli*, *Listeria*

monocytogenes, *Pseudomonas aeruginosa*, *Staphylococcus aureus* and *Salmonella Tennessee*, exhibiting more than 1 log reductions. In another study (Asri and others 2014), a silicon surface was silane functionalized for subsequent reaction with polyethyleneimine. The coated polyethyleneimine was alkylated through nucleophilic substitution to form a QAC resulting in a material capable of reducing microbial populations of *Staphylococcus epidermis* by more than 4 log cycles. Silanized stainless steel surfaces were also coated with QAC via alkylation of immobilized ethylene diamine resulting in antimicrobial activities of nearly 2 log cycles of *Staphylococcus aureus* and *Klebsiella pneumonia* (Jampala and others 2008).

As typical of antimicrobial materials literature, effectiveness of QAC modified materials are usually performed under conditions that maximize their biocidal efficacy, generally in bacterial suspensions in buffer or saline solutions. However, being charged substances, QAC have the potential of reacting and/or precipitating with organic molecules that can also exhibit charge, like proteins (Buffet-Bataillon and others 2012), which in turn may impact their antimicrobial activity. However, some works have reported that immobilized QACs retain antimicrobial activity even in the presence of proteins (Beyth and others 2010; Tiller 2011; Asri and others 2014), which suggests QAC may possess a versatile antimicrobial mechanism or a preferential affinity of microbial cells. Nevertheless, commercial applications of QAC modified food processing surfaces may be limited by fouling/charge neutralization by complex food components. Research on effectiveness in the presence of such food components, as well as effectiveness after exposure to chemically reactive cleaning and sanitization agents common in food processing, remains a need to demonstrate the commercial potential of QAC based

antimicrobial materials and coatings. It may also be possible to design new QACs (by careful R-group selection) that maximize their effectiveness in food equipment coating applications.

2.3.3 Cationic polymers

As with QAC, cationic polymers exert antimicrobial activity by destabilization of microbial membranes by ionic interchange with divalent cations present in the membranes. Unlike QAC, the positive charges provide (Feng and others 2006; Bratskaya and others 2007; Chua and others 2008; Elsabee and others 2008) antimicrobial activity regardless of the presence of hydrophobic alkyl chains (Kugler and others 2005; Lichter and others 2009). Among the polycations that have been studied for antimicrobial activity are polylysine (Fang and others 2014), chitosan (Mansilla and others 2013) and polyamines like polyethyleneimine and polyamidoamine (Wang and others 2010; Xia and others 2011). Their antimicrobial effectiveness has been widely demonstrated against Gram positive and Gram negative bacteria. Given their charged nature, they are commonly coated via layer-by-layer deposition (Feng and others 2006; Bratskaya and others 2007; Chua and others 2008; Elsabee and others 2008). They have also been covalently crosslinked onto surfaces (Yudovin-Farber and others 2010; Xia and others 2011). In a study that involved LbL deposition of carboxymethyl chitosan and carboxymethyl chitin onto corona activated polypropylene, both antifungal and antibacterial activity were demonstrated, achieving up to 5 log reductions (Elsabee and others 2008). In another study in which polyethyleneimine was covalently crosslinked with glutaraldehyde on silane-modified glass slides, it was possible to inactivate 5 log

Escherichia coli and *Bacillus subtillis* per cm^2 of modified material (Xia and others 2011).

Despite the well published demonstration of the antimicrobial efficacy of cationic polymers, when such materials are challenged by presence of particulates or organic matter, antimicrobial efficacy can be drastically diminished. In a study that involved surface modification of sands with polyethyleneimine (Onnis-Hayden and others 2011), antimicrobial activity was tested against both aqueous and waste-water containing suspensions of the same microbial load of *Escherichia coli*. Suspension in waste-water reduced antimicrobial efficacy from 5 to 2 log reductions. The observed reduction in antimicrobial effectiveness was likely a result of fouling by anionic compounds in the suspended organic matter. In addition to diminishing antimicrobial efficacy, such fouling could potentially condition a surface to promote bacterial adhesion and biofilm formation. For these reasons, in addition to standard "log reduction" antimicrobial activity assays, a proper evaluation of an antimicrobial coating should include microscopy or other analyses to evaluate the influence of the coating chemistry on fouling by food components and/or microorganisms. Integration of non-fouling and antimicrobial character (by cationic polymers or other antimicrobial approaches) may therefore represent a useful approach to overcome such challenges.

2.3.4 Antimicrobial peptides

Antimicrobial peptides impart antimicrobial activity against bacteria, viruses and fungi in a similar way as cationic polymers and QAC. Given their generally low molecular weight, they are believed to be able to interact with microbial cell membranes

and get entrapped within their structure, increasing their porosity and causing leakage of essential biomolecules which ultimately leads to cell death. These peptides are synthesized generally by microbial cells as a way to compete and survive in the environment. Over 800 naturally derived antimicrobial peptides have been studied (Glinel and others 2012; Perez Espitia and others 2012). Another approach that has been explored is the design and synthesis of biomimetic peptides (through techniques like ring-opening metathesis polymerization) with biological activity that mimic the antimicrobial effect of the natural origin peptides, and those synthetic substances may or may not contain amino acids (Sgolastra and others 2013).

Antimicrobial peptides can be covalently linked to food contact material surfaces by amines, carboxylic acids, thiols and hydroxyls inherent in their structure. Their ionic nature also enables them to be deposited through layer-by-layer assembly. A range of surfaces including silicon (Wang and others 2014), glass (Chen and others 2012), magnetic nanoparticles (Zhang and others 2012), titanium (Gao and others 2011), polystyrene (Han and others 2011) and stainless steel (Hequet and others 2011) have been explored for covalent immobilization of antimicrobial peptides. Some antimicrobial peptides have also been loaded through electrostatic interactions into anionic polymer carriers for subsequent deposition onto different substrates (Wang and others 2012). The well-studied antimicrobial peptide nisin has also been blended with polymers through solution casting technique (Bastarrachea and others 2010). In another study, the peptides magainin and nisin were attached to the surface of stainless steel and decreased adhesion of *Listeria ivanovii* by more than 60% (Hequet and others 2011). However, there are several limitations to be overcome prior to application in antimicrobial coatings for food

processing. They can be prone to hydrolysis and denaturation under pH and temperature extremes, which ultimately eliminates their antimicrobial effect.

2.3.5 Essential oils

Essential oils are natural, low molecular weight compounds possessing functional groups such as phenols, aldehydes, ketones, alcohols and hydrocarbons. They are produced by plants for protection against microorganisms and have been found to be antimicrobial against Gram positive and Gram negative bacteria, as well as against yeasts, fungi and viruses (Glinel and others 2012; Saad and others 2013; Seow and others 2014). Given their structural diversity, the mechanism of their biocidal activity is not completely understood, but is believed to include hydrophobic and hydrophilic interactions with the microbial cell membranes. This increases membrane permeability, leading to loss of vital molecules and ions, disruption to the production of energy and finally cell death (Bakkali and others 2008; Glinel and others 2012; Saad and others 2013). Much of the research in essential oil based antimicrobial materials has been in the form of edible films (Oussalah and others 2004; Avila-Sosa and others 2010; Avila-Sosa and others 2012; Da Rocha and others 2014). In this approach, the essential oils are mixed with polymers like chitosan, polysaccharides, cellulose derivatives or proteins, and materials are prepared by solution casting. Modification of surfaces of different materials that can be in direct contact with food has been done mainly in plastics like polyethylene and polypropylene, either through bulk modification (blending of the corresponding essential oil with the polymer) or by coating of the essential oil with a carrier. In a recent study, linalool and methylchavicol were incorporated into polyethylene films through

extrusion and antimicrobial activity was demonstrated against *Escherichia coli* (Suppakul and others 2011). In other work, polypropylene was coated with microcapsules containing thymol and carvacrol, and antimicrobial activity was shown against *Escherichia coli* O157:H7, *Staphylococcus aureus*, *Listeria innocua*, *Saccharomyces cerevisiae*, and *Aspergillus niger*) (Guarda and others 2011). Despite their demonstrated effectiveness, a major hindrance to the commercial application of essential oils is their native odor, particularly at concentrations necessary to achieve efficacy. Further, as with many low molecular weight antimicrobial agents, essential oils must necessarily migrate from the coating to be effective, meaning the coating would lose effectiveness over time. Finally, their antimicrobial activity can be substantially reduced in the presence of polysaccharides, proteins, lipids, oxygen, as well as exposure to high temperatures, light, and high pH levels (Glinel and others 2012; Seow and others 2014). Nevertheless, with increasing consumer demands for replacing synthetic additives with natural compounds, there is opportunity if research can overcome the stated limitations in essential oil based antimicrobial materials and coatings.

2.3.6 Light activated antimicrobials

Light activated antimicrobials refer to a wide range of photoactivated compounds which can be organic, aromatic compounds (e.g. porphyrin or chlorophyll derivatives (Huang 2005)) or inorganic oxides (e.g. titanium dioxide, TiO_2). Their antimicrobial activity can be achieved by exposure to light of a particular wavelength, resulting in generation of reactive oxygen species which can react with biomolecules (cell membranes, enzymes, nucleic acids) affecting microbial viability (Huang 2005; Noimark

and others 2013a). A range of such light activated antimicrobials have been explored for biomedical applications in treatment of localized, drug resistant infections, and recent research has explored their incorporation into materials for applications in polymer coatings and textiles (Sun and Hong 2013).

Light activated antimicrobials have been incorporated into polymers through solution casting, in which a solution of a dissolved polymer and the corresponding antimicrobial are poured into a mold followed by evaporation of the solvent (Decraene and others 2008a). They have also been incorporated into different polymers through swell encapsulation (Perni and others 2009; Ismail and others 2011; Noimark and others 2012; Noimark and others 2013b). TiO_2 based light activated antimicrobial materials have been prepared by oxidizing bulk metallic alloys containing titanium (Chrzanowski and others 2010) and deposition through arc ion plating (Chung and others 2008). In another work, a solid support was dip coated in an emulsion containing TiO_2 and subsequently thermally treated to promote TiO_2 crystallization on the surface (Yu and others 2003).

The biocidal efficacy of light activated antimicrobials embedded in different materials has been demonstrated to achieve several log reductions. In a study that involved incorporation of methylene blue into polysiloxane, up to a 3.5 log reduction in *Staphylococcus aureus* and *Escherichia coli* populations were achieved after short exposure to light at the corresponding wavelength (Perni and others 2009). In this work, addition of gold nanoparticles enhanced the activity of the photosensitizer by providing an additional source of reactive oxygen species. In another study, toluidine blue and rose Bengal were incorporated into cellulose acetate through solution casting and the light

activated modified material was able to inactivate up to 3 log cycles of *Staphylococcus aureus*, depending on the amount and presence of organic matter (Decraene and others 2008a). In a study involving surface modification of stainless steel with a thin film of TiO_2, it was possible to inactive *Bacillus pumilus* (a resistant Gram positive rod) by more than 0.5 log cycles (Yu and others 2003). A limitation of light-activated antimicrobials is their non-specific activity against organic matter. When the test conditions include some exposure to different levels of organic matter, antimicrobial activity can be drastically diminished to less than 1 log reduction (Decraene and others 2008b). In addition, no extensive stability studies have been made to evaluate robustness of photoactivated antimicrobials after incorporated into coatings. Nevertheless, their ability to repeatedly 'self-clean' on exposure to light makes them a promising opportunity for incorporation into coatings for food contact applications.

2.3.7 N-halamines

N-halamines are a class of antimicrobials in which one or more nitrogen atoms can be reversibly halogenated with chlorine, bromine or iodine. The mechanism behind their biocidal activity is not completely understood but there is general agreement that there is an oxidizing effect on microorganisms' membrane functions imparted by the nitrogen-stabilized halogen. Another possibility is the penetration of free (dissociated) halogen into the microbial cells, and subsequent disruption of the functions of vital biomolecules (Eknoian and others 1998; Kenawy and others 2007). A major interest in the application of N-halamines (particularly for food applications) is that after imparting their antimicrobial effect, N-halamines can be recharged by exposure to a halogen source

(most commonly chlorine) to provide repeated cycles of disinfection. Numerous nitrogenous structures are capable of forming antimicrobial N-halamines, with stabilities decreasing in the order of amine > amide > imide (Qian and Sun 2003; Tan and Obendorf 2007). Chlorine halogenation of N-halamines is most commonly studied because of the higher stability of the N–Cl bond as compared to N–Br or N–I bonds (Worley and Williams 1988). N-halamines can be part of an inorganic or organic compound (Worley and Williams 1988). Inorganic N-halamines are generally referred to as *chloramines*, and exhibit lower antimicrobial effect than free chlorine but are less reactive towards organic matter than free chlorine. Organic N-halamines can be classified in several groups including isocyanurates, hydantoins, N-chlorosuccinimide, Glycolurils, Sulfonchloramides, acyclic N-halamines and polymeric N-halamines (Williams and others 1987; Worley and Williams 1988; Williams and others 1991; Goddard and Hotchkiss 2008; Bastarrachea and others 2011; Bastarrachea and Goddard 2013).

A wide range of methods have been reported for the preparation of monomeric N-halamines, typically as cyclic organic compounds (Williams and others 1987; Williams and others 1991; Lauten and others 1992; Worley and others 1992; Kou and others 2009). Because of the potential toxicity of low molecular weight N-halamines, additional research has been performed in development of higher molecular weight, polymeric N-halamines. Cyclic N-halamines have been functionalized for subsequent covalent bonding to an already formed polymer substrate or surface (Worley and Sun 1996; Eknoian and others 1998; Williams and others 2005; Liang and others 2007; Kou and others 2009; Kocer and others 2010). In other work, acrylate derivatized hydantoin-containing monomers were copolymerized with methyl methacrylate or acrylamide (Sun

and Sun 2001; Sun and Sun 2003; Cao and Sun 2009; Kocer and others 2011b; Kocer 2012). Such N-halamine containing polymers could be dispersed in paints (Kocer and others 2011a), incorporated into nanostructures as electrospun nanofibers (Tan and Obendorf 2007; Ren and others 2013), or copolymerized onto nanoparticles (Dong and others 2011). Incorporation of N-halamine moieties into nanostructures enables high surface area (and therefore increased effectiveness per unit mass of material) however would likely need additional converting steps to be suitable for coating onto food processing equipment.

Recently, N-halamine containing coatings have been applied onto a range of substrates via layer-by-layer assembly, in which N-halamine functionality may come from one of the polyelectrolytes, bonds formed between polyelectrolytes, or N-halamine containing nanostructures entrapped between layers (Goddard and Hotchkiss 2008; Cerkez and others 2011; Bastarrachea and Goddard 2013; Bastarrachea and others 2013; Bastarrachea and others 2014). Deposited bilayers can be covalently cross-linked to improve coating stability, as would be needed in applications (such as food processing equipment) that are exposed to a range of pH values, surfactants, and exposure to ionic constituents (e.g. proteins, salts, hydrocolloids) which may impact stability of electrostatically bound coatings. N-halamines have demonstrated biocidal efficacy towards a range of Gram positive and Gram negative bacteria. A "sandwich" test is commonly used to quantify the antimicrobial activity of N-halamine coated materials, in which a small volume of (typically aqueous) inoculum is sandwiched between two coupons of modified material (Williams and others 2005; Tan and Obendorf 2007; Kou and others 2009; Cerkez and others 2011; Lee and Whang 2011; Kocer and others 2011a;

Kocer 2012). This sandwich method has been used to demonstrate inactivation rates of up to 8 log cycles (99.999999% reduction) (Kou and others 2009). Although a frequently reported method, it has significant practical limitations in terms of application to true environmental conditions, as the surface area to volume ratio between the N-halamine coated material and the bacterial suspension is typically in the 500 – 800 range, well beyond realistic ratios experienced by food processing equipment. Rotating submersion assays provide more commercially translatable antimicrobial activity data, in which coupons of coated material are submerged in larger volumes of inoculum and rotated to ensure continuous contact between material and inoculum for the course of the study (Bastarrachea and Goddard 2013; Bastarrachea and others 2013; Bastarrachea and others 2014).

The stability of N-halamine coatings has been investigated more thoroughly than that of other antimicrobial materials and coatings, likely because their interest is due to their rechargeable nature. N-halamines stability has been tested by imitating conditions of repeated usage or continuous exposure to cleaning agents, sources of light, repeated halogenation, etc. It has been reported that N-halamines exhibit optimal stability when their nitrogen atoms neighbor methyl groups and/or form part of a hydrophobic structure (Sun and Sun 2001; Cerkez and others 2011; Kocer and others 2011b). Kocer and others (2010) evaluated the stability of a hydantoinyl siloxane N-halamine coated onto cotton which suffered decomposition after continuous exposure to UV light when chlorinated. It was concluded that the chemical deterioration was due to breakage of an alkyl bond contained in the silane cross-linker used to attach the N-halamine on the cotton's surface. Stability of the bond linking antimicrobial moieties to a food processing equipment's

surface is therefore a critical factor in evaluating the commercial application of a particular coating. Continuous halogenation may also provoke breakage of the chemical bonds that hold N-halamine structures on modified substrates due to the oxidizing effect of halogen sources, particularly at high concentrations. It is therefore important to evaluate N-halamine stability under conditions typical of a food processing environment. For example, while researchers often evaluate N-halamine chlorination at concentrations exceeding 3000 ppm, the maximum concentration allowable for sanitation of food contact equipment is 200 ppm, which is likely to be less degradative to N-halamine modified surface, yet has been shown to effectively chlorinate N-halamine structures (Bastarrachea and others 2014).

N-halamine antimicrobial materials and coatings represent a unique approach to antimicrobial food processing equipment, as they regain activity after exposure to halogenated solutions, such as common in food contact material sanitizers. Such materials would therefore have enhanced potential for long-term usage in a processing environment, compared to materials and coatings for which the antimicrobial agent must migrate for effectiveness. As with other antimicrobial coatings, on-going research is needed to demonstrate effectiveness of N-halamine containing coatings in the presence of organic matter, after long term exposure to mechanical and chemical stresses, and at surface area to volume ratios typical of food processing environments.

2.4 Conclusions

The antimicrobial materials and technologies explored throughout this review still face several obstacles to be of common use in industry, like the need for approval for both the antimicrobial substance and the material in which it has been applied. As it was explained, antimicrobials can be anchored covalently onto the surfaces of different materials, which in theory would eliminate the risk of transfer onto the foods. However, as research has shown, coatings and surfaces can deteriorate and become unstable, which could lead to contamination of not approved antimicrobial substances onto the final food products (Wang and others 2010; Lee and Whang 2011; Kocer and others 2011b). This phenomenon also harbors the risk of development of antimicrobial resistance by the microorganisms, as well as environmental negative impacts (Das and others 2009; Munro and others 2009). Another obstacle relates to cost. The effectiveness of many approaches to render materials antimicrobial has been successfully studied and confirmed at a laboratory scale, but the cost of scaling them up makes their industrial application unrealistic. In addition (as it was also confirmed throughout this review), many technologies have proved to be effective at a laboratory scale under ideal conditions (chosen to maximize the antimicrobial effectiveness of the studied substance) that don't take into account several characteristics of the food processing environments (presence of organic matter, extreme levels of pH, oxidizing agents, physical stress, extreme temperatures, etc.) and that can hardly be extrapolated to real situations in industry. This brings the need for more extensive and challenging research to improve these technologies and make them more efficient, as well as the need for developing standard methods of antimicrobial evaluation in which industry can rely. There is also the need to

conduct research that can generate antimicrobial materials and coatings with the potential to be used continuously or to be regenerated, with limited or no loss of activity.

2.5 Acknowledgements

This work was supported by the National Institute of Food and Agriculture, U.S. Department of Agriculture under project number 2011-65210-20059 and in part by the Center for Hierarchical Manufacturing at The University of Massachusetts Amherst, an NSF Nanoscale Science & Engineering Center supported by the National Science Foundation under NSF Grant No. CMMI-0531171.

CHAPTER 3

DEVELOPMENT OF ANTIMICROBIAL STAINLESS STEEL VIA SURFACE MODIFICATION WITH N-HALAMINES: CHARACTERIZATION OF SURFACE CHEMISTRY AND N-HALAMINE CHLORINATION[2]

3.1 Abstract

N-halamine modification of materials enables the development of antimicrobial materials whose activity can be regenerated after exposure to halogenated sanitizers. Surface and bulk modification of polymers by N-halamines has shown great success, however modification of inorganic substrates (e.g. stainless steel) remains an area of research need. Herein we report the covalent surface modification of stainless steel to possess rechargeably antimicrobial N-halamine moieties. Bilayers of branched polyethyleneimine and poly(acrylic acid) were immobilized onto the surface of stainless steel and the number of N-halamines available to complex chlorine was quantified. Samples were characterized through contact angle, Fourier Transform Infrared Spectroscopy (FTIR), ellipsometry, dye assay for amine quantification, and X-ray photoelectron spectroscopy (XPS). Increasing the number of bilayers from one to six increased the number of N-halamines available to complex chlorine from 0.30 ± 0.5 to 36.8 ± 5.0 nmol cm^{-2}. XPS and FTIR confirmed successful covalent layer-by-layer deposition of the N-halamine bilayers. The reported layer-by-layer deposition technique resulted in a greater than seven-fold increase of available N-halamine compared to prior

[2] Submitted to Journal of Applied Polymer Science.

reports of N-halamine surface modifications. The N-halamine modified steel demonstrated antimicrobial activity (> 99.9% reduction) against the pathogen *Listeria monocytogenes*. Such surface modified stainless steel with increased N-halamine functionality, and therefore potential for rechargeable antimicrobial activity, supports efforts to reduce cross-contamination by pathogenic organisms in the food and biomedical industries.

Keywords: biological applications of polymers, ESCA/XPS, FTIR, surface modification, nanolayers

3.2 Introduction

Cross-contamination of pathogenic microorganisms is a major concern in the food and biomedical industries because of the impact to public health as well as the resulting financial impact of medical expenses (Centers for Disease Control and Prevention 2003; Centers for Disease Control and Prevention 2004). In the food industry, the growth and cross-contamination of pathogens like *Listeria monocytogenes*, *Escherichia coli*, and *Salmonella* spp. on the surface of food contact materials (work tables, conveyor belts, processing equipment) as well as non-contact materials (ventilation ducts, door knobs, etc.) pose a public health risk. There is also a substantial potential for economic losses due to the proliferation of spoilage microorganisms and resulting product loss. Further, some microorganisms are able to form stable communities called biofilms, which increases their resistance to traditional cleaning and sanitization methods (Maukonen and others 2003; Simões and others 2010; Møretrø and Langsrud 2011).

Stainless steel is a commonly used material in food processing facilities as well as in fabrication of biomedical devices (Maukonen and others 2003; Niinomi 2008; Gupta and Kumar 2008). However, several studies have shown its ability to harbor biofilms composed of microorganisms from different genera, including *Listeria*, *Staphylococcus*, *Escherichia, Bacillus* and *Pseudomona* (Cloete and Jacobs 2001; Parkar and others 2004; Sharma and others 2005; Kreske and others 2006; Marques and others 2007; Oulahal and others 2008). Currently, there is no available strategy to totally prevent or control the formation of biofilms. The most common techniques used are the application of disinfectants and heat, which are less effective on microorganisms that have formed a

stable biofilm (Simões and others 2010). There is therefore a continued need to reduce the adhesion, survival, and cross-contamination of pathogenic and spoilage organisms on stainless steel. Development of antimicrobial materials for which the antimicrobial activity is long-lasting and does not diminish via migration of the antimicrobial agent can help to support current cleaning and sanitization protocols in improving food safety.

N-halamines are antimicrobial structures in which a stable nitrogen-halogen complex can be rechargeably formed after contact with halogenated sanitizers (e.g. sodium hypochlorite, bromophors/iodophors). N-halamines can exist as amines, amides or imides and the halogen position can be occupied by an atom of chlorine, bromide, and iodide. N-halamines composed by amines exhibit higher stability than those composed by amides, which in turn are more stable than those composed by imides (Eknoian and others 1998). The stability is given by the ability of the N-halamine to provide an electron to the halogen atom, working as a sort of resonance system and avoiding the separation of the halogen from the rest of the molecule due to the loss of one of its electrons. Probably the most important feature of N-halamines is their ability to be regenerated with solutions containing the corresponding halogen, which makes them able to provide antimicrobial activity repeatedly. The halogen is released once it gets in contact with microorganisms, inactivates them, and the N-halamines can be regenerated again (with sodium hypochlorite/bleach commonly), making them ready for another cycle of disinfection (Eknoian and others 1998). N-halamine functionalized materials have been developed for a range of applications such as biocides in swimming pools and spas, disinfectants in water filtration systems, disinfectants of recreation water, and so on (Worley and Sun 1996). They have also been incorporated in fabrics to be used in the production of

different types of clothes (Sun and Sun 2002; Møretrø and Langsrud 2011). Both soluble and insoluble N-halamines have been developed with demonstrated activity against microorganisms, and both bulk and surface modification techniques have been employed to impart N-halamine activity to materials (Eknoian and others 1998; Sun and Sun 2002; Liang and others 2007; Goddard and Hotchkiss 2008; Kocer and others 2010). Surface modification in which the N-halamine moiety is covalently attached to a materials surface decreases the likelihood of N-halamine migration from the substrate, a potential regulatory benefit (Worley and Sun 1996). A few reports have been published on surface modification of polymeric materials with N-halamines, however there are no reports of such modifications on inorganic substrates like stainless steel.

The overall goal of the present work was to modify the surface of 316 stainless steel to possess rechargeably antimicrobial N-halamine functionality, and to increase the number of N-halamines by a sequential layer-by-layer deposition process. The objectives were to modify the surface of stainless steel through the layer-by-layer deposition of increasing number of bilayers of covalently linked branched polyethyleneimine (PEI) and polyacrylic acid (PAA), to evaluate the capacity to retain and release chlorine, and finally to characterize the materials through surface analytical techniques to confirm the chemical modification. The number of N-halamines and primary amines increased with the number of bilayers immobilized. Covalent bond formation between the applied polymers and stainless steel was confirmed through FTIR, ellipsometry, and XPS. No significant difference between control samples and treated samples was observed in contact angle ($P > 0.05$). More than 3 logarithmic reductions were obtained after challenging the 6 bilayer samples against *L. monocytogenes*.

3.2 Materials and methods

3.2.1 Materials

Stainless steel 316L #2B and #8 finish (non-mirror and mirror polished, respectively) was purchased from McMasterr-Carr (Chicago, IL). Isopropanol, acetone, sulfuric acid, hydrogen peroxide, toluene, hydrochloric acid (12 N), sodium hydroxide, HPLC grade water, and sodium chloride were purchased from Fisher Scientific (Pittsburgh, PA). The silane coupling agent 3-Glycidoxypropyltrimethoxysilane (GOPTS), sodium hypochlorite (5% chlorine), and AO7 dye (Orange (II) (Cert)) were purchased from Acros Organics (Fair Lawn, NJ). Branched polyethyleneimine (PEI, 25,000 Da) was purchased from Sigma-Aldrich (St. Louis, MO), and poly(acrylic acid) (PAA, 450,000 Da) was purchased from Scientific Polymer Products, Inc. (Ontario, NY). N-hydrosuccinimide (NHS) was purchased from Acros Organics. 1-(3-Dimethylaminopropyl)-3-ethylcarbodiimide hydrochloride (EDC-HCl) was purchased from ProteoChem, Inc. (Denver, CO). DPD total chlorine reagent powder was from Hach Company (Loveland, CO). *Listeria monocytogenes* FSL-J1-225 Scott A, was graciously provided by the laboratory of Dr. Lynne McLandsborough. Tryptic Soy Broth (TSB), Tryptic Soy Agar (TSA), and Neutralizing buffer (NB) were purchased from Becton, Dickinson and Company (Sparks, MD).

3.2.2 Stainless steel surface modification

Stainless steel 316L #2B finish was cut in 1 × 2.5 cm samples. Before surface modification, samples were subjected to cleaning, first with isopropanol then with acetone, and finally with deionized (DI) water under sonication (two 10 min cycles per solvent). Samples were then dried with purified air and immersed in piranha solution, prepared by mixing carefully sulfuric acid and hydrogen peroxide in a 7:3 volumetric ratio of sulfuric acid and 30% hydrogen peroxide for 20 min in order to clean the surface of the samples and create hydroxyl groups. After piranha solution treatment, samples were rinsed with DI water, dried with purified air, and left shaking overnight in toluene to precondition the surface prior to solvent-based silanization. Samples which had undergone piranha treatment and toluene soaking were dried with purified air and stored in clean glass Petri dishes as Control samples. Samples that were going to be subjected to further chemical modification were then immersed in a solution of toluene containing 2% (v/v) of the silane coupling agent GOPTS and shaken for 10 min. Once treated with GOPTS, samples were rinsed with copious toluene, dried with purified air, and heated for 2 h at 80 °C in order to promote covalent bond formation between the oxidized stainless steel surface and GOPTS. Cured, GOPTS treated samples were stored in clean glass Petri dishes as "GOPTS" treatment. The rest of the samples were treated as follows: to apply a single bilayer of polyethyleneimine and polyacrylic acid, samples were first immersed in a 0.1 M phosphate buffer solution, pH 7.8, containing 5 mg mL^{-1} of branched polyethyleneimine (PEI), and the zero-length cross-linker EDC-HCl and NHS in a concentration of 50 and 5 mM (respectively), and shaken for 30 min. Then, after having

been rinsed in copious DI water and dried with purified air, samples were immersed in a 0.1 M phosphate buffer solution, pH 7.8, containing 5 mg mL^{-1} of PAA and the same concentrations of EDC-HCl and NHS, shaken for 30 min, rinsed in copious DI water, and dried with purified air. The described procedure was repeated until completing up to six bilayers. Samples were randomly selected after each bilayer deposition to be subjected to surface analysis as described below. Figure 3.1 illustrates the overall chemistry of the chlorinated N-halamine surface modified stainless steel.

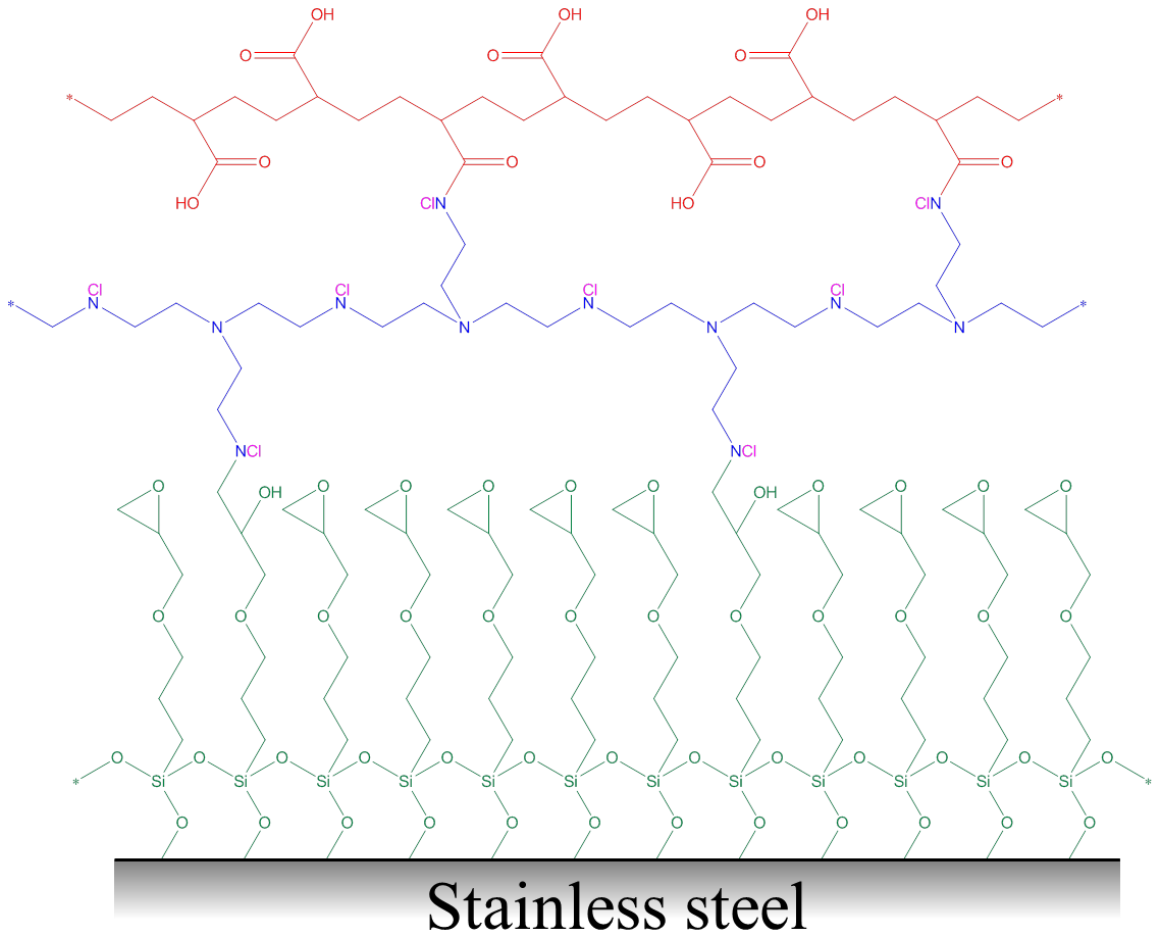

Figure 3.1 Schematic of chlorinated, N-halamine modified stainless steel prepared by layer-by-layer deposition technique.

3.2.3 N-halamine activation and determination of chlorination

Samples from the different treatments prepared as explained earlier were shaken for 15 minutes in individual test tubes containing DI water with 3000 ppm of chlorine, prepared by making the corresponding dilution from a sodium hypochlorite solution containing 5% of free chlorine. The chlorine content of the sodium hypochlorite solution was confirmed previously through the standard method D 2022–89, in which the

available chlorine content is determined through a iodometric titration with $Na_2S_2O_3$ 0.1 N (American Society for Testing and Materials 2008). Samples were rinsed with copious DI water after the 15 min of shaking, and dried with purified air. Then, the samples were transferred to individual test tubes with DI water. The ability of N-halamines to complex chlorine was determined through a modified N,N-diethyl-p-phenylenediamine (DPD) assay. DPD reagent was prepared by mixing one packet of DPD total chlorine reagent powder with 1 mL of DI water. A volume of 50 μL of DPD reagent was applied per every mL of DI water contained in the individual test tubes. Then, the samples were shaken for 2 min and the absorbance of the solutions in contact with them was measured at 512 nm. The chlorine concentration of the solutions was determined from a standard curve of sodium hypochlorite in DI water. The chlorination of N-halamines in nmol cm^{-2} was calculated by taking into account the volume of DI water in contact with the samples and the samples' dimensions. This procedure was performed 3 times (3 replicates), with 4 samples per treatment in every replicate.

3.2.4 Contact angle

Advancing (θ_A) and receding (θ_R) water contact angles were determined with a DSA100 (Krüss, Hamburg, Germany). A volume of 2.5 μL HPLC grade water was applied at a rate of 15 μL min^{-1} with an automatic dispenser. Measurements were performed under atmospheric conditions and were analyzed using the Drop Shape Analysis software, version 1.91.0.2 (Krüss, Hamburg, Germany). Hysteresis (H) was obtained from the difference between θ_A and θ_R. A total of 3 replicates were performed

for this evaluation, with 3 samples per treatment in every replicate and 3 measurements were done in every sample (9 measurements per replicate).

3.2.5 Fourier Transform Infrared Spectroscopy (FTIR)

Mirror polished stainless steel (316, 0.036" thick) was used as a substrate for bilayer deposition for FTIR and ellipsometry measurements (described below), to avoid artifacts resulting from inherent roughness in #2B finished stainless steel. Changes in surface chemistry were determined with an IRPrestige 21 spectrometer (Shimadzu Corp., Tokyo, Japan). Absorbance was measured in 3 different spots of each of three samples per treatment with a Monolayer Grazing Angle Accessory (Specac Ltd., Orpington Kent, UK) at an angle of incidence of 60°. A resolution of 4 cm^{-1} and a total of 200 scans were applied for every spot using square triangle apodization. Control samples (ie: piranha cleaned steel) were used as the background. The spectra were collected with IRsolution software (Shimadzu Corp., Tokyo, Japan), and after baseline correction, atmospheric correction and smoothing (20 points), spectra were analyzed with the Knowitall software (Biorad Laboratories, Philadelphia, PA). The areas of representative peaks were calculated with the IRsolution software. A total of 3 replicates were performed, with 3 samples per treatment in every replicate.

3.2.6 Ellipsometry

Before determination of thicknesses by ellipsometry, the refractive indices of PEI, PAA and GOPTS were confirmed with a digital refractometer from Sper Scientific model 300034 (Sper Scientific, Scottsdale, AZ). The thicknesses of the increasing bilayers of the different treatments were determined with a Rudolph research model auto SL-II automatic ellipsometer (Rudolph Research Analytical, Hackettstown, NJ) with an angle of incidence of 70° from the normal. The light source was a He-Ne laser with λ = 632.8 nm. Measurements were done in 3 different spots of a single sample. Three replicates were done for this evaluation, with 3 samples per treatment in every replicate.

3.2.7 Acid Orange 7 (AO7) dye assay

The quantification of primary amines on the samples' surface was performed as follows. Samples were immersed in individual test tubes containing 1 mM of AO7 dye (Orange (II) (Cert), Acros Organics, Fair Lawn, NJ) in DI water adjusted to a pH of 3 by hydrochloric acid. After the 3 h of shaking, the samples were rinsed in copious DI water (pH = 3) to remove noncomplexed dye. Samples were then transferred to individual test tubes containing DI water adjusted to a pH of 12 by sodium hydroxide in order to desorb the absorbed dye. Samples were then shaken for 15 min and the absorbance of the solutions in contact with the samples was measured at 455 nm. The AO7 concentration was determined from a standard curve of AO7 in DI water (pH = 12) and the primary amines content on the surface of the samples was calculated based on such concentration

and the samples' dimensions (Uchida and others 1993). Three replicates were performed for this assay, with 3 samples per treatment in every replicate.

3.2.8 X-ray photoelectron spectroscopy (XPS)

XPS analysis was performed with a Physical Electronics Quantum 2000 (Physical Electronics, Inc., Chanhassen, MN) with Al Kα excitation at a spot size of 100 μm at 25 W. Spectra were obtained at an angle of 45° relative to the samples' plane. Survey scans of every sample were collected at a pass energy of 187.85 eV with a step size of 1.6 eV. High resolution spectra were collected at a pass energy of 46.95 eV and with a step size of 0.4 eV. Atomic concentrations and high resolution spectra were analyzed with the MultiPak software version 6.1A (Physical Electronics, Inc., Chanhassen, MN). After linear background subtraction, high resolution spectra were fitted with the Gaussian-Lorentzian model (90% Gaussian was applied).

3.2.9 Antimicrobial activity assay

Coupons were prepared as explained earlier but with a final dimension of 1 × 1 cm. *L. monocytogenes* was used as the model organism to demonstrate antimicrobial activity because of its importance in food safety, having been reported to be the pathogen responsible for the most foodborne illness related deaths (Mead and others 2000). Bacterial suspensions were prepared by preparing a 1:100 dilution with sterile TSB from an overnight culture grown in the same type of broth. This subculture would be incubated

at 37 °C with rotation (150 rpm) for 4 h, time chosen basing on a previously prepared growth curve (Figure 3.2) in order to make sure microorganisms remained multiplying during the rest conditions. After the 4 h, a 1:1000 dilution from that culture would be prepared to have a final concentration of approximately 10^6 CFU mL^{-1}.

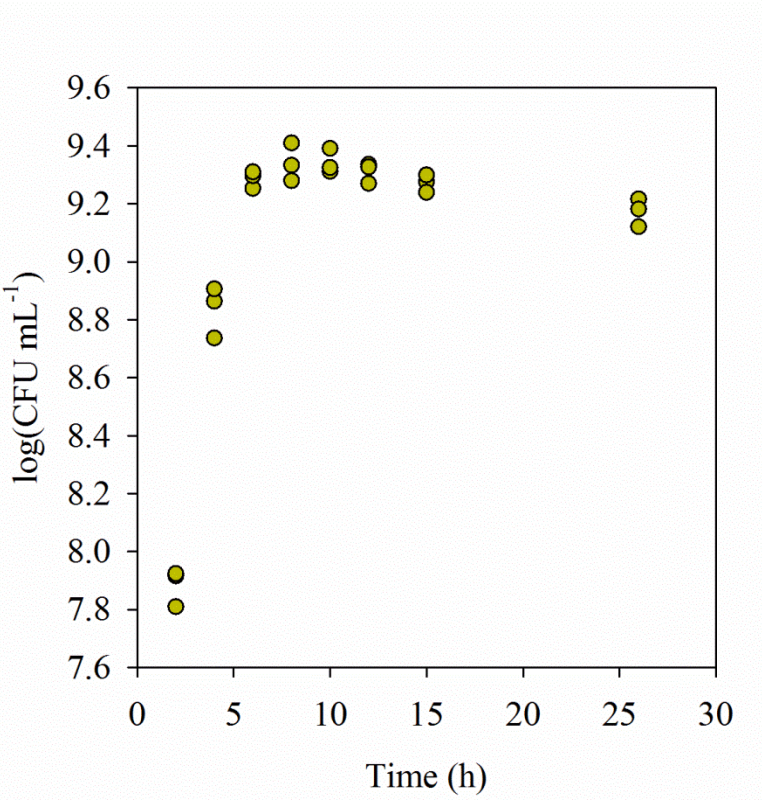

Figure 3.2 Growth curve of *L. monocytogenes*.

Stainless steel coupons from each treatment (1 × 1 cm^2) were submerged in 0.5 mL of the mentioned aqueous suspension of *L. monocytogenes* and incubated with rotation (35 rpm) at 32 ^oC in a carousel rotator. The position of the rotator was set in a way that allowed the coupons inside the test tubes to flip after completing a single turn, which allowed each side of them to be exposed to the bacterial suspensions (Figure 3.3).

Samples from the suspensions in contact with the coupons were taken after 2 and 4 h and serial dilutions were prepared with NB (the first dilutions to neutralize chlorine) and the next serial dilutions were prepared in saline water (0.9% NaCl). Then, the serial dilutions were plated on TSA and the plates were incubated for 48 hours at 37 ^{o}C. Colonies were counted with and antimicrobial activity was recorded as the log reduction in CFU mL^{-1}. Inoculation in TSA was done with an automated spiral plater Autoplater 4000 (Spiral Biotech Inc., Norwood, MA), and colonies counting was performed with a plate reader Scan® 500 (interscience, Saint-Non-la-Brèteche, France) in a range of 30 – 300 colonies using the instrument's software.

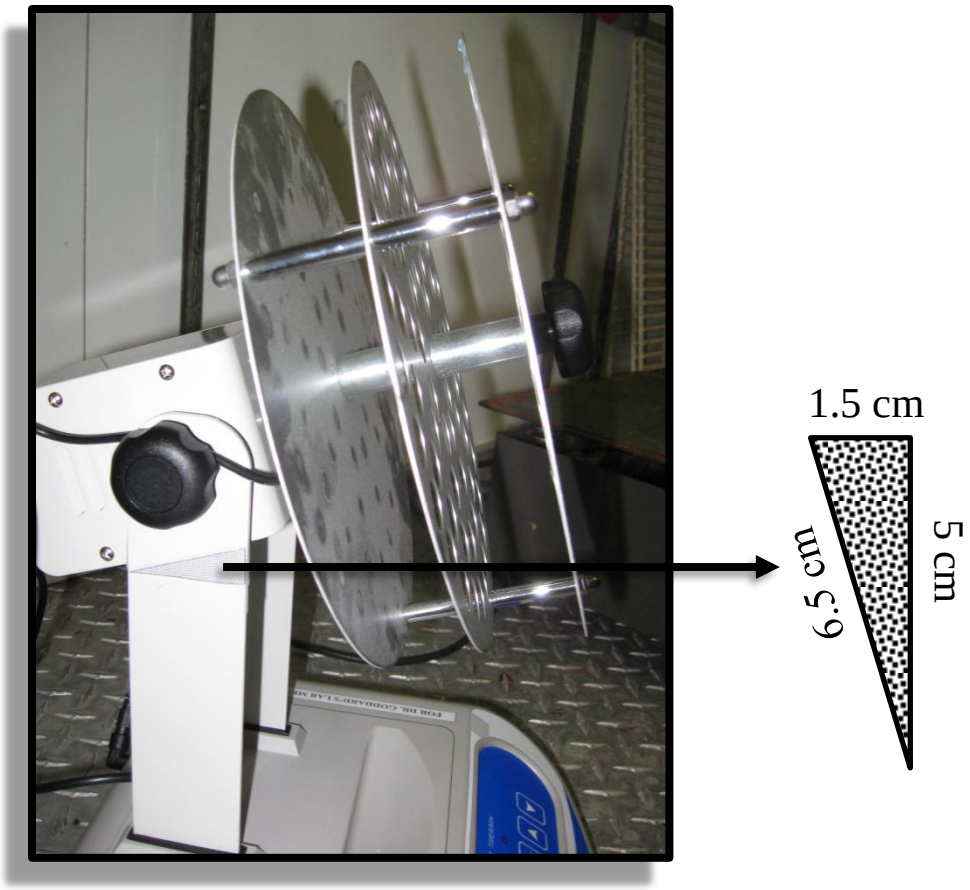

Figure 3.3 Rotator position and guide used for the antimicrobial activity assay.

In this assay, bacterial suspensions without being in contact with any type of coupons, not modified stainless steel, GOPTS, and not chlorinated 6 bilayers would serve as controls.

3.2.10 Atomic Force Microscopy

Mirror polished stainless steel samples were prepared as described previously for this analysis. Atomic Force Microscopy (AFM) was used to evaluate the roughness and surface morphology of the modified stainless steel samples with a Dimension 3100

Atomic Force Microscope (Digital Instruments, Inc., Santa Barbara, California). Tapping mode tips (Veeco, phosphorus n-doped Si, f_0: 312 – 342 kHz) were used on cantilevers having a resonance frequency in the range of 290 – 410 kHz. AFM images were flattened, filtered, and analyzed through the SPIP software (Scanning Probe Image Processor, Image Metrology, Denmark).

3.2.11 Statistical analysis

One-way analysis of variance (ANOVA) followed by Tukey's pairwise comparisons was conducted between treatments using Minitab version 16.1.1 (Minitab Inc., State College, PA) with a confidence interval of 95%. As appropriate, regression analysis was also evaluated at a 95% confidence interval.

3.3 Results and Discussion

3.3.1 N-halamine activation and determination of chlorination

The ability of control and bilayer N-halamine modified stainless steel to complex with chlorine after contact with 3000 ppm sodium hypochlorite was quantified by a modified DPD assay (Figure 3.4). No chlorination was observed for the GOPTS treated stainless steel, as expected. The Control (clean stainless steel) treatment exhibited trace chlorination, likely due to hydrophilic behavior brought by the piranha solution, however this trace chlorination was not significantly different from GOPTS treated ($P > 0.05$). The

level of N-halamine content increased with increasing bilayer deposition, with a quadratic relationship from 1 to 6 bilayers ($P > 0.05$).

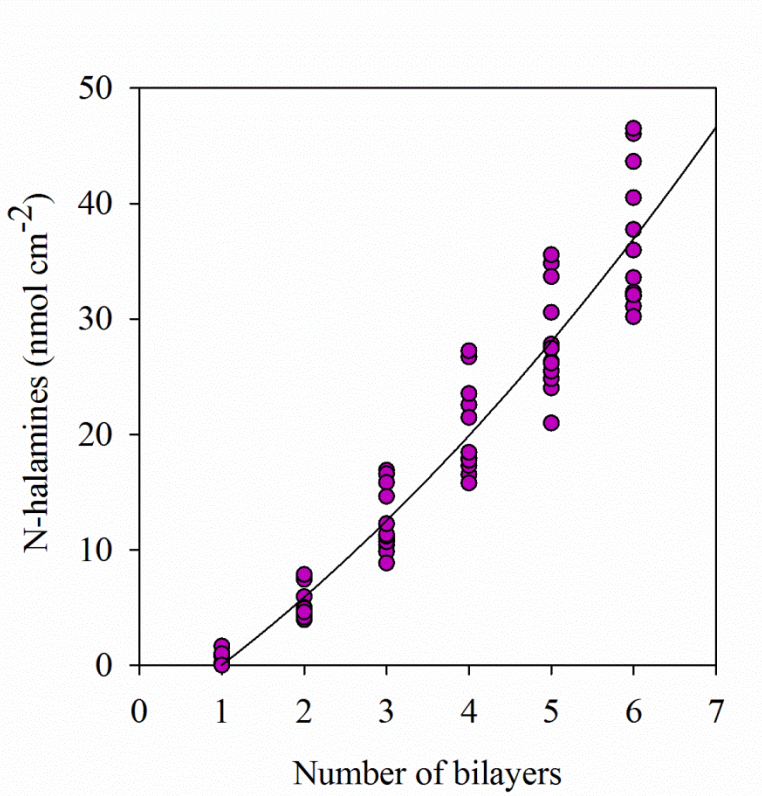

Figure 3.4 Relationship observed between the N-halamine content and the number of covalently bound bilayers (data points represent the results of 3 replicates).

3.3.2 Contact angle

Water contact angles (advancing, receding, and hysteresis) were measured for control and modified steel to determine the effect of N-halamine bilayer deposition on wettability (Table 3.1). The only treatment that exhibited significantly different advancing contact angle (θ_A) ($P < 0.05$), when compared to the rest of the treatments was GOPTS treated. Such behavior can be attributed to the hydrophobic nature of GOPTS,

which made the stainless steel surface have a higher value of θ_A compared to the rest of the treatments. None of the treatments of steel modified with N-halamine forming bilayers (one to six bilayers) was significantly different from the Control in θ_A. However, the values of θ_A for 1 bilayer and 3 bilayers were significantly different ($P < 0.05$), suggesting an increase in hydrophilicity as the number of bilayers increases from 1 to 3. It is likely that the hydrophobic influence of the underlying GOPTS monolayer is more evident with only a single bilayer than when several bilayers are immobilized. None of the treatments of steel modified with N-halamine forming bilayers was significantly different from the Control in θ_R ($P > 0.05$). As observed with θ_A, and the only treatment significantly different from the rest was that of GOPTS treated steel ($P < 0.05$). A substantial variability was observed from the bilayer modified steel in the measured values of θ_A and θ_R. The more heterogeneous or rough a surface is, the more evident the fluctuations among contact angle measurements will be (Long and Chen 2006). The reason behind this phenomenon may be related to a non-uniform distribution of the introduced chemical species on the substrate's surface (stainless steel in this case), creating zones of varying hydrophilic or hydrophobic nature (Adamson AW 1997; Makamba and others 2005). Such lack of uniformity may also explain the observed variability in the values of *H*. Some areas in the sample may exhibit a higher tendency to absorb water, whereas other areas will tend to repel it. Additionally, surface topography can also increase or decrease adsorption of water, which relates to the surface roughness. Hence, the effect in wettability caused by a change in surface chemistry can be amplified by an irregular surface, leading to a less predictable behavior in *H* (Drelich and others 2011).

Table 3.1 Advancing and receding water contact angle, and contact angle hysteresis.

Treatment	Advancing Contact Angle θ_A (Degrees)	Receding Contact Angle θ_R (Degrees)	Contact Angle Hysteresis H (Degrees)
Control	$37.1 \pm 4.5^{ac*}$	33.8 ± 4.0^{a}	3.3 ± 0.7^{a}
GOPTS	65.0 ± 3.0^{b}	55.1 ± 7.3^{b}	9.9 ± 4.4^{b}
1 bilayer	41.0 ± 3.6^{a}	34.3 ± 3.4^{a}	6.7 ± 1.2^{ab}
2 bilayers	27.4 ± 6.8^{ac}	23.7 ± 5.9^{a}	3.6 ± 1.7^{a}
3 bilayers	23.6 ± 4.9^{c}	20.0 ± 5.0^{a}	3.6 ± 0.8^{a}
4 bilayers	27.8 ± 0.9^{ac}	23.4 ± 0.6^{a}	4.5 ± 1.1^{a}
5 bilayers	32.5 ± 12.1^{ac}	27.2 ± 10.6^{a}	4.5 ± 1.5^{ab}
6 bilayers	28.6 ± 3.9^{ac}	23.7 ± 4.4^{a}	5.0 ± 0.6^{ab}

*Values are means of 3 replicates ± 1 SD. Treatments with the same letter within the same column are not significantly different ($P > 0.05$).

3.3.3 Fourier Transform Infrared Spectroscopy (FTIR)

The results from grazing angle FTIR analysis confirmed that the surface of the treated stainless steel possessed increasing quantities of N-halamines with increasing bilayer deposition. Figure 3.5 shows representative spectra from 0 (GOPTS treated) to 6 bilayers in the range from 1875 to 1365 cm^{-1}, which includes absorbance bands characteristic of amine, amide, and carbonyl functionalities. A characteristic band was observed at around 1535 cm^{-1}, which can be attributed to the N–H bond in plane bend of secondary amides. An increasing absorbance in this band suggests the formation of covalent bonds between the primary amines of PEI and the carboxylic acid groups of PAA, an important observation which supports the covalent nature of the N-halamine modification of stainless steel. A more subtle band was observed at about 1638 cm^{-1}, which corresponds to the scissors vibration of primary amines. Another band formed at about 1680 cm^{-1}, which can be related to the C=O stretch of secondary amides. At about 1750 cm^{-1}, a band was exhibited which may suggest the formation of acid anhydrides.

The chlorine from unreacted EDC-HCl may have favored the formation of acid anhydrides, which can form from the condensation of the polar heads of two carboxylic acids in the presence of chlorine. A less evident band was seen at 1420 cm^{-1}, belonging to the O–H bond in plane bend of carboxylic acids (Smith 1999). The area beneath the spectra in the range of 1680 – 1395 cm^{-1} was calculated for stainless steel modified with one to six bilayers (Figure 3.6). The area in the chosen range was observed to increase with a quadratic relationship ($P < 0.05$) as the number of bilayers increased. This observation is in good agreement with prior FTIR analysis of PEI attached to steel, which show characteristic bands in the 1200 – 1600 cm^{-1} range (Plagge and others 2007).

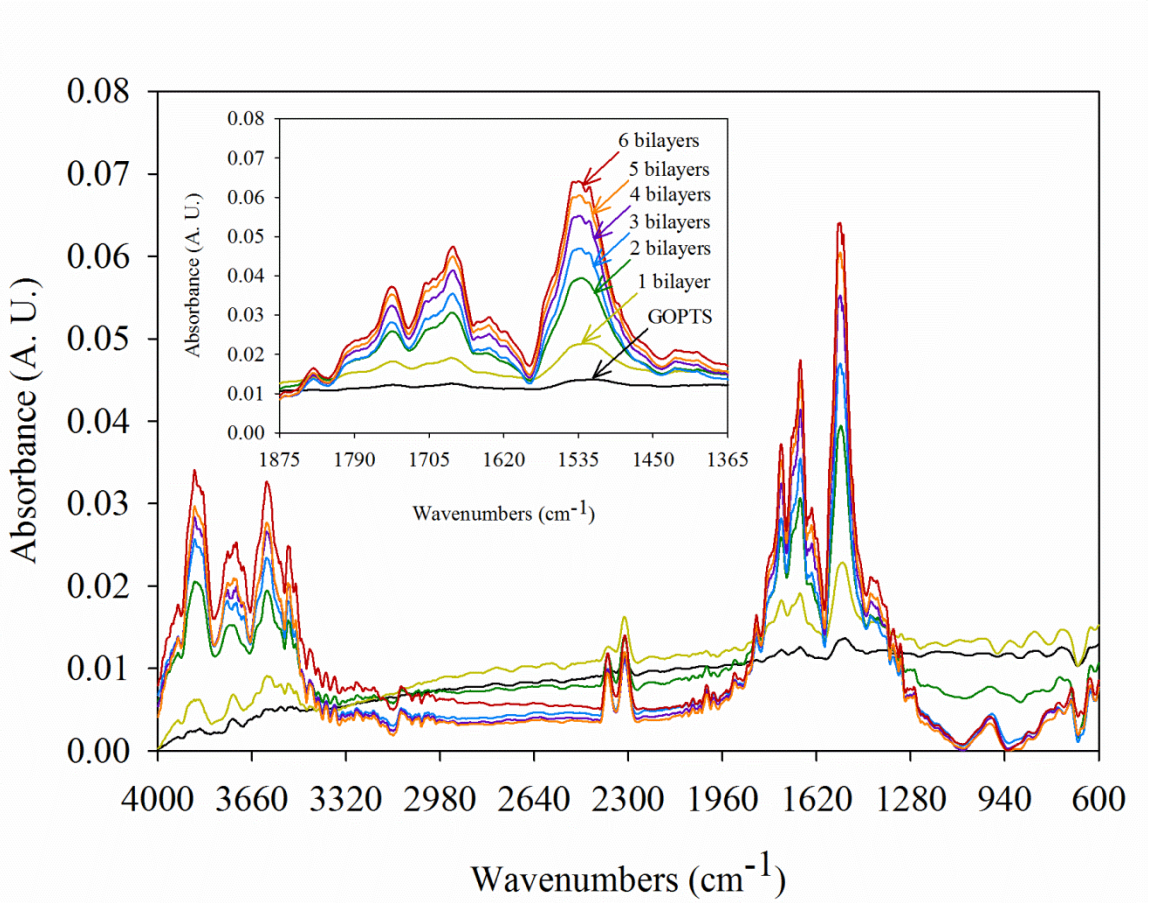

Figure 3.5 Representative FTIR spectra between 1875 to 1365 cm^{-1} of GOPTS treated steel to steel modified with up to six N-halamine forming bilayers.

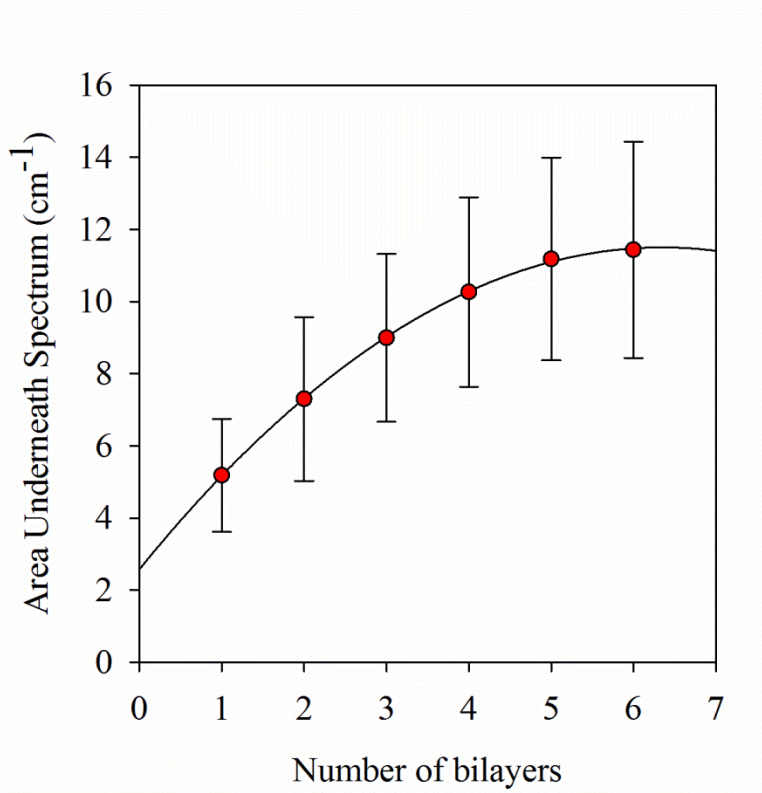

Figure 3.6 Relationship between the area beneath the spectra and the number of bilayers. Values are means of 3 replicates ± 1 standard deviation.

3.3.4 Ellipsometry

Spectroscopic ellipsometry was performed to quantify the equivalent thickness of increasing numbers of N-halamine forming bilayers after deposition onto stainless steel (Figure 3.7). A non-linear behavior was observed between the number of bilayers and the increasing thickness, in which a substantial increase in thickness took place from 3 to 4 bilayers. From 4 to 6 bilayers, there was a notably less pronounced increase in the corresponding thickness with deposition of each sequential bilayer. Different phenomena can explain this condition. From 1 to 3 bilayers, a higher proportion of reactive groups from the PEI and/or PAA polymers may have bound with available surface groups on the

stainless steel substrate, leaving fewer groups available for ionization and/or swelling which leads to a less pronounced increase in thickness. This would imply that the behavior shown by the increase in thickness as the number of bilayers increases depends not only on the amount of PEI or PAA deposited, but in the spatial arrangement in which such deposition takes place. At the pH of the phosphate buffer used (7.8), most of the carboxylic acids of PAA have a negative charge ($pK_a \approx 4.8$) (Guzman and others 2011a). On the other hand, above a pH of 3, about 70% of the amine groups of PEI are protonated (Zhao and others 2005). It can be assumed that as more available sites of interaction are formed (after having covered must of the substrate's surface), and more positively charges from PEI are exposed, more negatively charged PAA chains will diffuse and be attracted to the previously added PEI chains by electrostatic interactions, leading finally to the formation of covalent bonds. This phenomenon may be another reason behind the observed behavior in the increase of thickness. Additionally, a non-linear growth in the thickness of polymer bilayers can be explained by the reorganization and interdiffusion of any of the polymers within bilayer system. Another possible phenomenon is the formation of "islands" from the application of the first layer or bilayer, instead of a uniform layer. Such islands can later join together (coalesce) as more layers of polymers are deposited. This has been observed in previous works involving layer-by-layer deposition of PEI and PAA, which suggests an increase in roughness from the formation of such islands with increasing number of deposited multi layers (Tsukruk and others 1997; Guzman and others 2011b).Our observations on bilayer thickness as determined by ellipsometry are also in good agreement with previously published work. Deposition of

carbon nanofibers in four PEI/PAA bilayers on polyurethane foam resulted in a total thickness of 87 nm (Kim and others 2011).

A power relationship was found between area beneath spectra / thickness and number of bilayers (Figure 3.8). This behavior may support the idea of the initial formation of "islands" in the surface of the substrate, which represent a low initial concentration of the chemical species attached. However, the average initial thickness is low if it is correlated with the initial concentration of the polymers. Such ratio decreases as the number of bilayers increases (at least in the analyzed range), as the thickness raises in a non-linear behavior.

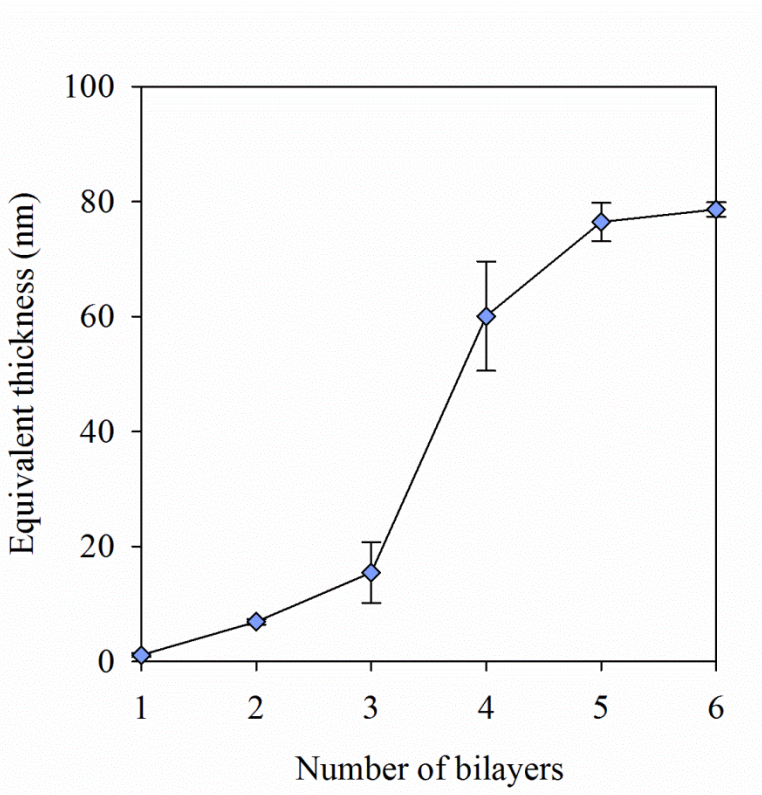

Figure 3.7 Thickness of N-halamine forming bilayers as determined by spectroscopic ellipsometry. Values are means of 3 replicates ± 1 standard deviation.

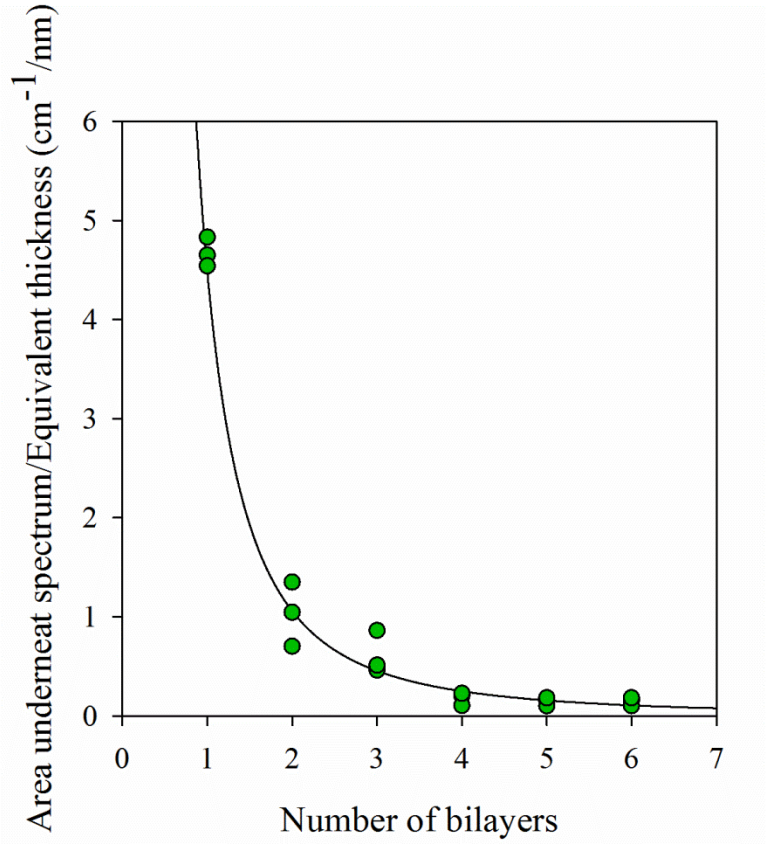

Figure 3.8 Relationship found between the ratio of the area underneath spectra and the equivalent thickness and number of bilayers (data points represent the results of 3 replicates).

3.3.5 Acid Orange 7 (AO7) dye assay

An increase in the primary amine content was observed as the number of bilayers increased (Figure 3.9), proportional to the increase in N-halamine chlorination (Figure 3.3). N-halamines are capable of forming on amines (both primary and secondary), amides, and imides, with amines reported to stabilize the N-halamine:halogen complex most strongly (Eknoian and others 1998). Branched PEI has a ratio of primary, secondary and tertiary amines of 1:2:1. Our results suggest that approximately 50% of the available

amines on the PEI component of each bilayer were able to complex chlorine as antimicrobial N-halamines.

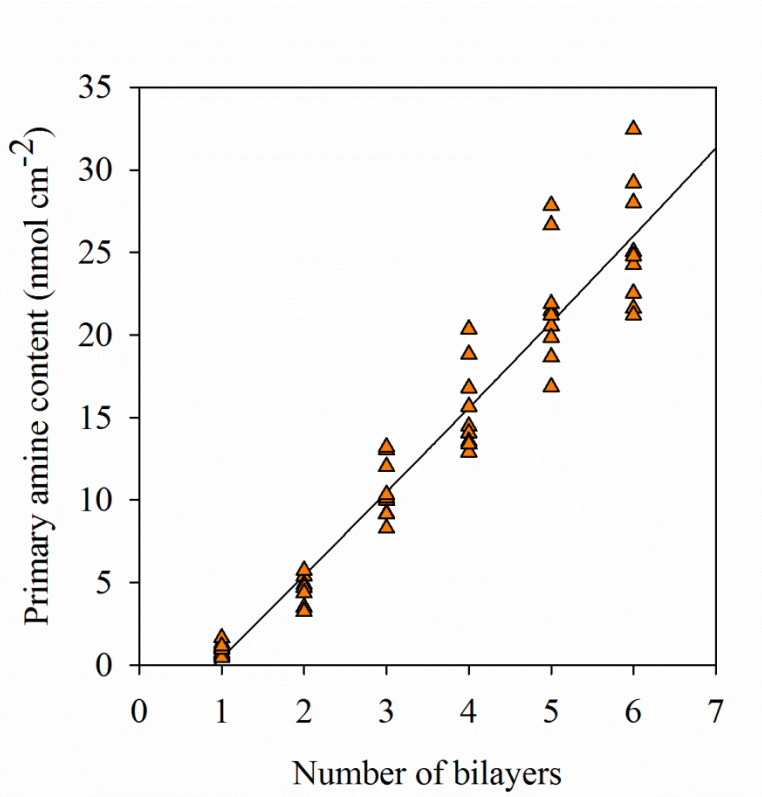

Figure 3.9 Relationship observed between the primary amine content and the number of covalently bound N-halamine forming bilayers from 1 to 6 bilayers (data points represent the results of 3 replicates).

3.3.6 X-ray photoelectron spectroscopy (XPS)

XPS survey scans as well as high resolution C 1s and Si 2p spectra were performed to quantify the change in surface atomic composition and specific bond formation after stainless steel was surface modified by GOPTS treatment and with each layer-by-layer bilayer deposition (Table 3.2). The oxidation of stainless steel in the control samples as a result of piranha treatment was confirmed by the high oxygen

percentage. GOPTS treatment introduced 3.48% Si, as expected from successful silanization. At an incidence angle of 45°, the applied beam has an analysis depth of approximately 2.5 nm, whereas the first bilayer of PEI and PAA was determined by ellipsometry to present a thickness of ~ 1.1 nm. As such, it is expected that the 1 bilayer atomic composition will contain a small amount of silicon and chromium, as observed, as the beam is interrogating the underlying GOPTS. From two to six bilayers however, the overall thickness comprised of PEI/PAA exceeds the XPS sampling depth of 2.5 nm, and the resulting atomic compositions are expected to be similar for each increasing bilayer. Our experimentally determined atomic compositions support this hypothesis. The values obtained closely approximated the theoretical proportion of carbon, oxygen and nitrogen present in a mixture of equal amounts of PEI and PAA (neglecting the presence of hydrogen, which is undetectable by XPS) and taking into account their monomeric formulas:

$–(C_2H_4NHC_2H_4N(C_2H_4NH_2)C_2H_4NH)_n–$ for PEI and $–(CH_2CH(COOH))_n–$ for PAA. Theoretical atomic percentages are calculated as follows: 52.5% C, 22% O, 16% N, and 9.5% H (58% C, 24.3% O, and 17.7% N taking only C, O and N into account).

Table 3.2 Representative atomic concentrations obtained from XPS (%).

Treatment	C	N	O	Si	Cr	Mn	Co	S	Mo
Control	17.5		55.2		10.6	3.2	5.1	4.9	3.5
GOPTS	32.0		54.7	3.5	4.2		3.3		
1 bilayer	54.6	8.7	32.2	1.8	2.7				
2 bilayers	67.5	11.4	21.1						
3 bilayers	67.8	13.7	18.5						
4 bilayers	67.4	12.6	20.1						
5 bilayers	65.7	13.7	20.6						
6 bilayers	66.7	12.9	20.4						

Figure 3.10 shows representative survey XPS spectra obtained from Control, GOPTS treated, single bilayer, and 2 – 6 bilayer modified stainless steel. Table 3.3 displays the relative percentages of the chemical species found from the high resolution spectra of C 1s and Si 2p in the evaluated treatments.

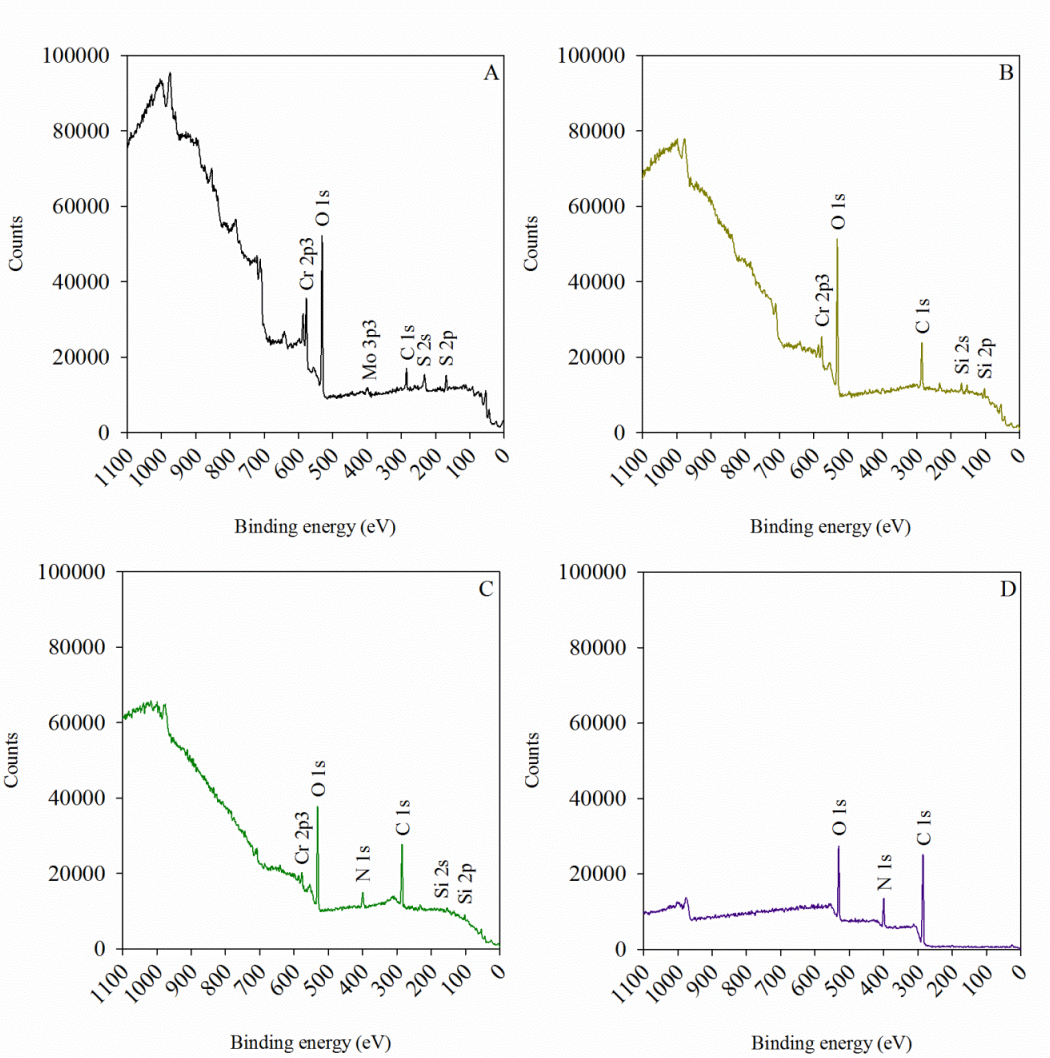

Figure 3.10 Representative survey XPS spectra of Control (A), GOPTS modified (B), single bilayer modified (C), and characteristic spectrum from 2 – 6 bilayer modified stainless steel (D).

Table 3.3 Representative relative percentages obtained from the deconvolution of high resolution C 1s and Si 2p XPS spectra.

	C 1s				
Treatment	285 – 284 eV (C–C/C–H)	287 – 286 eV (C–O)	288 – 287 eV (C=O/ O–C=O)	286 – 285 eV (C–N/C–O)	288 – 287 eV (N–C=O/ O–C=O)
Control	65.7	22.3	12.0		
GOPTS	51.7	38.0	10.4		
1 bilayer	50.6			33.6	15.8
2 bilayers	54.6			26.9	18.5
3 bilayers	50.9			29.2	20.0
4 bilayers	56.2			22.4	21.4
5 bilayers	57.3			22.7	20.0
6 bilayers	53.8			25.3	21.0
	Si 2p				
Treatment		102 – 101 eV (Si–O–C)		102 – 101 eV (Si–O–Si)	
Control					
GOPTS		91.6		8.4	
1 bilayer		79.0		21.0	
2 bilayers					
3 bilayers					
4 bilayers					
5 bilayers					
6 bilayers					

For the case of the Control and GOPTS treatments, the deconvolution of the high resolution spectrum of C 1s exhibited the presence of the chemical species C–C/C–H, C–O, and C=O/O–C=O, in the binding energy ranges of 284 – 285 eV, 286 – 287 eV, and 287–288 eV, respectively (Figure 3.11 A and 3.11 B). The deconvolution of the high resolution spectrum of Si 2p showed two bands of which the highest values fell approximately at 102 – 101 and 104 – 103 eV, corresponding to the chemical species of Si–O–C and Si–O–Si, respectively (Figure 3.11 C). This demonstrates the formation of the covalent bond between the substrate (stainless steel) and GOPTS, as well as the formation of covalent bonds between molecules of GOPTS. After piranha solution treatment, –OH groups are formed, which are able to react with GOPTS forming covalent bonds after curing. Then, the covalently attached molecules of GOPTS are able to

crosslink with themselves. The high resolution spectrum of C 1s from the treatments with 1–6 bilayers presented 3 bands from its deconvolution, and that can be attributed to the chemical species C–C/C–H, N–O/C–O, and N–C=O/O–C=O/C=O, in the ranges of 284 – 285 eV, 285 – 286 eV, and 287 – 288 eV, respectively (Figure 3.11 D). Similar results have been observed in previous studies involving the interaction between PEI and substances containing carboxylic acids, as well as in studies involving GOPTS and its incorporation in oxidized surfaces (Makamba and others 2005; Ma and others 2006; Pollock and others 2007). This confirms the formation of amides from the reaction between the carboxylic acid groups of PAA and the primary amines of PEI. Overall, the XPS results support those of grazing angle FTIR. When interpreted in parallel with the ellipsometry data, the experimentally determined atomic percentages gained by XPS analysis closely match theoretical atomic percentages of the predicted surface chemistry, suggesting that the desired layer-by-layer N-halamine surface modifications were successfully achieved.

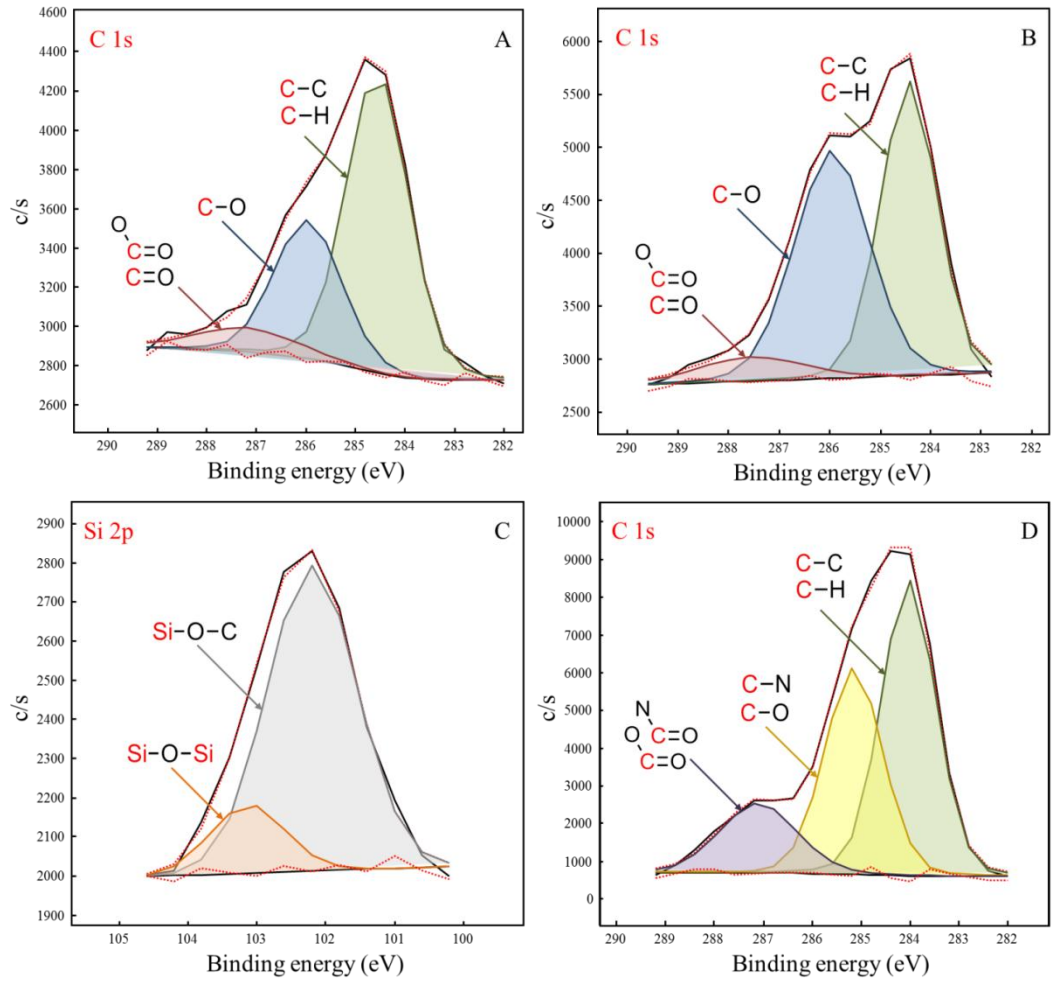

Figure 3.11 Representative deconvoluted high resolution XPS spectra. A and B represent the high resolution spectra of C 1s from Control and GOPTS modified steel, respectively; C represents the high resolution spectrum of Si 2p (GOPTS treatment); D shows a representative high resolution C 1s spectrum of stainless steel modified by deposition of 1 to 6 N-halamine forming bilayers.

3.3.7 Antimicrobial activity assay

Table 3.4 shows the results of the antimicrobial activity assay. As it can be seen, coupons having 6 bilayers were the only ones able to reach inactivation below the limit of detection (Figure 3.12), generating a reduction of more than 3 logarithmic cycles (> 99.9% reduction). What is remarkable about this method is that it contrasts with the

commonly used approach employed in previous works about modified surfaces with N-halamines, in which a very small volume of bacterial suspension is put in contact with a proportionally very large surface area of modified material (Sun and others 2001; Williams and others 2005; Tan and Obendorf 2007; Kou and others 2009; Cerkez and others 2011; Lee and Whang 2011; Kocer and others 2011a; Kocer and others 2011b; Ren and others 2013).

Table 3.4 Antimicrobial activity assay results.[*]

Treatment	Time (h)	Log (CFU mL^{-1})
Bacterial suspension	2	6.15 ± 0.09^{a}
	4	6.14 ± 0.52^{a}
Control stainless steel	2	5.64 ± 0.32^{ab}
	4	5.60 ± 0.48^{ab}
GOPTS	2	5.99 ± 0.21^{ab}
	4	5.94 ± 0.10^{ab}
Not chlorinated 6 bilayers	2	6.00 ± 0.26^{ab}
	4	6.15 ± 0.14^{a}
1 bilayer	2	5.70 ± 0.60^{ab}
	4	5.89 ± 0.32^{ab}
2 bilayers	2	6.01 ± 0.06^{ab}
	4	5.62 ± 0.25^{ab}
3 bilayers	2	5.70 ± 0.21^{ab}
	4	5.67 ± 0.53^{ab}
4 bilayers	2	5.17 ± 0.18^{ab}
	4	5.15 ± 0.13^{b}
5 bilayers	2	5.18 ± 0.19^{b}
	4	5.17 ± 0.20^{b}
6 bilayers	2	$< 2.00 \pm 0.00^{c}$
	4	$< 2.00 \pm 0.00^{c}$

[*]Values are means of 3 replicates ± 1 SD. Treatments with the same letter within the same column are not significantly different ($P > 0.05$).

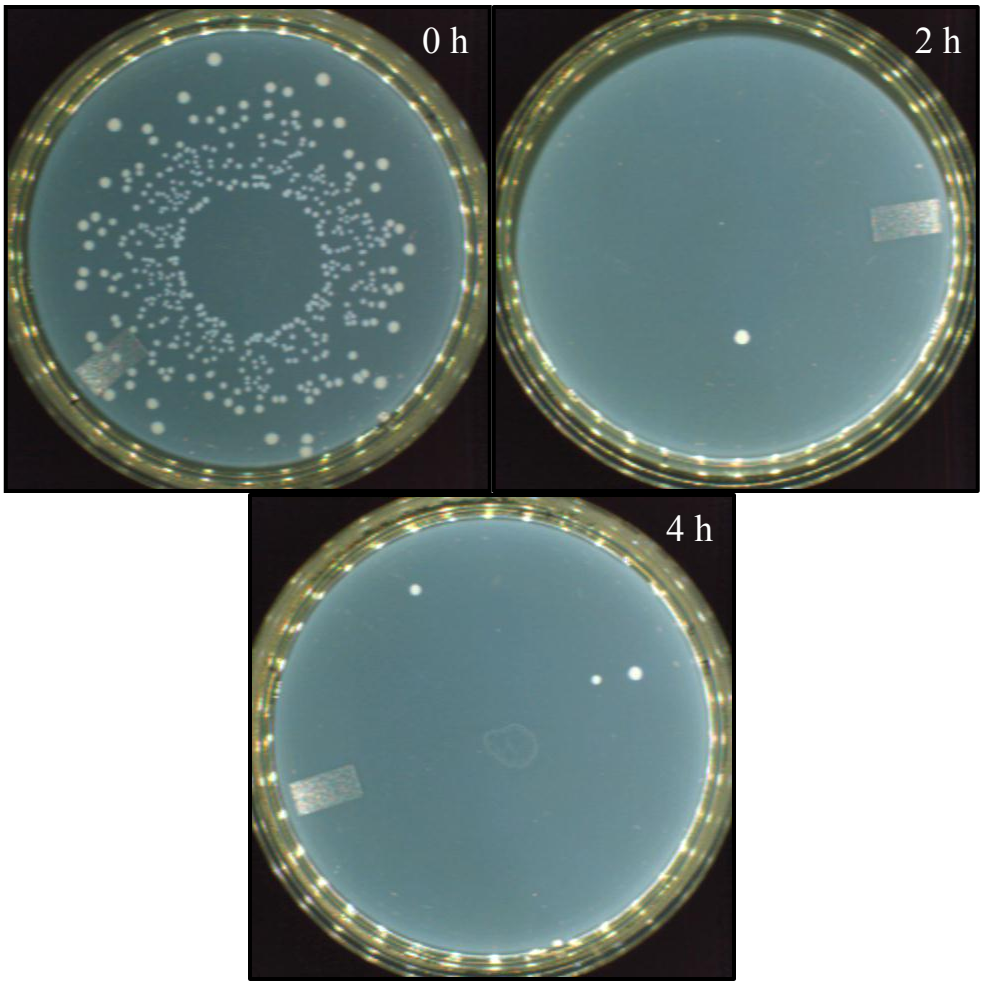

Figure 3.12 Petri dishes showing the reduction in microbial load given by 6 bilayers coupons after 2 and 4 h (bacterial suspension at time 0 plated as 10^{-3}, and at 2 and 4 h dilution plated as10^{-2}).

3.3.8 Atomic Force Microscopy

Figure 3.13 shows the images obtained from the AFM analysis. The results suggest the formation of isolated patches at the beginning of the deposition of bilayers of PEI and PAA. A non-uniform topography can be observed from 4 bilayers to 6 bilayers. The vertical axis (*Z* coordinate) divisions in the images represent 30 nm. This confirms the results obtained from ellipsometry. The values of roughness obtained were as follows (in nm): 5.656 (Control), 2.656 (GOPTS), 3.530 (1 bilayer), 5.851 (2 bilayers), 3.738 (3 bilayers), 11.143 (4 bilayers), 10.036 (5 bilayers), 13.384 (6 bilayers). This suggests a substantial increase in roughness as more bilayers are deposited, which can be related to the variability observed earlier in the contact angle analysis for the values of θ_A, θ_R and H.

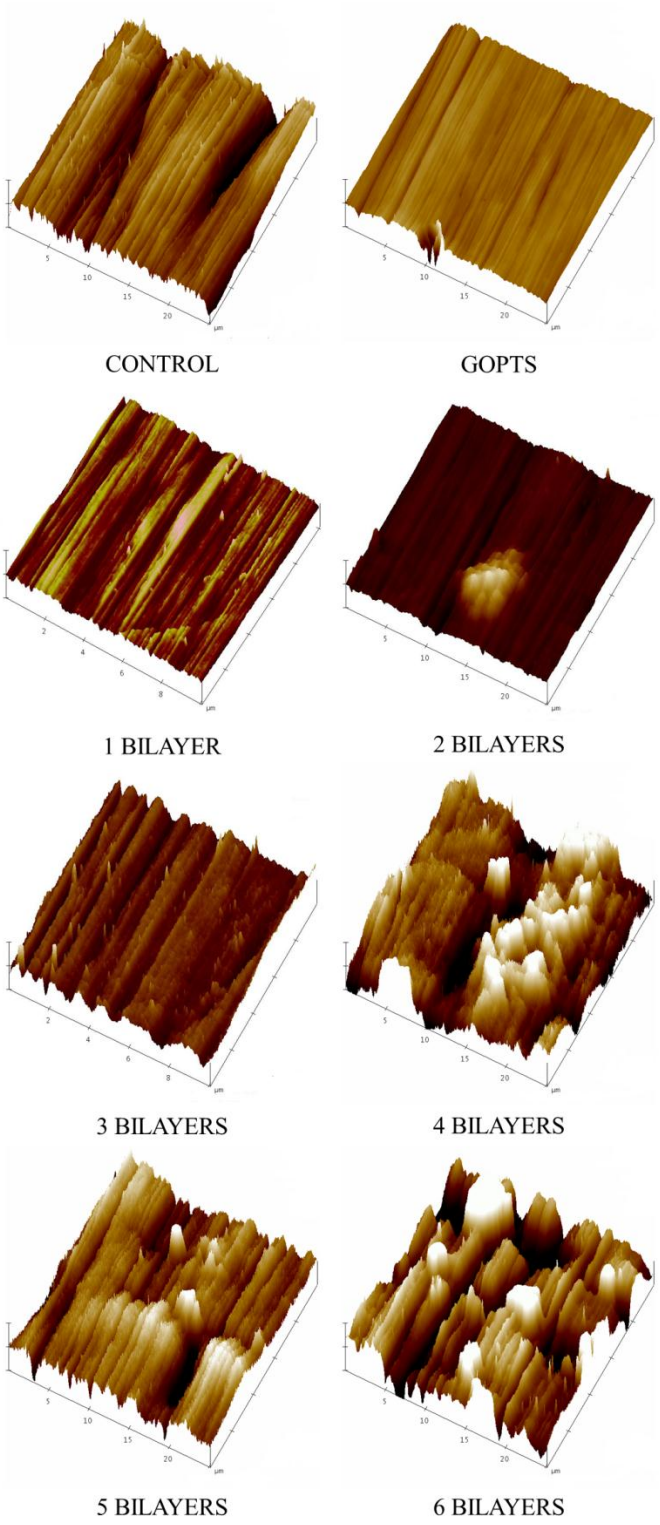

Figure 3.13 AFM analysis results.

3.4 Conclusions

We have demonstrated the ability to modify the surface of 316 stainless steel using a covalent layer-by-layer deposition of N-halamine forming PEI and PAA. Prior work demonstrated that using similar chemistry, a single bilayer of PAA-PEI immobilized onto polyethylene film surfaces exhibited significant antimicrobial activity (Goddard and Hotchkiss 2008). In addition to developing a surface modification technique to adapt such N-halamine modification to stainless steel, our goal in this work was to evaluate the influence of increasing bilayers on the number of available antimicrobial N-halamines. However, in order to retain bulk material properties, we wanted to limit the changes in surface chemistry to the top 100 nm or less. For this reason, we limited the number of bilayers evaluated in this study to six. Formation of covalent bonds was confirmed through FTIR and XPS between PEI and PAA, as well as the covalent attachment of GOPTS to the substrate's surface. Results of surface analysis in this work are in agreement with other reports in which PAA and PEI are immobilized onto supports in a layer-by-layer fashion.

Chlorination assays confirmed that the increasing quantity of amides and amines which present with increasing bilayer deposition were able to be chlorinated to form antimicrobial N-halamine moieties. The N-halamine modified steel with 6 bilayers demonstrated antimicrobial activity (> 3 logarithmic reductions or > 99.9% reduction in viable organisms) against *L. monocytogenes*, an important food borne pathogen.

3.5 Acknowledgements

This material is based upon work supported by the National Institute of Food and Agriculture, U.S. Department of Agriculture under project number 2011-65210-20059 and in part by the Center for Hierarchical Manufacturing at UMass Amherst, an NSF Nanoscale Science & Engineering Center supported by the National Science Foundation under NSF Grant No. CMMI-0531171. The authors would also like to thank Prof. D. Julian McClements for use of his Krüss DCA for contact angle analysis, Prof. Lynne McLandsborough for assistance with antimicrobial activity assays, Prof. Dr. Thomas J. McCarthy and Jacob Hirsch for use of their Rudolph SLII for ellipsometry measurements and their Physical Electronics Quantum 2000 for XPS analysis, and Dr. Sekar Dhanasekaran for assistance and use of his Dimension 3100 Atomic Force Microscope.

CHAPTER 4

INACTIVATION OF LISTERIA MONOCYTOGENES ON A POLYETHYLENE SURFACE MODIFIED BY LAYER-BY-LAYER DEPOSITION OF THE ANTIMICROBIAL N-HALAMINE[3]

4.1 Abstract

Modification of food contact surfaces to be antimicrobial represents an approach to address the problem of cross-contamination in the food industry. The effect of increasing levels of surface modification on low density polyethylene (LDPE) through application of N-halamines on the inactivation kinetics of *Listeria monocytogenes* Scott A was evaluated. Increasing levels of modification were applied through layer-by-layer deposition on LDPE surface (1 to 5 bilayers of polyethyleneimine and poly(acrylic acid)). Surface modification was achieved and confirmed through Fourier transform infrared spectroscopy (FTIR). From 1 to 5 bilayers, the N-halamine content ranged from 3.42 ± 1.2 to 27.30 ± 3.5 nmol cm^{-2}. More than 4 logarithmic cycles (> 99.99%) reduction was reached against *L. monocytogenes* Scott A after different contact times depending on the level of modification, that varied from 50 to 110 minutes (from 5 to 2 bilayers). Inactivation kinetics followed a sigmoidal behavior. A reusability evaluation was performed with coupons having 5 bilayers. The coupons were able to inactivate in more than 4 logarithmic cycles the initial microbial load in the first 2 cycles, but from the third cycle the antimicrobial activity had been lost. FTIR analysis exhibited loss of the applied bilayers after 5 cycles. Then, another regeneration study was carried on in which coupons

[3] Submitted to Journal of Food Engineering.

with 5 bilayers were chlorinated, dechlorinated and rechlorinated for 10 cycles using 2 concentrations of chlorine (200 and 3000 ppm), for a shorter period of time for chlorination (5 min). FTIR results showed a less detrimental effect on the surface chemistry from using a shorter chlorination time.

Keywords: N-halamines, surface treatment, layer-by-layer deposition, surface modification, inactivation kinetics, antimicrobial materials.

4.2 Introduction

Cross contamination of pathogenic microorganisms from food contact surfaces continues to be a concern in the food industry in terms of both the potential health risk and financial burden (Centers for Disease Control and Prevention 2003; Centers for Disease Control and Prevention 2004). Surfaces on which food products get in contact during the production process (conveyor belts, work tables, processing equipment, and so on) are probably the most common source of cross contamination, since different pathogenic microorganisms exhibit ability to adhere to such surfaces and form stable biofilms. This increases their resistance against different methods of disinfection, such as the application of chemicals and heat (Maukonen and others 2003; McLandsborough and others 2006; Simões and others 2010; Møretrø and Langsrud 2011). Polyethylene is one of the most versatile polymers, with broad applicability in the food industry. It can be found in pipes, tubing, fittings, trays, industrial containers, industrial sheets (conveyor belts) and so on (Carraher 2010).

Listeria monocytogenes (*L. monocytogenes*) is a well-known foodborne pathogen of special concern among the vulnerable population. It is able to survive and grow under refrigeration temperatures. Additionally, some strains are able to survive milk pasteurization, present adaptability to diverse environments, tolerance to salts and acids, and competitiveness against other microorganisms (Elkest and Marth 1988b). For these reasons, *L. monocytogenes*, is a good target microorganism for evaluation of new antimicrobial materials technology (Jin et. al., 2009).

In the food industry, hypochlorites are highly effective disinfectants, able to inactivate a wide range of microorganisms. In addition, they don't represent a risk against humans at the concentrations normally applied (0.6 – 200 ppm), are cheap and easy to use. They are the most common source of chlorine as a disinfectant. Sodium hypochlorite (NaClO) is probably the most common choice. It decomposes into hypochlorous acid (HClO) and sodium hydroxide (NaOH) in aqueous solutions. HClO is thought to provide the germicidal effect by entering the cell's cytoplasm, and once there, a possible liberation of nascent oxygen provokes cell's death. Other possible inactivation mechanisms include enzymatic inhibition and cell wall disruption (Elkest and Marth 1988a).

N-halamines are halogenated nitrogenous structures with antimicrobial activity. The most common halogen used to generate N-halamines is chlorine, and they can be chlorinated with NaClO solutions. Iodine and bromine also form N-halamine structures. In addition to inactivating microorganisms, a unique feature of N-halamines is their ability to be reused repeatedly; the halogen atom is released in presence of organic matter and/or microorganisms, inactivates them, and the N-halamine structure can be regenerated after subsequent exposure to a halogen solution (Eknoian and others 1998). This class of antimicrobials has been used in different applications such as water filtration systems, disinfectants in pools, fabrics for clothing, and so on (Worley and Sun 1996). However, their potential application in the food industry has not been explored extensively (Goddard and Hotchkiss 2008; Bastarrachea and Goddard 2013). The effectiveness of N-halamines has been evaluated by applying them in a variety of materials (Worley and others 2003; Williams and others 2005). Their concept is

promising given the fact that chlorine is prone to react with organic matter, which could be overcome by making it possible to be available from surfaces (and be regenerated) (Møretrø and Langsrud 2011).

Microbial inactivation has been usually assumed to be a process that exhibits first order kinetics, in which the number of microorganisms decreases exponentially with time (Peleg 2006). However, a number of studies have shown that this is not always the case (Linton and others 1996; Juneja and others 1997; Huemer and others 1998; Ingham and Uljas 1998; Penna and Moraes 2002; Van Boeijen and others 2008). To the best of our knowledge, no inactivation kinetics work has been reported on N-halamines. The objectives of the present work are to surface modify low density polyethylene (LDPE) with increasing levels (bilayers) of N-halamines, evaluate the chemical modification of their surface, challenge them against *L. monocytogenes*, and evaluate the effect of increasing levels of bilayers on the inactivation kinetics.

4.3 Materials and Methods

4.3.1 LDPE surface modification

Low density polyethylene (LDPE) was rendered antimicrobial by N-halamine surface modification using a layer-by-layer deposition process, modified from that reported in previous works (Goddard and Hotchkiss 2008; Bastarrachea and Goddard 2013). LDPE film with a thickness of 125 μm (kindly donated by Honam Petrochemical Corp., South Korea) was cut into 1 × 1 cm coupons and cleaned under sonication at 40

kHz, first with isopropanol (Fisher Scientific, Pittsburgh, PA), then with acetone (Fisher Scientific, Pittsburgh, PA), and finally with deionized (DI) water (2 cycles per solvent and 10 min per cycle). Then, the coupons were left drying overnight in a closed chamber at room temperature with a relative humidity (RH) of < 20%. Once dried, each side of the coupons was subjected to UV irradiation for 15 min with a Jelight Co. model 42 UVO Cleaner (Irvine, CA). After UV irradiation, the coupons were subjected to a layer-by-layer deposition process described as follows. Coupons were shaken at room temperature for 30 min in a 0.1 M phosphate buffer solution (pH 7.8) containing 5 mg mL^{-1} of branched polyethyleneimine (PEI, 25,000 Da, Sigma-Aldrich, St. Louis, MO), and the zero-length cross-linkers 1-(3-Dimethylaminopropyl)-3-ethylcarbodiimide hydrochloride (EDC-HCl, ProteoChem, Inc., Denver, CO) and N-hydrosuccinimide (NHS, Acros Organics, Fair Lawn, NJ) at a concentration of 50 and 5 mM (respectively). After rinsing in copious DI water, the coupons were immersed in a 0.1 M phosphate buffer solution (pH 7.8) containing 5 mg mL^{-1} of poly(acrylic acid) (PAA, 450,000 Da, Scientific Polymer Products, Inc., Ontario, NY) with the same concentrations of EDC-HCl and NHS, shaken for 30 min at room temperature and rinsed in copious DI water. The application of one layer of PEI and one layer of PAA would represent a single bilayer. The described procedure was repeated until completing 5 bilayers. After every bilayer application, coupons were selected at random to be used for further experiments, and left drying overnight in a dry chamber (RH < 20%). Once dried, coupons were stored in glass Petri dishes in the dark until usage. Figure 4.1 shows a scheme of surface chemistry of the N-halamine modified LDPE.

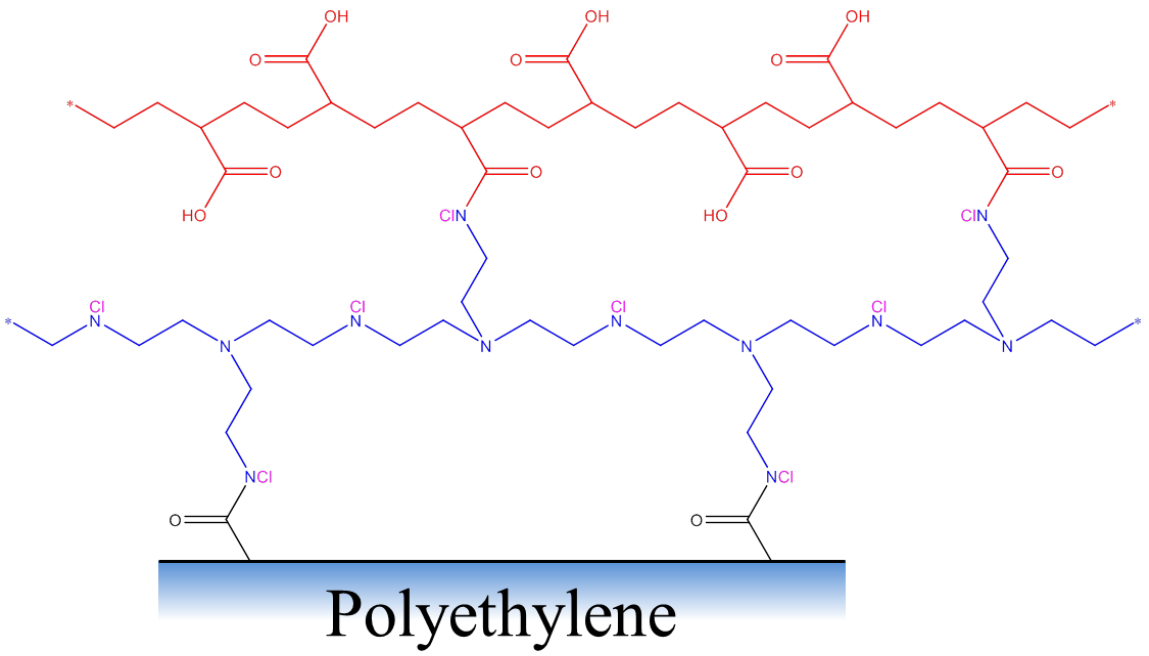

Figure 4.1 Scheme of a single chlorinated bilayer of PEI and PAA covalently attached onto LDPE (Goddard and Hotchkiss 2008; Bastarrachea and Goddard 2013).

4.3.2 N-halamine activation and quantification

An aqueous chlorine solution was prepared from DI water and a NaClO (bleach) solution containing 5% chlorine (Acros Organics, Fair Lawn, NJ). The concentration of chlorine in the bleach solution was confirmed by iodometric titration (American Society for Testing and Materials 2008). Modified and not modified (clean) LDPE coupons were immersed in a solution containing 3000 ppm of chlorine and shaken at room temperature for 15 min. Then, the coupons were rinsed in copious DI water to remove non-complexed chlorine. To determine the amount of chlorinated N-halamines on the coupons, a modified N,N-diethyl-p-phenylenediamine (DPD) assay was followed. Individual coupons from the different treatments were immersed in test tubes containing 2 mL of DI

water. DPD reagent was made by mixing one packet of DPD total chlorine reagent powder (Hach Company, Loveland, CO) with 1 mL of DI water. A volume of 50 μL of the DPD total chlorine reagent was applied to the 2 mL of DI water in contact with the coupons. Then, after shaking the coupons for 2 min for color formation, the absorbance of the solutions in the test tubes containing them was measured at 512 nm. The concentration of chlorine was determined from a standard curve prepared with solutions of known concentrations of chlorine. The N-halamine quantification was carried out by taking into account the exposed area of the coupons, the concentration of chlorine given by them, and the volume of the DI water in the test tubes. The results were expressed in nmol of chlorine cm^{-2}. Three replicates were done for every treatment, with 3 coupons per replicate.

4.3.3 Attenuated Total Reflectance Fourier Transform Infrared Spectroscopy (ATR-FTIR)

Changes in surface chemistry from the modified LDPE coupons (not chlorinated) were evaluated with an IRPrestige 21 spectrometer (Shimadzu Corp., Tokyo, Japan). For a total of 3 replicates, absorbance was measured in 3 different spots per coupon, and 3 coupons were analyzed per treatment. A resolution of 4 cm^{-1} and 32 scans were applied for every spot using Happ-Genzel apodization. Spectra from all the treatments were obtained from the IRsolution software (Shimadzu Corp., Tokyo, Japan) and analyzed with the Knowitall software (Biorad Laboratories, Philadelphia, PA). Quantitative analysis was done by calculating the area under representative bands from the collected spectra using the IRsolution software.

4.3.4 Inactivation kinetics study

L. monocytogenes Scott A (FSL-J1-225) bacterial suspensions used for testing were prepared as follows. Stock cultures were maintained in tryptic soy broth (TSB, Difco, Becton Dickinson, Sparks, MD) with 25% glycerol at -80 °C. One loopful of stock was inoculated onto tryptic soy agar (TSA, Difco, Becton Dickinson, Sparks, MD) by quadrant streak technique (in order to obtain individual colonies) and incubated at 37 °C for 24 h. Then, a single colony was inoculated in TSB and incubated overnight at 37 °C. Following overnight incubation, a 1:100 dilution from the overnight culture was prepared with new and sterile TSB, and incubated at the same temperature until reaching a microbial load of ~ 9 Log(CFU mL^{-1}), which was estimated by plating and confirmed by measuring optical density (OD) at 600 nm. After incubation, bacterial suspensions were prepared by diluting this culture with deionized water to have a microbial load of ~ 6 Log(CFU mL^{-1}).

Chlorinated coupons from all the treatments were challenged against *L. monocytogenes* Scott A as follows. Ten coupons from every treatment were put in contact with 1 mL of bacterial suspension and incubated at 32 °C with rotation at 60 rpm. This temperature was chosen because it is within the range of maximum effectiveness of chlorine against *L. monocytogenes* Scott A, 25 – 35 °C (Elkest and Marth 1988a). After 2 h, serial dilutions were prepared with neutralizing buffer (Difco, Becton Dickinson, Sparks, MD) and plated onto TSA with an automated spiral plater Autoplater 4000 (Spiral Biotech Inc., Norwood, MA). Bacterial suspensions with added volumes of soda bleach solution imitating the concentrations of chlorine given by the different treatments

would be used as positive controls. The positive controls were prepared by adding to the 1 mL of bacterial suspensions the necessary amount of diluted bleach solution to mimic the concentration given by the modified LDPE coupons in the same volume of deionized water (the concentrations are shown in Table 4.1). As negative controls, bacterial suspensions alone, bacterial suspensions with 10 coupons of not modified LDPE, and bacterial suspensions with 10 coupons of not chlorinated 5 bilayers LDPE were tested. TSA plates were incubated at 37 °C for 48 h. Colonies were counted with a plate reader Scan® 500 (interscience, Saint-Non-la-Brèteche, France) in a range of 30 – 300 colonies using the instrument's software. Colonies were also counted by manually inoculating 1 mL of the 10^{-1} dilution onto TSA in order to lower the detection limit. This antimicrobial evaluation was repeated 3 times (3 replicates). The detection limit was 10 CFU mL^{-1}.

For the inactivation kinetics study, those treatments that were able to reduce the microbial load in more than 4 logarithmic cycles (> 99.99%) from the antimicrobial evaluation were evaluated as follows. Using the same conditions as in the antimicrobial evaluation, test tubes containing ten coupons of the corresponding treatments were collected at different points in time. Dilutions were prepared and plated onto TSA as described above. After 48 h of incubation at 37 °C, colonies were counted with the same criteria. For every treatment, the inactivation kinetics evaluation was repeated 2 times (2 replicates). In order to compare the inactivation behavior given by positive controls, the same evaluation was conducted with bacterial suspensions containing the same amounts of chlorine given by the modified LDPE coupons.

4.3.5 Reusability and regeneration study

LDPE coupons having 5 bilayers that had been chlorinated using the same conditions explained before (3000 ppm of chlorine for 15 min) were subjected to up to 10 cycles of antimicrobial inactivation. The protocol followed was the same described in the previous section. A total of 10 coupons were put in contact with bacterial suspension having ~ 6 Log(CFU mL^{-1}), and incubated under the same conditions described previously (2 h, 32 °C, and with rotation at 60 rpm). Serial dilutions were prepared likewise and the corresponding TSA plates were incubated for 48 h at 37 °C. After the 2 h of incubation in an inactivation cycle, the coupons were rinsed with copious sterile DI water and rechlorinated to be put in contact with new bacterial suspension. The described procedure was repeated 10 times.

A regeneration study was also carried on with coupons having 5 bilayers as follows. Two chlorine concentrations were tested (200 and 3000 ppm). Individual coupons were chlorinated and dechlorinated 10 times in order to determine the final content of N-halamines, which was obtained through DPD assay.

Coupons from the two evaluations described were also subjected to FTIR analysis following the same protocol described in previously.

4.3.6 Data analysis

When appropriate, the general linear model analysis followed by Tukey's pairwise comparisons was conducted between treatments using Minitab version 16.1.1

(Minitab Inc., State College, PA) with a confidence interval of 95%. Linear regression analysis was also evaluated at a 95% confidence interval when appropriate. For the inactivation kinetics study, data points were fitted with the following sigmoid isothermal semi-logarithmic models (Peleg 2003; Peleg 2006):

$$\log\left(\frac{N}{N_0}\right) = -\frac{at}{(b+t)} - \frac{ct}{(d-t)} \quad (1)$$

$$\log\left(\frac{N}{N_0}\right) = -\frac{at}{(1+b)(c-t)} \quad (2)$$

Where N/N_0 is the momentary survival ratio, N_0 is the initial microbial population, N is the microbial population at a certain point in time, t is the time in min, and a, b, c and d are temperature dependent coefficients. Nonlinear regression analysis and equation solving was conducted using GraphPad Prism 5 version 5.04 (GraphPad software Inc., La Jolla, CA) and Mathematica 9.0.0.0 (Wolfram Research, Champaign, IL).

4.4 Results and Discussion

4.4.1 N-halamine activation and quantification

Prior work has demonstrated the ability to impart N-halamine antimicrobial activity on stainless steel using a layer-by-layer approach, and on polyethylene using a single layer. The results obtained here for multilayer modification of polyethylene with N-halamine forming polyelectrolytes are in accordance with what has been reported in

previous studies (Goddard and Hotchkiss 2008; Bastarrachea and Goddard 2013). A linear relationship ($P < 0.05$) was observed between the N-halamine content and the number of bilayers (Figure 4.2). Clean, unmodified LDPE presented no N-halamines, as expected from the absence of the nitrogenous structures, and the hydrophobic nature of LDPE. The content of N-halamines (in nmol cm^{-2}) given by the chlorinated samples from 1 to 5 bilayers is shown in Table 4.1, as well as the effective concentration of chlorine of 10 coupons of every treatment in a volume of 1 mL of DI water. The effective chlorine concentrations were calculated to determine chlorine concentrations to be added to bacterial suspensions to prepare the positive controls used in the antimicrobial evaluation.

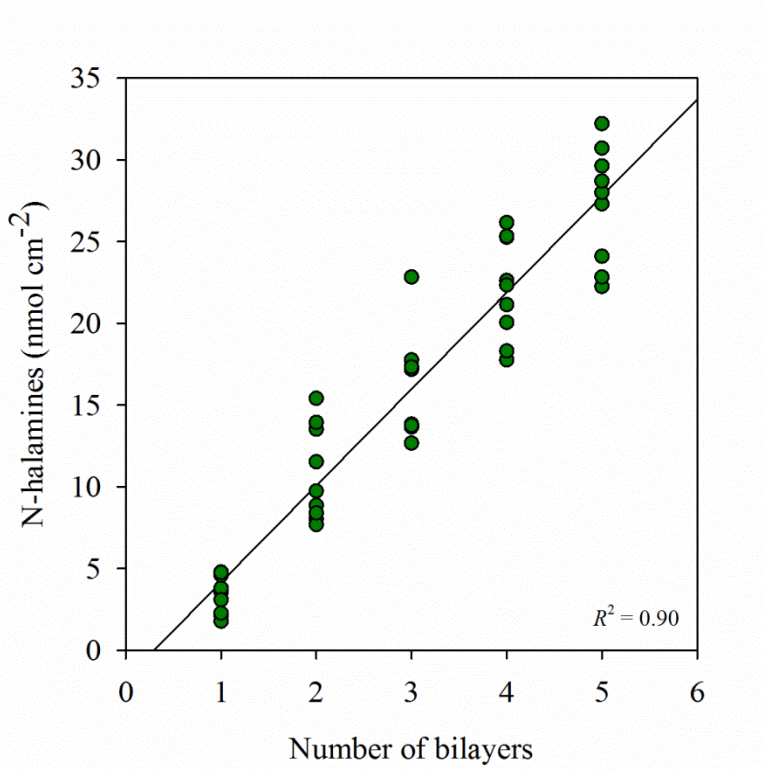

Figure 4.2 Relationship found between the N-halamine content and the number of bilayers.

Table 4.1 N-halamine content and chlorine concentration given by every treatment (values are average of 3 replicates ± 1 standard deviation).

Number of bilayers	N-halamine content (nmol cm^{-2})	Chlorine concentration (ppm)*
1	3.4 ± 1.2	2.4 ± 0.8
2	10.8 ± 2.9	7.7 ± 2.1
3	16.3 ± 3.2	11.6 ± 2.3
4	22.1 ± 3.1	15.7 ± 2.2
5	27.3 ± 3.5	19.4 ± 2.4

*Given by 10 coupons of the corresponding treatment in 1 mL of DI water.

4.4.2 Attenuated Total Reflectance Fourier Transform Infrared Spectroscopy (ATR-FTIR)

Surface chemical modification was confirmed through ATR-FTIR. Figure 4.3 shows the collected representative spectra from all the treatments. The formation of the carbonyl group can be seen from the representative spectrum given by LDPE after UV irradiation in the range between 1740 and 1720 cm^{-1}. Covalent bond formation between PEI and PAA is demonstrated from the band found in the range between 1570 and 1515 cm^{-1} exhibited by all the treatments with modified surface. This range corresponds to the N–H bond in plane bend from secondary amides. The presence of carboxylic acids from PAA is exhibited from the band found in the range between 1440 and 1395 cm^{-1}, characteristic of the O–H bond in plane bend of carboxylic acids. The observed region between 1650 and 1550 corresponds to the N–H bond of primary and secondary amines (scissor vibrations of the N–H bond and N – H bend, respectively). Finally, the increase in absorbance in the range between 1680 and 1630 can be attributed to the C=O stretch of secondary and tertiary amides (Smith 1999). Quantitative ATR-FTIR spectral analysis was performed using the area beneath the spectra in the absorbance range between 1800 and 1395 cm^{-1}. Figure 4.4 shows the relationship between the area beneath the spectra

and the number of bilayers. A linear relationship ($P < 0.05$) was found with a correlation slightly better ($R^2 = 0.95$) than that obtained by N-halamine quantification ($R^2 = 0.90$) (Figure 4.2). This improvement in correlation is expected, as FTIR analysis is a direct surface analysis technique, whereas N-halamine quantification by DPD analysis requires a secondary colorimetric assay with continuous color development. Nevertheless, FTIR and N-halamine quantification results are in agreement that increasing bilayer deposition resulted in increased number of antimicrobial N-halamines on the surface of modified LDPE.

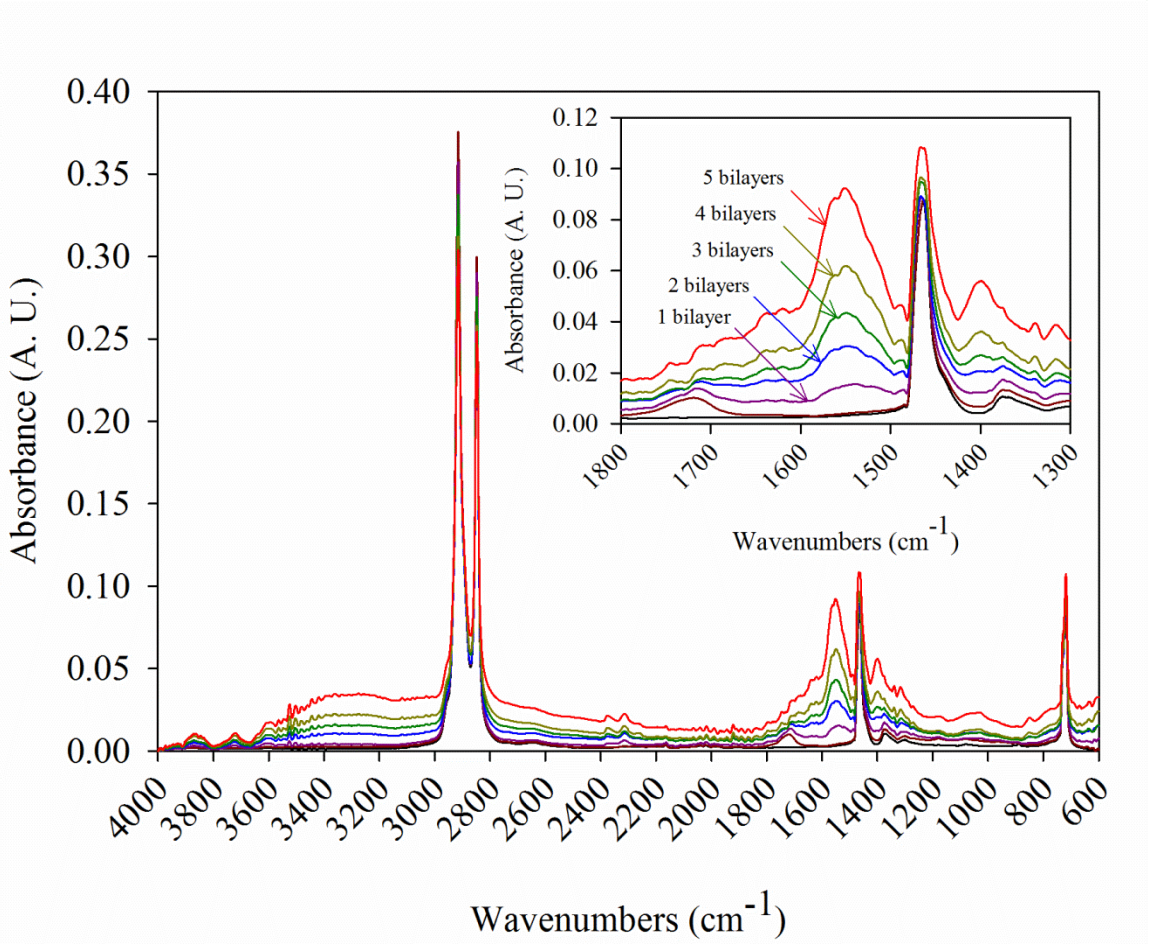

Figure 4.3 ATR-FTIR spectra from all the treatments (the two first spectra from bottom to top correspond to clean LDPE and UV irradiated LDPE, respectively).

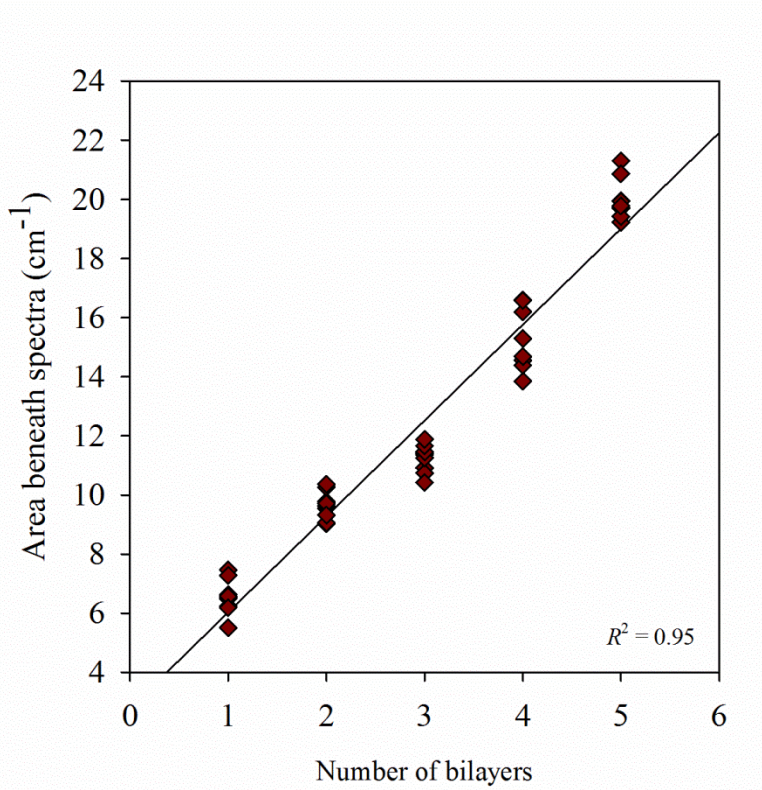

Figure 4.4 Relationship found between the area beneath the spectra and the number of bilayers in the range between 1800 and 1395 cm^{-1}.

4.4.3 Antimicrobial activity and inactivation kinetics study

Antimicrobial activity of control and N-halamine modified LDPE films are reported in Table 4.2, along with controls including bacterial suspension alone, LDPE that was N-halamine modified but not chlorinated, and finally positive controls corresponding to the equivalent amount of chlorine at each number of bilayers as determined in Table 4.1. Antimicrobial activity was determined by incubating 10 coupons of every treatment under 1 mL of *L. monocytogenes* Scott A suspension containing ~ 6 Log(CFU mL^{-1}) with rotation for 2 h at 32 °C. LDPE coupons with 1

bilayer, as well as their positive controls, exhibited a microbial load more than 1 logarithmic cycle lower than the control bacterial suspension. Treatments containing 2 or more bilayers (and their corresponding positive controls) were able to inactivate the initial load of *L. monocytogenes* Scott A under the limit of detection, providing more than 4 logarithmic reductions (> 99.99%) in 2 h. Clean LDPE and coupons containing 5 bilayers without chlorine had no inactivation effect. The lack of antimicrobial activity by modified, but not chlorinated, LDPE is important in establishing that the observed antimicrobial activity is specifically due to the chlorinated N-halamine structure, and that non-specific surface chemistry:microorganism interactions were not involved.

Table 4.2 Antimicrobial activity of control and modified LDPE (values are average of 3 replicates ± 1 standard deviation).

Treatment	Microbial load after 2 h (Log(CFU mL^{-1}))*
Bacterial suspension	5.94 ± 0.1^{a}
Clean LDPE	5.66 ± 0.1^{b}
Not chlorinated 5 bilayers	5.89 ± 0.1^{a}
1 bilayer	4.19 ± 0.2^{c}
2 bilayers	$< 1.00 \pm 0.00^{e}$
3 bilayers	$< 1.00 \pm 0.00^{e}$
4 bilayers	$< 1.00 \pm 0.00^{e}$
5 bilayers	$< 1.00 \pm 0.00^{e}$
1 bilayer (positive control**)	4.78 ± 0.1^{d}
2 bilayers (positive control)	$< 1.00 \pm 0.00^{e}$
3 bilayers (positive control)	$< 1.00 \pm 0.00^{e}$
4 bilayers (positive control)	$< 1.00 \pm 0.00^{e}$
5 bilayers (positive control)	$< 1.00 \pm 0.00^{e}$

*Treatments followed by the same letter are not significantly different ($P > 0.05$).
**Positive control refers to bacterial suspension exposed to an equivalent chlorine concentration as reported in Table 4.1.

Figure 4.5 shows representative Petri dishes from the corresponding serial dilutions prepared from each treatment after 48 h of incubation at 37 °C.

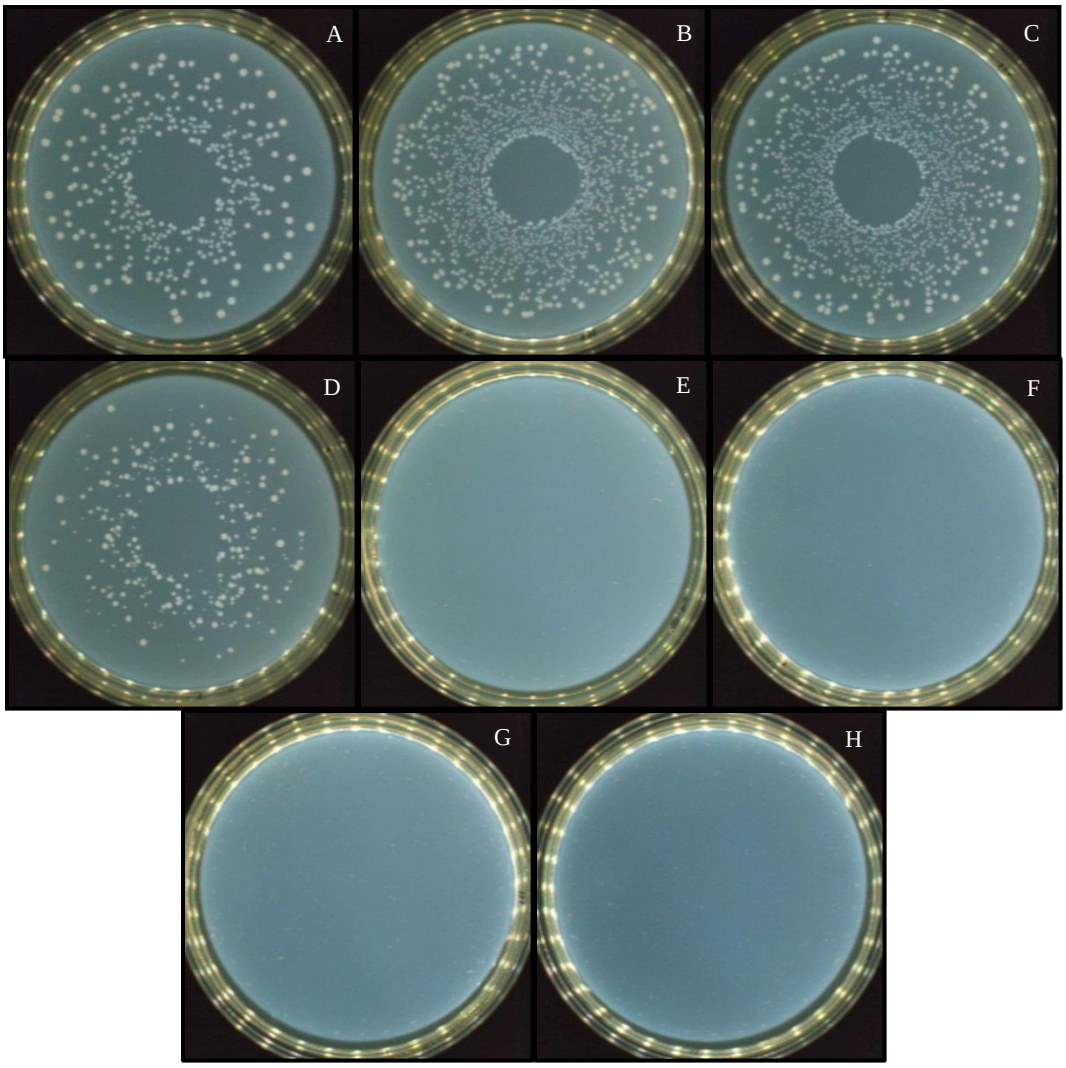

Figure 4.5 Representative Petri dishes from the antimicrobial evaluation after 48 h of incubation at 37 °C (A: bacterial suspension; B: clean LDPE; C: not chlorinated 5 bilauers; D: 1 bilayer; E: 2 bilayers, F: 3 bilayers; G: 4 bilayers; H: 5 bilayers). Controls plated as 10^{-3}, and for 2 – 5 bilayers, 10^{-1}.

Inactivation kinetics of LDPE modified with up to 5 bilayers of N-halamines was determined to quantify the relationship between the logarithm of the survival ratio and time in min from the evaluated treatments (Figure 4.6). The non-linear regression analysis results are shown in Table 4.3. It was not possible to fit the obtained data with Equation 2 with a good correlation. A good correlation between the obtained data and

Equation 1 was observed. However, the value of R^2 decreased as the number of bilayers (and corresponding amount of N-halamines) decreased. Also, the time to reach the limit of detection and provide more than 4 logarithmic reductions increased as the number of bilayers decreased. Figure 4.7 shows the trendlines given by Equation 1.

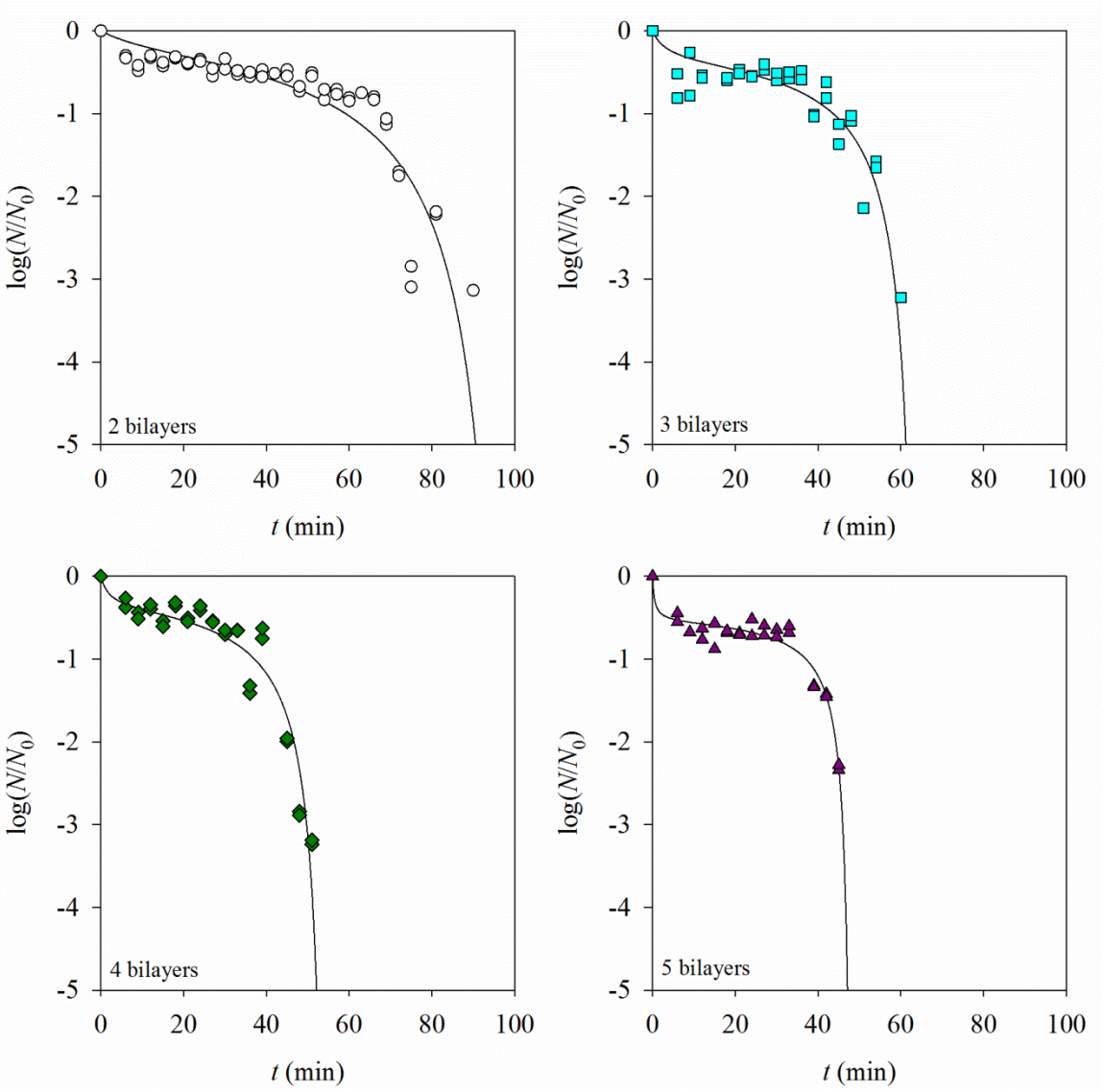

Figure 4.6 Inactivation kinetics (data points fitted with Equation 1 represent the results of 2 replicates).

Table 4.3 Non-linear regression analysis results from the inactivation study.

Number of bilayers	Equation 1 coefficients				R^2
	a	*b* (min)	*c*	*d* (min)	
2	0.27	12.00	0.55	101.00	0.83
3	0.39	3.50	0.32	65.50	0.87
4	0.40	2.00	0.31	55.60	0.92
5	0.55	0.50	0.14	48.62	0.96

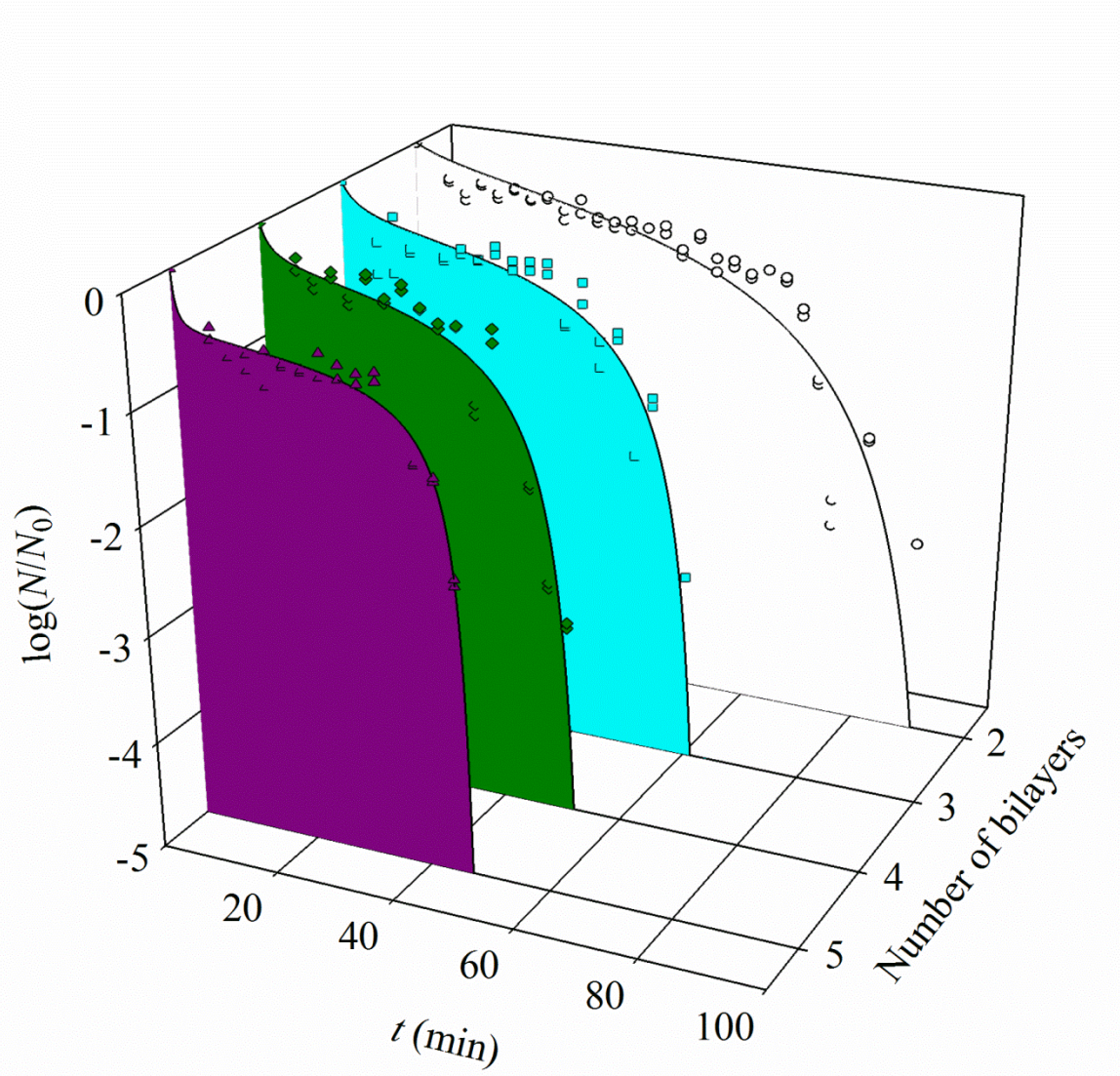

Figure 4.7 Trend lines and data points obtained after fitting the inactivation kinetics data with Equation 1.

The decrease in the degree of correlation may be explained by the fact that a sigmoidal behavior represents a mixed population. At first, a sudden reduction in the initial population may be observed, suggesting the death of the weakest portion of the microorganisms, followed by a plateau that shows resistance against the applied inactivation method, which then leads to a sudden and substantial decrease in the microbial load (Peleg 2006). As a treatment against microorganisms becomes more aggressive, as with the increase in N-halamines with increasing bilayers, the microbial population will react in a more uniform manner since even the strongest cells will be unable to show resistance. On the other hand, if the intensity of the applied inactivation treatment is lowered, more dispersion in the collected data may be observed since within a non-homogeneous population there may be diverse degrees of sensitivity, possibly derived from different degrees of injury.. Having the values of the parameters of Equation 1, it is possible to determine the theoretical time necessary to achieve a specific number of logarithmic reductions by solving (Peleg 2003):

$$\left(c - a - \log\left(\frac{N}{N_0}\right)\right)t^2 + \left(ad + cb + d\log\left(\frac{N}{N_0}\right) - b\log\left(\frac{N}{N_0}\right)\right)t + bd\log\left(\frac{N}{N_0}\right) = 0 \qquad (3)$$

After solving Equation 3 for each level of bilayers, a theoretical reduction of 99.999% (5 logarithmic cycles) would be reached after 90.54, 64.62, 54.06, and 47.65 min for 2, 3, 4 and 5 bilayers, respectively. Likewise, a theoretical reduction of 6 logarithmic cycles would be reached after 92.20, 65.33, 54.64, and 47.92 min for 2, 3, 4 and 5 bilayers, respectively.

In Table 4.3 and Figure 4.8 the relationships between the factors *a*, *b*, *c* and *d* in Equation 1 and the number of bilayers can be observed. Factors *a* and *c* exhibited a linear behavior, whereas factors *b* and *d* showed a power law behavior. Factor *a* increment reflects that the characteristic plateau observed in this kind of curve takes place at a lower level of survival ratio. For instance, a higher value of *a* reflects a more drastic initial reduction of microorganisms. The exhibited decrease in factor *c* is an indicator of how fast the plateau will be interrupted for the downward concavity to appear. A high value of *c* indicates a more drastic treatment and, consequently, a shorter time in which the downward concavity will start to form. Factors *b* and *d* seem to exhibit a decrease in value as the treatment against the microorganisms becomes more aggressive. A low value of *b* results in a faster and more pronounced decrease in the number of microorganisms that is reflected in a more evident upward concavity. Likewise, a low value of *d* will result in a more pronounced downward concavity that appears sooner. Having these values and knowledge of their behavior may be useful to further predict how the kinetics would behave at a theoretical more drastic treatment. In particular, the value of *d*, (the time at which the second denominator of Equation 1 becomes 0), can be an estimate of the time to reach nearly complete inactivation.

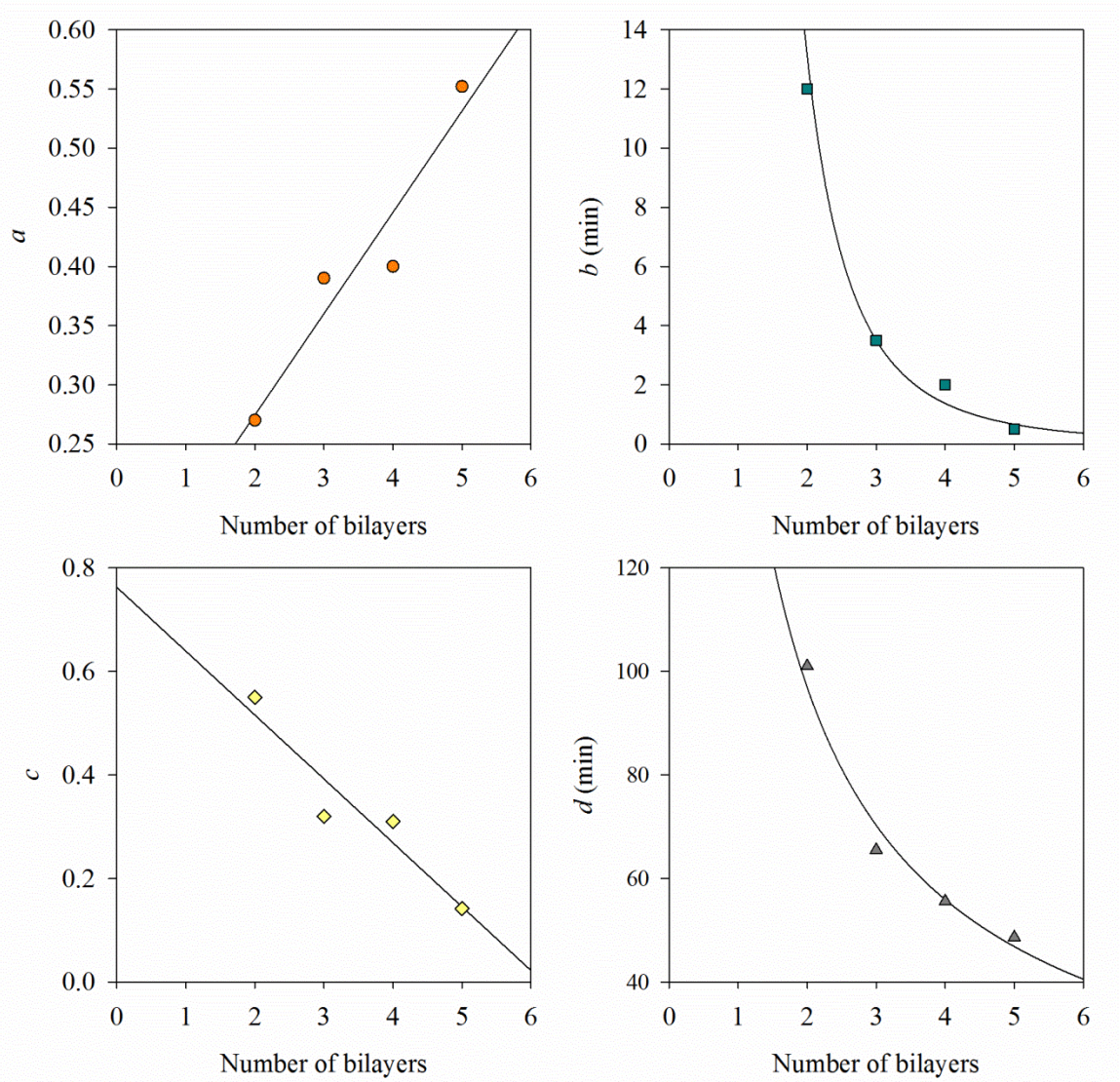

Figure 4.8 The magnitude of the coefficients of Equation 1 as a function of the number of deposited bilayers.

All the positive controls (Figure 4.9) were able to reduce the initial microbial population by more than 99.99% (4 logarithmic cycles) after 6 min, (the limit of detection was already reached by that time). This is in accordance with what has been reported in previous works on the effect of chlorine against *L. monocytogenes*, in which 1 logarithmic reduction can be reached in less than 1 min under a chlorine concentration as

low as 10 ppm (Elkest and Marth 1988a; Elkest and Marth 1988b). This suggests that, even though both the modified LDPE coupons and their corresponding positive controls were able to provide the same level of inactivation, the mechanism in which such inactivation takes place is different.

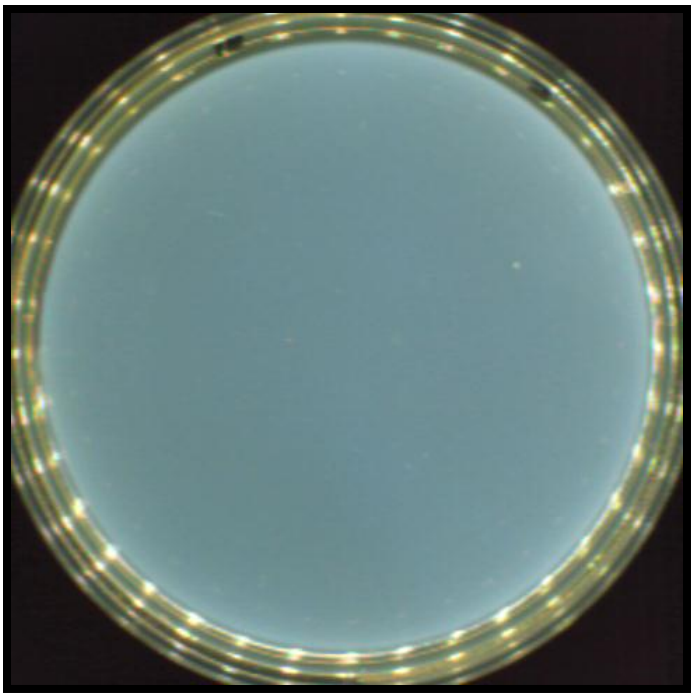

Figure 4.9 Representative Petri dish after incubation of samples taken from positive controls (dilution plated as 10^{-1}).

A problem that can be found when using free chlorine from any source to decontaminate water is precisely its potential interaction with nitrogenous compounds, which commonly results in the formation of chloramines. Indeed, HClO from bleach solutions reacts with the nitrogen-containing molecules. The result is a covalent bond formation between nitrogen and chlorine, with the subsequent formation of a water molecule (Amiri and others 2010):

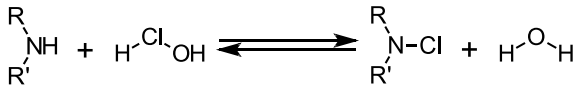

(4)

The germicidal effect of chlorine may be overestimated if this phenomenon takes place. This kind of chlorine-containing chemical species react in the same way free chlorine from bleach solutions does when quantification techniques like the DPD assay are conducted. However, their effect over microorganisms is much weaker and slower than that given by the commonly used sources of chlorine (Amiri and others 2010). A possible advantage of this kind of compound, including N-halamine modified LDPE, could be their ability to provide an extended antimicrobial effect. Several studies have been conducted with chlorinated nitrogenous compounds and their inactivation mechanism (if demonstrated) remains unclear (Fayyad and Al-Sheikh 2001; Amiri and others 2010). From this information, it becomes apparent that a similar phenomenon takes place with N-halamines. The process of microbial inactivation seems to consist of membrane oxidation from the exposure to Cl^+ when it dissociates from the N-halamine structure (Kenawy and others 2007). The degree of inactivation given by N-halamines can be equivalent to that given by the same concentration of free chlorine (or more precisely, by HClO), but in a substantially slower rate. As discussed above, this can represent some advantages if a steady, long-lasting effect is expected and some drawbacks if a fast microbial reduction is required.

Another explanation for the slower inactivation given by N-halamines as compared to free chlorine states that the chlorinated N-halamine is the main source of inactivation, rather than the HClO formed formed from hydrolysis equilibrium (Williams

and others 1988). This may suggest that direct contact between microorganisms and the antimicrobial surface (as in this research) is necessary for inactivation, and the limiting factor of the process may be cells diffusion from solution to the antimicrobial surface.

4.4.4 Reusability and regeneration study

The coupons tested were able to inactivate the initial population of *L. monocytogenes* in more than 5 logarithmic cycles for the first 2 cycles. From the third cycle, it was not possible to determine the number of survivors since the right dilutions were not plated (Figure 4.10). Figure 4.11 shows the FTIR results comparing the spectra of 5 bilayers as prepared, after the 5 antimicrobial evaluations, and after the 10 rechlorination cycles evaluated. It is possible to observe the depletion of the band that could originally be found in the 1600 – 1500 cm^{-1} range, which belongs to the N–H bond in plane bend from secondary amides (Smith 1999).

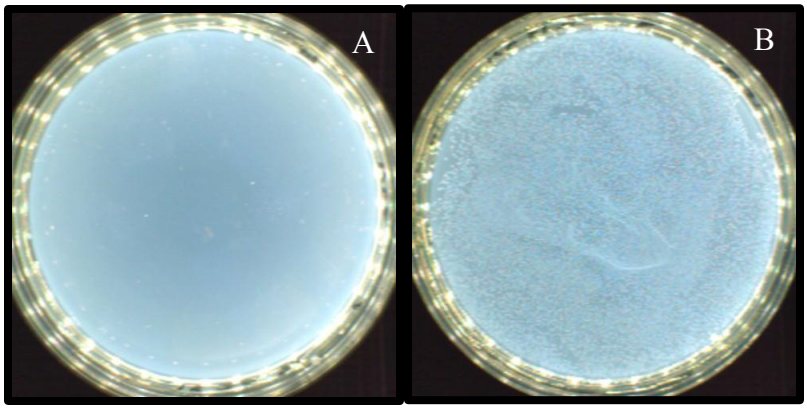

Figure 4.10 Petri dishes showing the 10^{-1} dilution given by 5 bilayers after 2 (A) and 3 cycles (B).

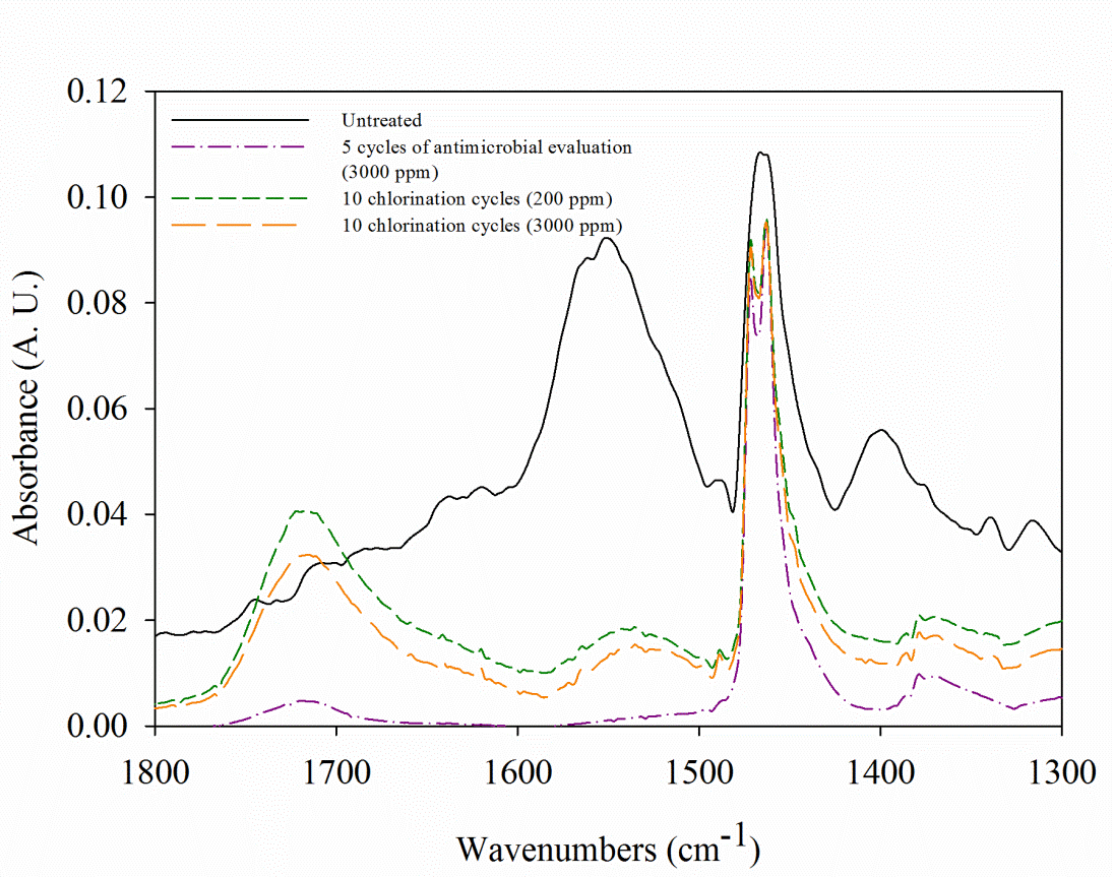

Figure 4.11 ATR-FTIR spectra of 5 bilayers coupons subjected to the reusability and regeneration study.

From that information it can be interpreted that the entire 5 bilayers lost the bonds that attached them onto the surface of LDPE, possibly due to the hydrolysis sodium

hypochlorite (and the high levels of pH its solutions in water exhibit) can provoke in amides (McKenna and Davies 1988; Cheshmedzhieva and others 2009) (Figure 4.12), especially under the concentration used.

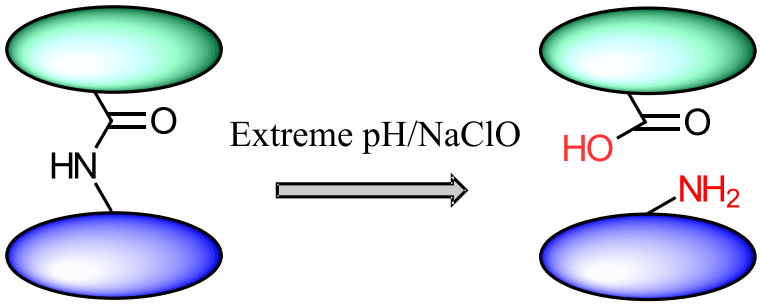

Figure 4.12 Hydrolysis of amides by the action of extreme levels of pH and/or sodium hypochlorite.

As a consequence of the loss of activity, a small regeneration study was performed as it was explained before. The results are shown in Table 4.4.

Table 4.4 Regeneration study results.*

Cycle	Chlorine concentration (ppm)	N-halamines (nmol cm^{-2})
0	200	37.5 ± 2.0^{a}
	3000	31.7 ± 2.9^{a}
10	200	13.2 ± 3.0^{b}
	3000	6.3 ± 2.1^{c}

*Values are average of 3 replicates ± 1 standard deviation. Treatments followed by the same letter are not significantly different ($P > 0.05$).

As it can be observed, the use of a lower concentration of chlorine brings a significantly lower loss of N-halamines after the 10 cycles evaluated. The effect of using 5 min of chlorination instead of 15 min can also be seen from Figure 4.11. The decrease

in the band that corresponds to the N–H bond in plane bend from secondary amides is less pronounced than that observed after the 10 cycles of antimicrobial reuse. There is also a substantial increase in the band that corresponds to the carbonyl (C=O) group in the 1740 and 1720 cm^{-1} range, possibly caused by oxidation of sodium hypochlorite.

4.5 Conclusions

In this work, the surface of LDPE was modified by layer-by-layer deposition of polyelectrolytes which form N-halamines after exposure to sodium hypochlorite. ATR-FTIR results confirmed successful surface modification of LDPE, showing the formation of covalent bonds between PEI and PAA and higher presence of the corresponding chemical species at increasing levels of bilayers. N-halamine modified LDPE was effective in reducing the presence of *L. monocytogenes* Scott A in more than 99.99%, and the overall effect on the microbial population was comparable to that given by free chlorine. The inactivation kinetics study demonstrated a delayed inactivation by the N-halamine modified LDPE compared to the inactivation by an equivalent free chlorine concentration. Such behavior can be predicted by the applied sigmoidal model with good correlation. To the best of our knowledge, this is the first study made on the inactivation kinetics given by a sort of N-halamines. These results may be useful in designing antimicrobial materials which can extend the sanitizing capability of free chlorine beyond initial sanitization. Several applications in the food industry could be benefited from this approach (containers, industrial sheets, conveyor belts, tubes, fittings, piping, and so on).

However, improvements and further research will be necessary to improve the stability and reusability of the coated bilayers.

4.6 Acknowledgements

This material is based upon work supported by the National Institute of Food and Agriculture, U.S. Department of Agriculture under project number 2011-65210-20059 and in part by the Center for Hierarchical Manufacturing at UMass Amherst, an NSF Nanoscale Science & Engineering Center supported by the National Science Foundation under NSF Grant No. CMMI-0531171.

CHAPTER 5

ANTIMICROBIAL N-HALAMINE MODIFIED POLYETHYLENE: CHARACTERIZATION, BIOCIDAL EFFICACY, REGENERATION AND STABILITY[4]

5.1 Abstract

Development of antimicrobial materials which regenerate antimicrobial activity represents a novel technology in preventing microbial cross-contamination. We report a method for the application of regenerably antimicrobial N-halamines onto the surface of polyethylene (PE) materials through layer-by-layer (LbL) assembly of polyethyleneimine and poly(acrylic acid). A total of 5, 10, 15 and 20 bilayers were applied. Modified PE had from 49.3 to 293.5 nmol cm^{-2} antimicrobial N-halamines from 5 to 20 bilayers after 10 minutes of chlorination. Each variant of N-halamine modified PE was able to reduce by > 5 logarithmic cycles *Listeria monocytogenes*. The stability of N-halamine modified PE was characterized after extended exposure to chlorine, acidic solutions, and an alkaline cleaner. After an initial conditioning period, materials generated more than double the quantity of N-halamines present on as prepared materials, retaining regenerability for up to 100 chlorination cycles. After the equivalent of 300 washing cycles by buffers (pH values 3, 5, and 7) or a commercial alkaline detergent, there was no change in the number of antimicrobial N-halamines on the modified materials. These results indicate that the reported layer-by-layer deposition technique results in antimicrobial N-halamine materials capable of long term reuse and exposure to harsh chemicals as expected in a

[4] Submitted to Journal of Food Science.

food processing environment. Such robust, regenerably antimicrobial materials could be an effective technology in the food industry to prevent cross contamination of pathogenic and spoilage microorganisms.

Keywords: N-halamines, Layer-by-layer assembly, antimicrobial materials, surface modification, polyelectrolyte multilayers.

5.2 Introduction

Cross contamination of pathogenic and spoilage microorganisms from food contact surfaces remains a significant challenge in the safety, quality, and security of our food supply. Further, microorganisms can develop resistance against different control measures if they are allowed to proliferate on contaminated surfaces (Sidhu and others 2001; Kenawy and others 2007). The financial and public health impact of such cross-contamination raises an interest in the development of new technologies such as antimicrobial materials to help prevent cross contamination. There has been a particular interest in the application of polymeric coatings with antimicrobial properties given the fact that, unlike low molecular weight antimicrobial substances, polymers may represent a lower risk of residual toxicity and contamination due to their lower solubility (Centers for Disease Control and Prevention 2003; Centers for Disease Control and Prevention 2004; Møretrø and Langsrud 2011). N-halamines are a unique class of antimicrobial compound which consist of a nitrogen atom covalently linked to a halogen, commonly chlorine. The nitrogen atom (which can belong to an amine, an amide, or an imide) can be chlorinated after exposure to a source of chlorine, such as solutions of NaClO (bleach). This chlorination can be repeated numerous times, resulting in so-called "regenerable" antimicrobial activity. The exact mechanism of their antimicrobial activity is not fully agreed upon, but is likely either via dissociation of chlorine into aqueous solution or by direct oxidation of critical components in the cell membrane (Worley and Sun 1996; Eknoian and others 1998; Kenawy and others 2007). Irrespective of exact mechanisms, such N-halamine antimicrobials have been evaluated both as small

molecular weight substances and polymeric coatings on plastics, textiles, and metals, against a wide range of microorganisms, showing promising antimicrobial activity (Worley and others 2003; Williams and others 2005; Goddard and Hotchkiss 2008; Cerkez and others 2011; Bastarrachea and Goddard 2013; Bastarrachea and others 2013).

To demonstrate the commercial potential of any coating designed for use in a harsh environment (like in food processing), stability studies must be performed. Such studies are unfortunately often omitted in place of single-use studies, limiting their potential for commercial translation. Long term stability is particularly important for N-halamine antimicrobial coatings, which interest lies in their regenerability and potential for long term reuse. Prior reports often suggest limited stability in N-halamine modified materials, indicating a need for improving methods for producing such materials (Goddard and Hotchkiss 2008; Kocer and others 2010; Cerkez and others 2013). An emerging technique in surface modification (by N-halamine coatings) which can be applied onto the surface of many materials (polymers, stainless steel) is layer-by-layer deposition (LbL). LbL deposition is simple, rapid, scalable to coating large substrates, and involves the consecutive adhesion of coatings of alternating charges. Coatings are reported to be stable owing to their numerous electrostatic interactions, hydrogen bonding, and Van der Waals forces. Covalent cross-links can also be introduced to enhance stability of LbL coatings (Decher 1997; Stockton and Rubner 1997; Cerkez and others 2011; Bastarrachea and others 2013; Bastarrachea and Goddard 2013).

The goal of the present study was to modify the food contact surface of polyethylene (PE) through LbL assembly of polyethyleneimine (PEI) and poly(acrylic acid) (PAA) to generate a stable, regenerably antimicrobial N-halamine coating. A total

of 5 to 20 bilayers were deposited via LbL assembly onto ultraviolet light functionalized PE, in which a single bilayer is composed of covalently crosslinked PEI and PAA. Materials were characterized in terms of N-halamine content, surface chemistry, antimicrobial effectiveness against *Listeria monocytogenes*, and stability against a commercial alkaline detergent and buffers of pH values 3, 5, and 7.

5.3 Materials and Methods

5.3.1 Layer-by-layer assembly onto PE

PE film donated by Honam Petrochemical Corp. (South Korea) was cut into 1 × 1 cm coupons and cleaned by sonication in isopropanol (Fisher Scientific, Pittsburgh, PA), then acetone (Fisher Scientific, Pittsburgh, PA), and finally deionized (DI) water (two cycles of 10 min per solvent). Once cleaned, the coupons were left drying overnight at room temperature over anhydrous calcium sulfate. After drying, each side of the PE coupons was functionalized through UV-Ozone (UV-O_3) irradiation for 15 min with a Jelight Co. model 42 UVO Cleaner (Irvine, CA). Once UV-O_3 irradiated, the LbL assembly process was conducted as follows. To deposit a single bilayer, coupons were immersed in a 0.1 M potassium phosphate monobasic and dibasic (Fisher Scientific, Pittsburgh, PA) buffer (pH 7.8) containing 5 mg mL^{-1} of branched polyethyleneimine (PEI, 25,000 Da, Sigma-Aldrich, St. Louis, MO) and shaken for 5 min at room temperature. Then, the coupons were rinsed with copious DI water and immersed in the same phosphate buffer containing the same concentration of poly(acrylic acid) (PAA,

450,000 Da, Scientific Polymer Products, Inc., Ontario, NY) and shaken for the same amount of time at room temperature, followed by rinsing in copious DI water. This procedure was repeated until completing 5 bilayers. Then, coupons were immersed in the same phosphate buffer containing the cross-linker 1-(3-Dimethylaminopropyl)-3-ethylcarbodiimide hydrochloride (EDC-HCl, ProteoChem, Inc., Denver, CO) and N-hydrosuccinimide (NHS, Acros Organics, Fair Lawn, NJ) at concentrations of 50 and 5 mM, respectively, and shaken for 2 h to covalently cross-link the bilayers. Coupons were then rinsed in copious DI water and the entire procedure for applying 5 bilayers was repeated until completing 10, 15 and 20 bilayers. After every cycle of covalent bond formation with EDC-HCl and NHS, coupons from every treatment were rinsed with copious DI water, chosen randomly, left drying overnight, and kept in closed glass Petri dishes until usage. Figure 1 shows a scheme of the change in surface chemistry applied on PE.

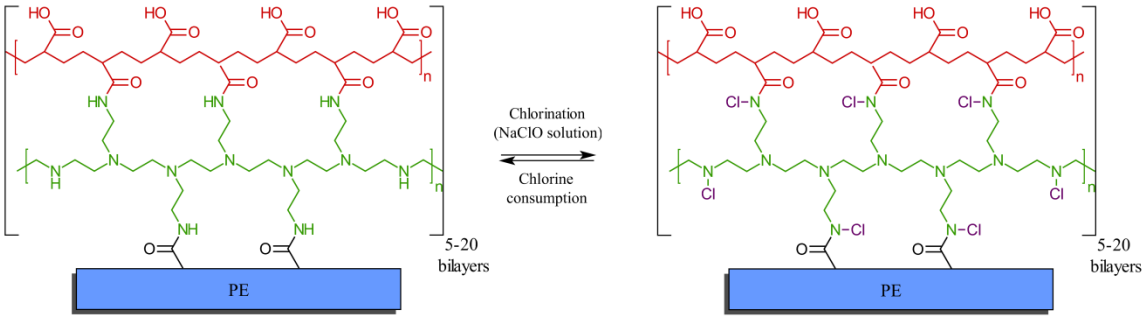

Figure 5.1 Scheme showing the change in surface chemistry applied on PE.

5.3.2 Attenuated Total Reflectance Fourier Transform Infrared Spectroscopy (ATR-FTIR)

The surface chemistry of native (clean) and N-halamine modified PE (both as prepared and after stability studies) was analyzed by ATR-FTIR with an IRPrestige 21 spectrometer (Shimadzu Corp., Tokyo, Japan). Area underneath the spectra of absorbance bands representative of the chemical species indicative of PEI and PAA was quantified on control and modified PE using the IRsolution software (Shimadzu Corp., Tokyo, Japan). ATR-FTIR analysis was conducted using Happ-Genzel apodization at a resolution of 4 cm^{-1}. A total of 32 scans were taken for every spot and 3 spots were analyzed for every coupon (at least 1 coupon per replicate of each corresponding evaluation or treatment). Spectra interpretation was conducted with the KnowItAll software (Biorad Laboratories, Philadelphia, PA).

5.3.3 Chlorination of N-halamine modified PE

Coupons with 5, 10, 15 and 20 bilayers were exposed to 200 ppm of chlorine (1 mL cm^{-2}) for up to 40 min. This concentration was selected because it is the upper limit allowed for disinfection by federal agencies (Rutala and Weber 2008). The chlorine content of the NaClO bleach solution used (Acros Organics, Fair Lawn, NJ) was confirmed through iodometric titration (American Society for Testing and Materials 2008). Coupons were randomly chosen over time, rinsed with copious DI water to remove not bound chlorine, and the number of antimicrobial N-halamines was quantified through a colorimetric modified DPD assay described previously (Goddard and

Hotchkiss 2008; Bastarrachea and Goddard 2013; Bastarrachea and others 2013). Briefly, DPD reagent (N,N-diethyl-p-phenylenediamine DPD total chlorine reagent powder, Hach Company, Loveland, CO) was prepared by mixing 1 pack of DPD total chlorine reagent powder with 1 mL of DI water. Coupons were immersed in individual test tubes containing 2 mL of DI water to which 50 μL of the DPD reagent was added. Then the coupons were shaken for 5 min inside the test tubes for color formation. Absorbances were measured at 512 nm and the N-halamine content was quantified from a standard curve prepared with known concentrations of chlorine and expressed as nmol cm^{-2}. Samples were analyzed in duplicate, with 3 replicates per treatment.

5.3.4 Antimicrobial evaluation

Bacterial suspensions of *L. monocytogenes* Scott A obtained from Dr. Martin Wiedmann (Food Science Department, Cornell University, Ithaca, NY) were prepared as follows. A loopful of stock culture stored in TSB with 25% glycerol at – 80 °C was streaked onto tryptic soy agar (TSA, Difco, Becton Dickinson, Sparks, MD) by quadrant streak technique and incubated at 37 °C for 24 h. Then, a single colony was inoculated into tryptic soy broth (TSB, Difco, Becton Dickinson, Sparks, MD) and incubated overnight at the same temperature. A 1:100 dilution was prepared from the overnight culture with fresh and sterile TSB and incubated at 37 °C until the microbial load was approximately 9 Log(CFU mL^{-1}) during the exponential phase (Bastarrachea and Goddard 2013). The culture was further diluted in DI water to a final microbial concentration of approximately 6 Log(CFU mL^{-1}), which was confirmed by plating on

TSA 100 μL of serial dilutions prepared in 0.9% saline water. Three coupons from every treatment were put in contact with 1 mL of this bacterial suspension and incubated at 32 °C for 2 h with rotation (60 rpm). Such temperature was chosen because previous works reported that at 25 – 35 °C chlorine exhibits its highest effectiveness against *L. monocytogenes* (Elkest and Marth 1988b). After the 2 h of incubation, bacterial suspensions were diluted 1:10 in neutralizing buffer (Difco, Becton Dickinson, Sparks, MD) to quench any residual chlorine, followed by serial dilutions in 0.9% saline water, plating onto TSA plates with an automated spiral plater Autoplater 4000 (Spiral Biotech Inc., Norwood, MA), and incubation for 48 h at 37 °C. To lower the detection limit to 1 log(CFU mL^{-1}), the entire 1 mL of the first dilution (with the neutralizing buffer) was also plated onto 3 TSA plates manually (333 μL per plate). After the 48 h of incubation, colonies were counted with the plate reader Scan® 500 (interscience, Saint-Non-la-Brèteche, France). The antimicrobial evaluation was repeated 3 times per treatment (3 replicates). Bacterial suspension alone, unmodified PE coupons chlorinated with 200 ppm of chlorine (1 mL cm^{-2}) for 10 min, and 20 bilayers N-halamine modified PE which had not been subjected to chlorination served as negative controls. The latter was chosen as a negative control given the fact it was the treatment with the highest level of surface modification, in order to confirm that any observed antimicrobial activity was a result of chlorinated N-halamines and not due to other surface:bacterial interactions. N-halamine modified PE coupons with 5, 10, 15 and 20 bilayers were chlorinated with 200 ppm of chlorine (1 mL cm^{-2}) for 10 min (determined by preliminary experiments to be the time of N-halamine saturation) before the antimicrobial evaluation. Bleach added to bacterial suspensions in a concentration calculated to match the expected N-halamine content of

the N-halamine modified PE coupons after 10 min of chlorination served as the positive control.

5.3.5 N-halamine regeneration and stability

N-halamine modified PE coupons with 20 bilayers were subjected to 100 cycles of chlorination with 200 ppm of chlorine in individual test tubes (1 mL cm^{-2}) with 15 s of exposure time. After every cycle of chlorination, coupons were rinsed with DI water and chlorine was removed (quenched) from the surface by exposing the coupons to 0.1 N sodium thiosulfate (Acros Organics, Fair Lawn, NJ) with the same volume to surface area ratio (1 mL cm^{-2}) for 15 s. Then, coupons were rinsed again in DI water to be subjected to another cycle of chlorination. The N-halamine content was determined every 10 cycles through the DPD assay described earlier. To evaluate the stability of the N-halamines after extended exposure to an alkaline detergent used in washing food contact materials, PE coupons with 20 bilayers were chlorinated for 10 min and then rinsed in copious DI water (10 min was selected as the chlorination time since at this point chlorine content reaches an equilibrium). The initial chlorine content after the first chlorination was determined from a separate set of samples. The rest of the samples were put in contact with a solution of the cleaning agent Liquinox (Alcanox, Jersey City, NJ; ingredients: water, sodium alkylbenzene sulfonate, alcohol ethoxylate, coconut diethalonamide, sodium xylene sulfonate, and tripotassium EDTA) with a pH value of 8.6 ± 0.1 in individual test tubes (1 mL cm^{-2}) using the maximum concentration (1% v/v) and 10 times the ratio between detergent solution volume and surface area recommended by the

provider. The tubes were kept at 20 °C under rotation at 60 rpm for the equivalent of 100 washing cycles. Then, after removing the coupons from the detergent solution and rinsing with DI water, the remaining N-halamine content of the coupons was determined through the DPD assay. After N-halamine quantification, coupons were rechlorinated under the same scheme used at the beginning (200 ppm of chlorine for 10 min) and the N-halamine content was determined through the DPD assay from randomly selected coupons. The remaining coupons were subjected to another 100 cycles of washing. The described procedure was repeated until completing the equivalent of 300 washing cycles. A similar experiment was designed to determine the stability of N-halamine modified materials after exposure to pH values typical of acidic and neutral foods using buffers of pH values of 3, 5 and 7 prepared by mixing citric acid monohydrate (Acros Organics, Fair Lawn, NJ) 0.1 M and sodium phosphate dibasic (Fisher scientific, Pittsburgh, PA) 0.2 M. For the N-halamine regeneration and stability studies described above, coupons with 20 bilayers (the highest level of surface modification) were used since (as discussed below) coupons having 10, 15 and 20 bilayers harbor statistically the same number of N-halamines ($P > 0.05$), and according to ATR-FTIR, coupons with 15 and 20 bilayers exhibit the same surface chemistry. Three replicates were performed for each of the mentioned evaluations, with at least 1 coupon per replicate.

5.3.6 X-Ray Photoelectron Spectroscopy (XPS)

The surface chemistry of native and N-halamine modified PE (both as prepared and after stability studies) was further characterized by XPS to understand changes in

bond formation at the top several nanometers. XPS analysis was carried out with a Physical Electronics Quantum 2000 (Physical Electronics, Chanhassen, MN) using Al Kα excitation at a spot size of 100 μm at 25 W. An angle of 45° (relative to the coupons' surface) was used to collect spectra. To collect survey scans a pass energy of 187.85 eV using a step size of 1.6 eV was applied. A pass energy of 46.95 eV was applied to obtain high resolution spectra (C 1s, O 1s and N 1s). Atomic concentrations and high resolution spectra were analyzed with the MultiPak software version 6.1A (Physical Electronics, Chanhassen, MN); high resolution peaks were fitted with the Gaussian-Lorentzian model after linear background subtraction (90% Gaussian was applied). Reported atomic percentages are representative of analyses conducted on two separate spots.

5.3.7 Storage study

In order to evaluate the stability of the chlorine bond in the modified PE samples, coupons having 5 bilayers were first chlorinated for 10 min with 200 ppm of chlorine as explained earlier. Coupons with 5 bilayers were chosen because at this level of surface modification they exhibited more predictability in terms of N-halamine content. Coupons were stored in individual test tubes containing DI water (1 mL cm^{-1}) at 3 different temperatures: 4, 20 and 37 °C. At different points in time, coupons were randomly collected, rinsed in copious DI water, and the N-halamine content was determined through the DPD assay as described previously.

5.3.8 Statistical analysis

To determine significant difference between treatments, the general linear model followed by Tukey's pairwise comparisons was applied when appropriate, with a confidence interval of 95% using the software Minitab version 16.1.1 (Minitab Inc., State College, PA).

The one phase exponential association model was used to fit the data of the N-halamine chlorination study:

$$NH = NH_{asympt}(1 - e^{-Kt}) \quad (1)$$

where NH is the momentary N-halamine content in the coupons (nmol cm^{-2}), NH_{asympt} is the asymptotic N-halamine content, which indicates the theoretical maximum value of N-halamines that can be reached, K is the exponential rate constant (min^{-1}) and t is the time (min). Nonlinear regression analysis was conducted with GraphPad Prism 5 version 5.04 (GraphPad software Inc., La Jolla, CA) for each of the 3 replicates run for every treatment.

For the storage study, data collected from the N-halamine determination at different points in time for each storage temperature were fitted with the Weibull model:

$$\log\left(\frac{M_t}{M_0}\right) = -kt^n \quad (2)$$

where M_t is the N-halamine content at time t in a coupon, M_0 is the initial N-halamine content, k is the kinetic constant (h^{-1}), t is the time in h, and n is the shape factor. Non-linear regression analysis was performed with the GraphPad Prism 5 version 5.04 software.

5.4 Results and Discussion

5.4.1 Attenuated Total Reflectance Fourier Transform Infrared Spectroscopy (ATR-FTIR)

ATR-FTIR spectra were collected on native (clean) and N-halamine modified PE (Figure 5.2). After UV-O_3 irradiation, PE exhibited the characteristic absorbance band of the carbonyl group (C=O), in the range that corresponds to that functional group (1740 to 1720 cm^{-1}). A characteristic band formed in all the N-halamine-modified PE coupons within the 1650 and 1590 cm^{-1} range that corresponds to the vibration given by the N–H bond of primary and secondary amines. Another characteristic band was exhibited within the 1570 and 1515 cm^{-1} range from 5 to 20 bilayers that belongs to the N–H bond in plane bend of secondary amides, confirming the formation of covalent bonds between alternating layers of PEI and PAA. Another band was exhibited (more evidently from 10 to 20 bilayers) in a range that corresponds to tertiary amines (1360 – 1310 cm^{-1}). Another broad band was observed in a range that belongs to the oscillation of the N–H bond of primary and secondary amines (900 – 660 cm^{-1}). The presence of carboxylic acids was confirmed from the formation of a couple of bands as the number of bilayers increased in the range that corresponds to the C–O bond of carboxylic acids and derivatives, 1320 –

1210 cm^{-1} and 1075 – 1000 cm^{-1}, respectively. A broad band was also observed in the range that corresponds to the normal polymeric O–H vibration, 3400 – 3200 cm^{-1}.

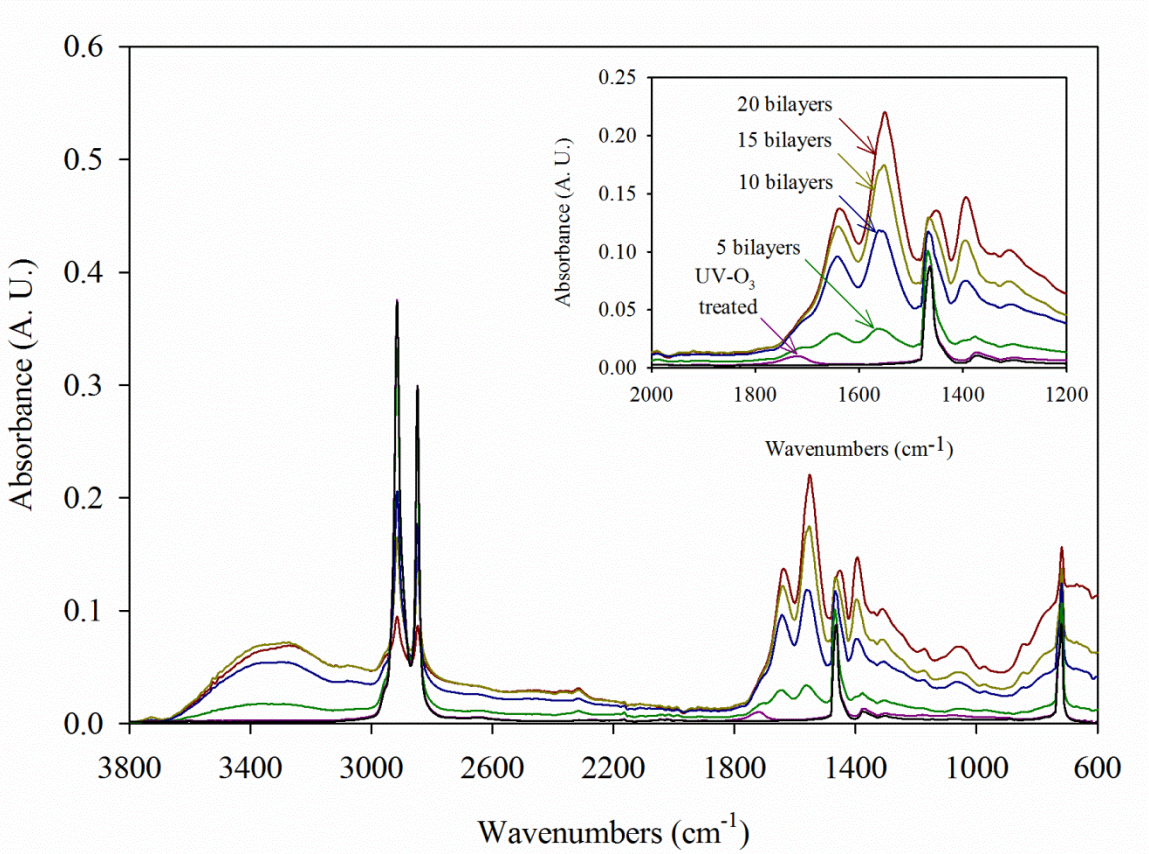

Figure 5.2 Representative ATR-FTIR spectra before chlorination. Spectrum of clean PE is shown at the bottom and above it the spectrum of UV-treated PE.

The increase in the quantity of N-halamine forming amines and amides with increasing bilayers, as determined by analyzing the area underneath FTIR spectra for characteristic absorbance bands is reported in Figure 5.3. Wavenumber ranges of 1700 to 1600 cm^{-1} and 1600 to 1500 cm^{-1} were analyzed for primary/secondary amines and secondary amides, respectively. An apparent plateau is reached as the number of bilayers increases, showing no significant difference in the values of area underneath spectra ($P >$

0.05) between 15 and 20 bilayers for either group of chemical species. It is interesting to note that the amounts of amides to amines increases as number of bilayers increases. At 5 and 10 bilayers, there is no significant difference between the values of area underneath spectra between amines and amides ($P > 0.05$), but that difference becomes significant ($P < 0.05$) from 15 bilayers. These results suggest that more covalent bonds are formed (via cross-linking) as more bilayers and more cycles of treatment with EDC-Cl and NHS are applied. Increasing covalent bond formation would mean there are fewer sites available for attachment of additional bilayers, which supports the results observed in Figure 4, below. Such increasing covalent bond formation also supports the enhanced stability of the bilayers after exposure to harsh cleaners (Li and others 2009; Bastarrachea and Goddard 2013). From these results, it was decided that N-halamine modified PE with 20 bilayers would be used for the N-halamine regeneration and stability studies, below.

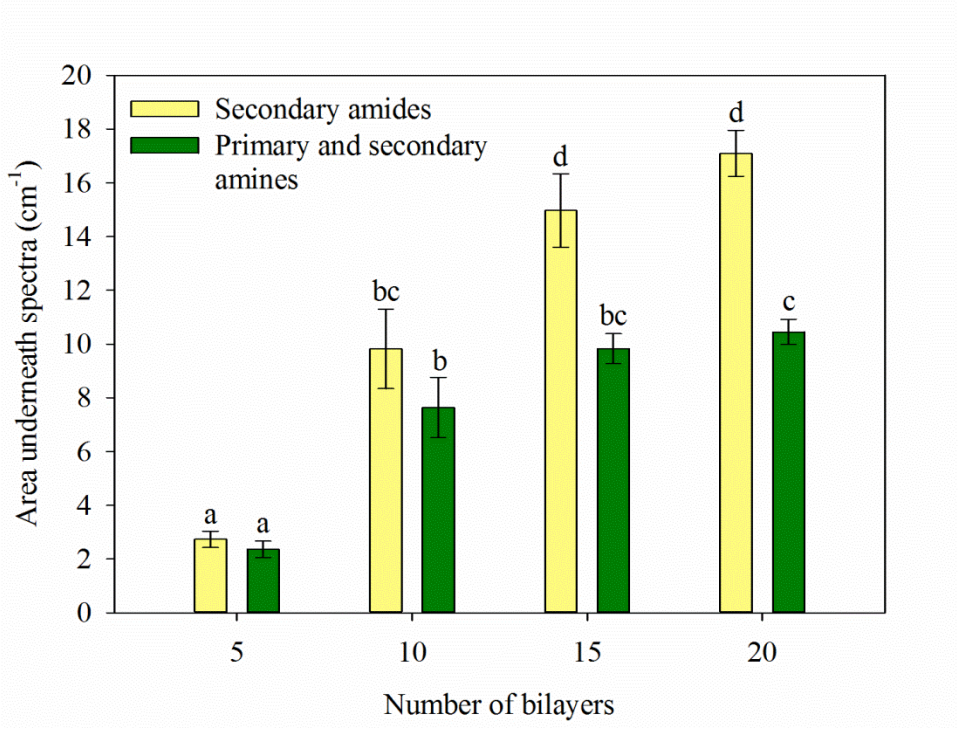

Figure 5.3 Change in area underneath spectra from ATR-FTIR as a function of number of bilayers. Values represent the average of 3 replicates. Treatments followed by the same letters are not significantly different ($P < 0.05$).

5.4.2 Chlorination of N-halamine modified PE

N-halamine chlorination data were fitted to the one phase exponential model (Equation 1), in order to determine the asymptotic or maximum theoretical amount of N-halamines that could be imparted after exposure to 200 ppm of chlorine, as reported in Figure 5.4. Kinetics parameters are reported in Table 1 to show the influence of the number of bilayers on NH_{asympt} and K.

Table 5.1 Exponential association model's (Equation 1) parameters.*

Number of bilayers	NH_{asympt} (nmol cm^{-2})	K (min^{-1})	R^2
5	49.3 ± 5^a	1.74 ± 1.28^a	0.91 ± 0.01
10	258.9 ± 61^b	0.21 ± 0.09^b	0.95 ± 0.05
15	223.1 ± 39^b	0.21 ± 0.04^b	0.90 ± 0.05
20	293.5 ± 53^b	0.12 ± 0.03^b	0.95 ± 0.01

*Results are the average of 3 replicates ± 1 standard deviation. Treatments followed by the same letter in the same column are not significantly different ($P > 0.05$). Modified PE coupons with 5, 10, 15 and 20 bilayers were immersed in 200 ppm of chlorine solution and selected randomly over time to quantify their N-halamine content.

The asymptotic number of N-halamines (NH_{asympt}, in nmol cm^{-2}) increased significantly between 5 and 10 bilayers ($P < 0.05$), but did not continue to increase from 10 to 20 bilayers. Similarly, the rate at which the asymptotic level of N-halamines is achieved (K) was significantly ($P < 0.05$) faster for 5 bilayers than the other treatments, which exhibited similar K values ($P > 0.05$). These results support the observation from the ATR-FTIR analysis results that the amount of amines and amides plateaus between 15 and 20 bilayers. From the observed results, it was decided that for further experiments, the chlorination time applied would be 10 min, since from this point, a saturation in the chlorine content starts to be reached (Figure 5.4).

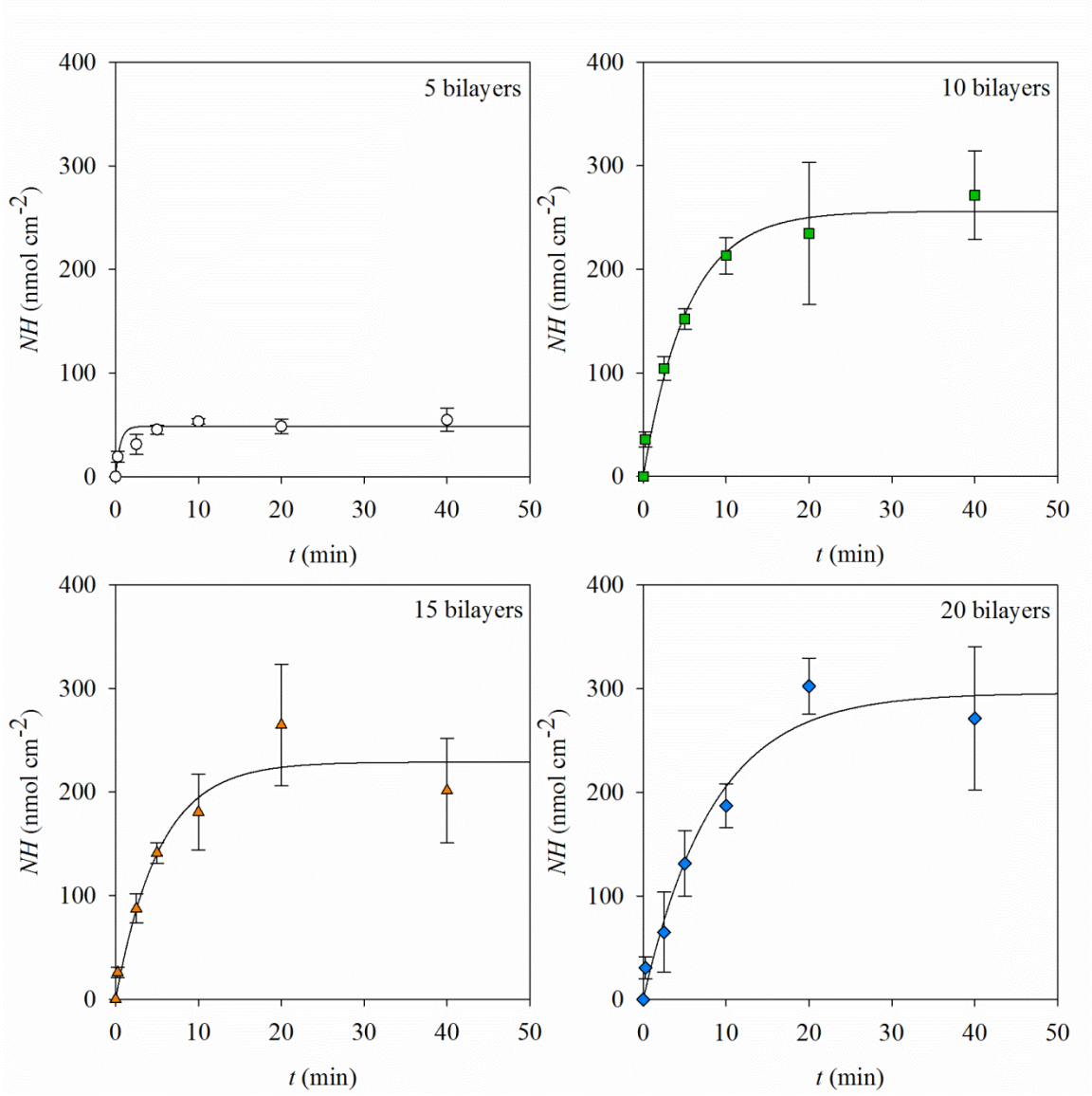

Figure 5.4 N-halamine chlorination of modified PE (data points represent the average values of 3 replicates fitted with Equation 1, with 2 values per replicate). Modified PE coupons with 5, 10, 15 and 20 bilayers were immersed in 200 ppm of chlorine solution and selected randomly over time to quantify their N-halamine content.

5.4.3 Antimicrobial evaluation

Native PE (clean), unchlorinated N-halamine modified PE with 20 bilyers, and chlorinated N-halamine modified PE coupons were subjected to an antimicrobial activity

assay, in which coupons were incubated at 32 °C for 2 h in a starting inoculum of approximately 6 Log(CFU mL^{-1}) *L. monocytogenes* (Figure 5.5). Each variant of chlorinated N-halamine modified PE coupons (from 5 to 20 bilayers) exhibited greater than 5 logarithmic microbial reductions (the limit of detection for the assay) as compared to the negative controls after 2 h of incubation. Similarly, positive controls (in which sodium hypochlorite was added directly to the suspension of *L. monocytogenes* in a concentration equivalent to the number of N-halamines present on modified PE coupons) reached inactivation below the limit of detection (< 1 log(CFU mL^{-1}) or > 5 logarithmic reductions reduction). This is in accordance with previous studies (Elkest and Marth 1988a; Elkest and Marth 1988b; Bastarrachea and others 2013).

As expected, none of the negative controls (bacterial suspension alone or in contact with either native or unchlorinated N-halamine modified PE with 20 bilayers) exhibited an antimicrobial effect (Figure 5.6). These results support our conclusion that the observed antimicrobial activity was a result of the chlorination of the N-halamine modified PE samples and not a result of nonspecific surface interactions.

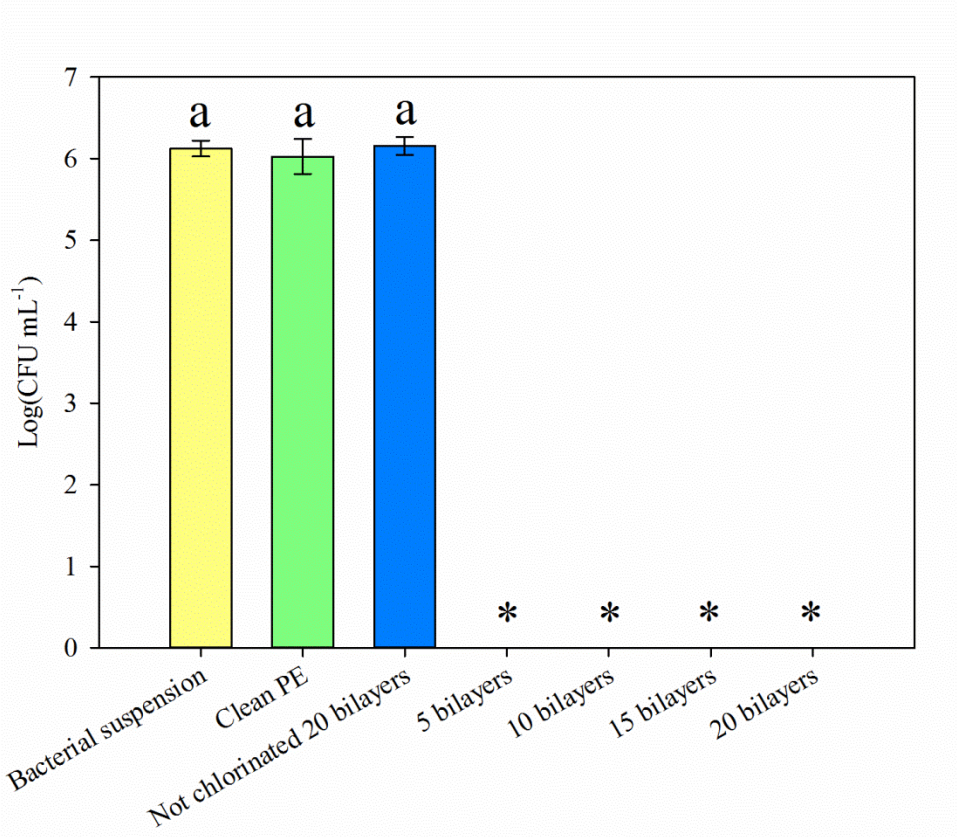

Figure 5.5 Antimicrobial evaluation results. Bars represent the average of 3 replicates. Treatments with the same letter are not significantly different ($P > 0.05$), * indicates result below the limit of detection (< 1 log(CFU mL^{-1})).

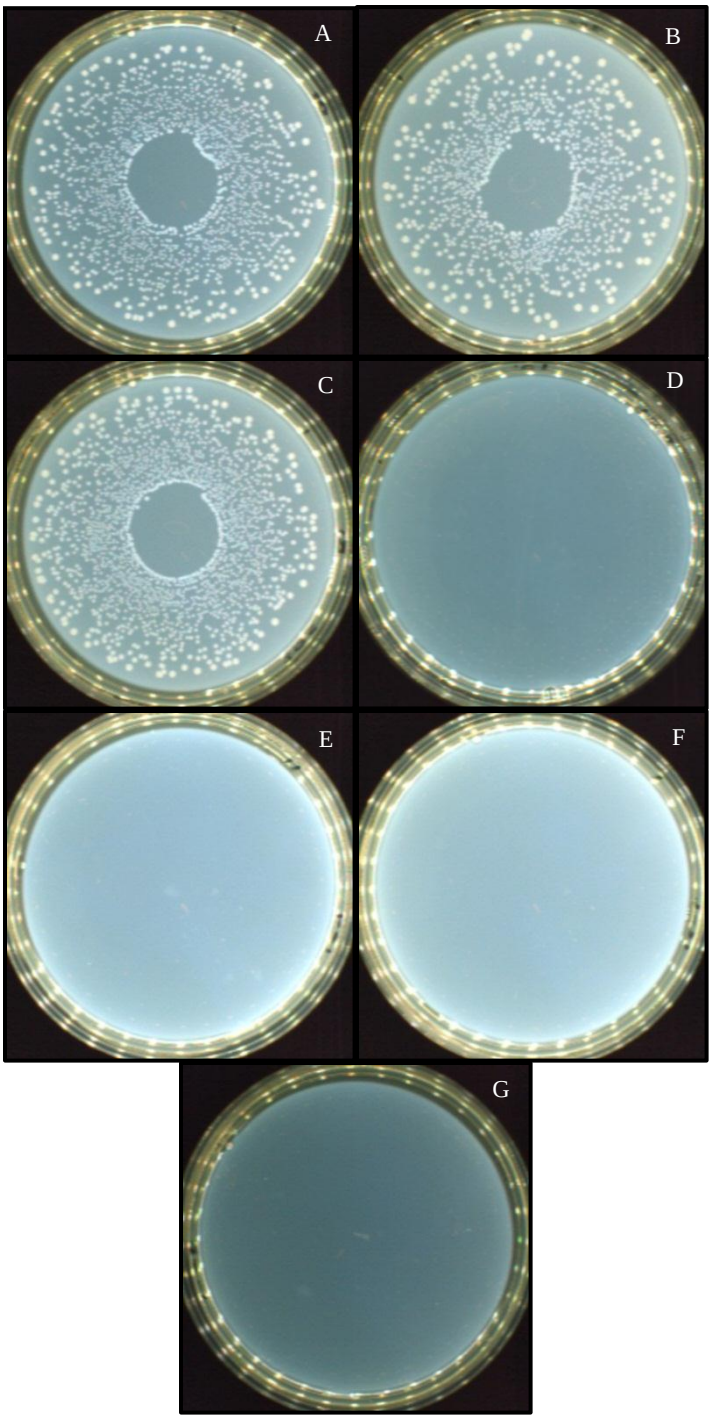

Figure 5.6 Representative Petri dishes from the antimicrobial evaluation after 48 h of incubation at 37 °C (A: bacterial suspension; B: clean PE treated with 200 ppm of chlorine; C: not chlorinated 20 bilayers; D: 5 bilayers, E: 10 bilayers; F: 15 bilayers; G: 20 bilayers). Controls were plated as 10^{-3}, and treated treatments as 10^{-1}.

5.4.4 N-halamine regeneration and stability

The influence of repeated rechlorination (up to 100 cycles) on surface chemistry and N-halamine chlorination are reported in Figure 5.7. It can be observed that the N-halamine content exhibited a steady increase during the initial 30 chlorination cycles, after which the N-halamine content fluctuates between approximately 80 and 140 nmol cm^{-2}. Evaluation of initial and final ATR-FTIR spectra help to explain these phenomena. The ATR-FTIR spectra suggest that after 100 chlorinations there was some rupture of amide bonds (reduced absorbance at 1570 – 1515 cm^{-1}) into amines (increased absorbance at 1650 – 1590 cm^{-1}) and carboxylic acids (increased absorbance at 1740 – 1720 cm^{-1} and 1320 – 1210 cm^{-1}). This change in surface chemistry may explain the observed fluctuations in N-halamine content during the repeated cycles of chlorination. It is possible that after repeated chlorinations, there is a breaking and reforming of amide bonds. The observed increase in N-halamine content during the initial 30 rechlorination cycles may also be a consequence of the hydrolysis of amide bonds and indicates that a conditioning period may be necessary to achieve the full antimicrobial potential of such materials. The subsequent fluctuations in the N-halamine content, as mentioned before, may be produced by a competition between amides and amines to bind chlorine (El Achari and others 1993; Hazell and others 1994; Hazen and others 1998), although this fluctuation is unlikely to significantly affect antimicrobial activity as materials with significantly lower quantities of N-halamines are also capable of achieving 5 log microbial inactivation. Further, the alkaline NaClO may promote the hydrolysis of amides (Cheshmedzhieva and others 2009), and it has also been reported that NaClO can

promote crosslinking in proteins involving amine groups (Matoba and others 1985). The observed variability in the N-halamine content after repeated chlorination may therefore be explained from a possible repeated hydrolysis and condensation of amides. Nevertheless, the retention of a substantial number of N-halamines on the modified groups, and retention of overall spectral intensity in FTIR results, suggest that the N-halamine coating deposited herein is stable to repeated chlorinations.

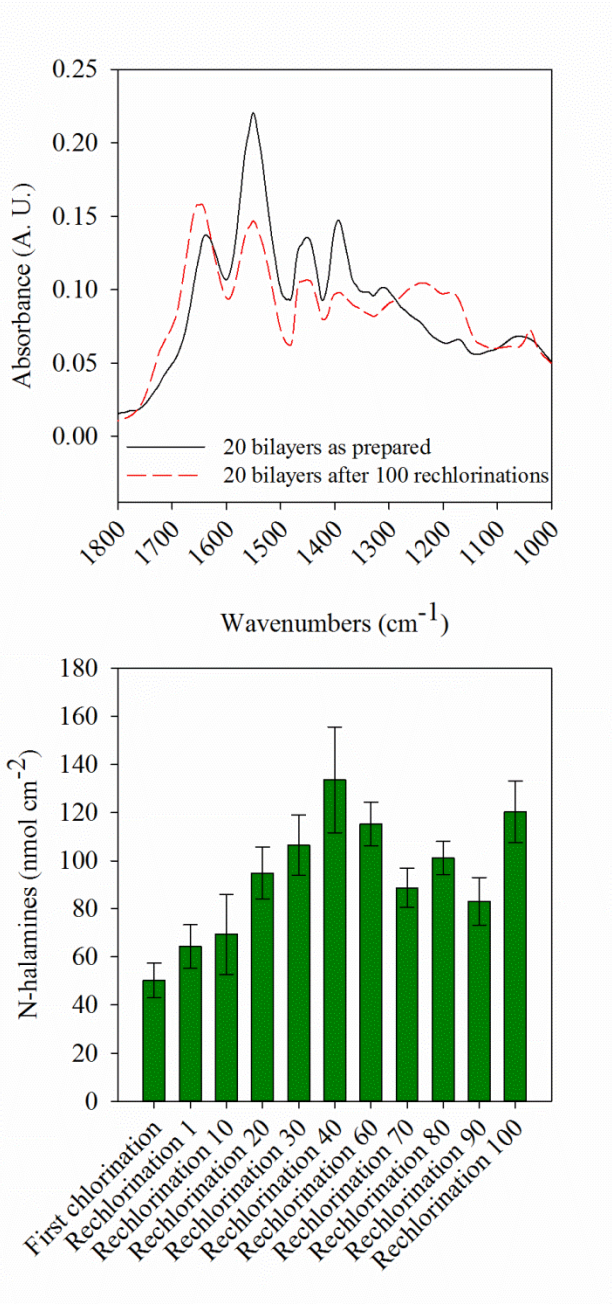

Figure 5.7 ATR-FTIR spectrum of 20 bilayer N-halamine modified PE after repeated rechlorination (top) and N-halamine regeneration of such coupons (bottom). Coupons were subjected to repeated chlorination by immersion in solutions with 200 ppm of chlorine, which was quenched with 0.1 N sodium thiosulfate between chlorinations.

The influence of extended exposure to detergents and wash buffers of acidic to neutral pH on the stability of N-halamine modified PE was quantified and is reported in

Figure 5.8. In all cases, after 300 equivalent wash cycles, N-halamine modified materials retained their ability to regenerate N-halamines in quantities equivalent to as prepared materials. In addition, the remaining chlorine in the coupons showed increased stability as more washing cycles were applied, as noted by the increase in retained chlorine after washing, prior to rechlorination. That increased stability was more evident as the pH of the washing solution decreased. Figure 5.9 shows representative ATR-FTIR spectra before and after the application of the equivalent of 300 washing cycles of every solution. The changes in surface chemistry exhibited by the 20 bilayers coupons subjected to the 100 cycles of chlorination (Figure 5.7) were observed in the coupons subjected to the stability studies with Liquinox and the buffers, in which there is an apparent rupture of amide bonds with the subsequent formation of amines and carboxylic acids. As it was mentioned before, the chemical bond chlorine atoms form with amines possesses more stability than the bond chlorine builds with amides. If at lower levels of pH the formation of amines from the hydrolysis of amides takes place faster, such stability will be evident after fewer washing cycles. Similar stable behaviors have been observed in N-halamine compounds during storage at different levels of pH (Worley and Williams 1988). After exposure to 300 equivalent washing cycles by Liquinox detergent (pH 8.6), or wash buffers of pH values 3, 5, or 7, the antimicrobial materials had equivalent ($P > 0.05$) numbers of N-halamines as prepared materials. These results support that the antimicrobial coating is stable and retains antimicrobial character after repeated use.

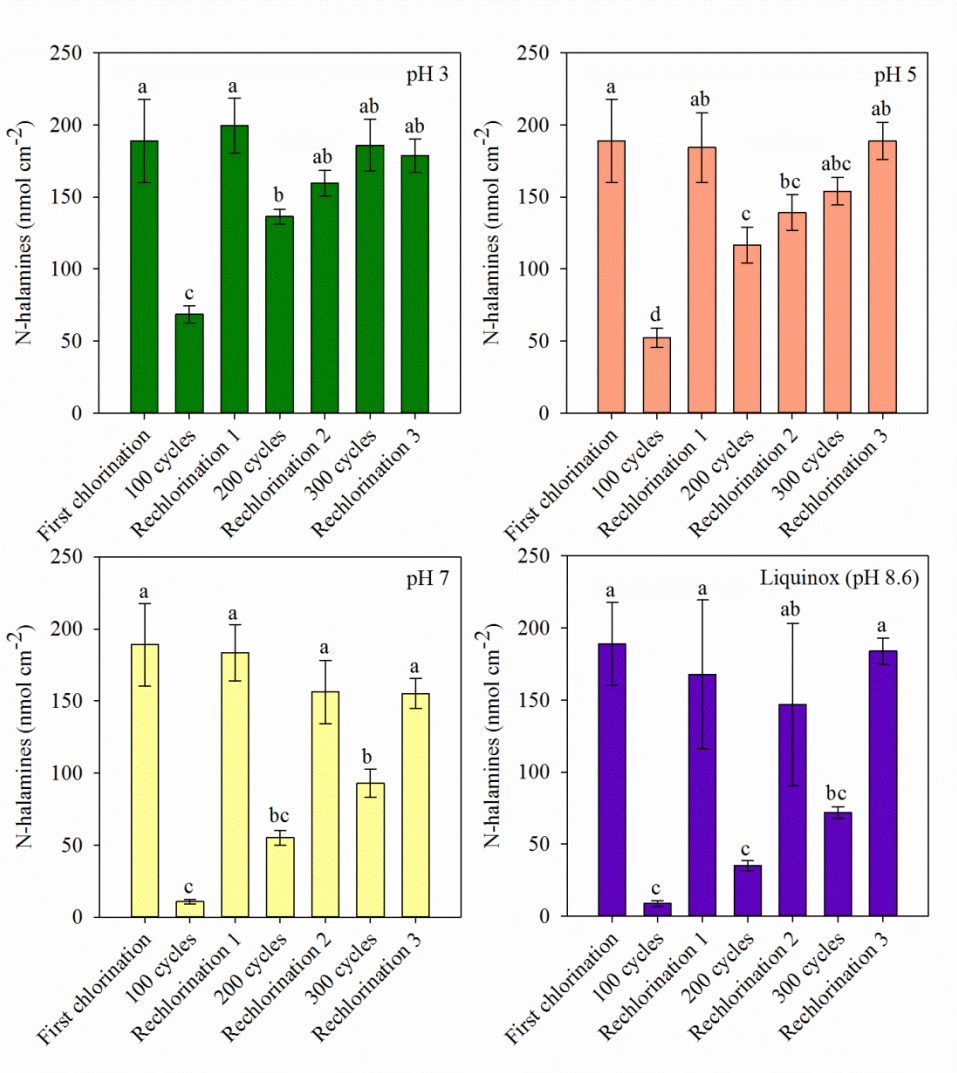

Figure 5.8 Stability studies of modified PE coupons having 20 bilayers toward repeated washing. Treatments represent average values of 3 replicates ± 1 standard deviations. Treatments with the same letter are not significantly different ($P > 0.05$).

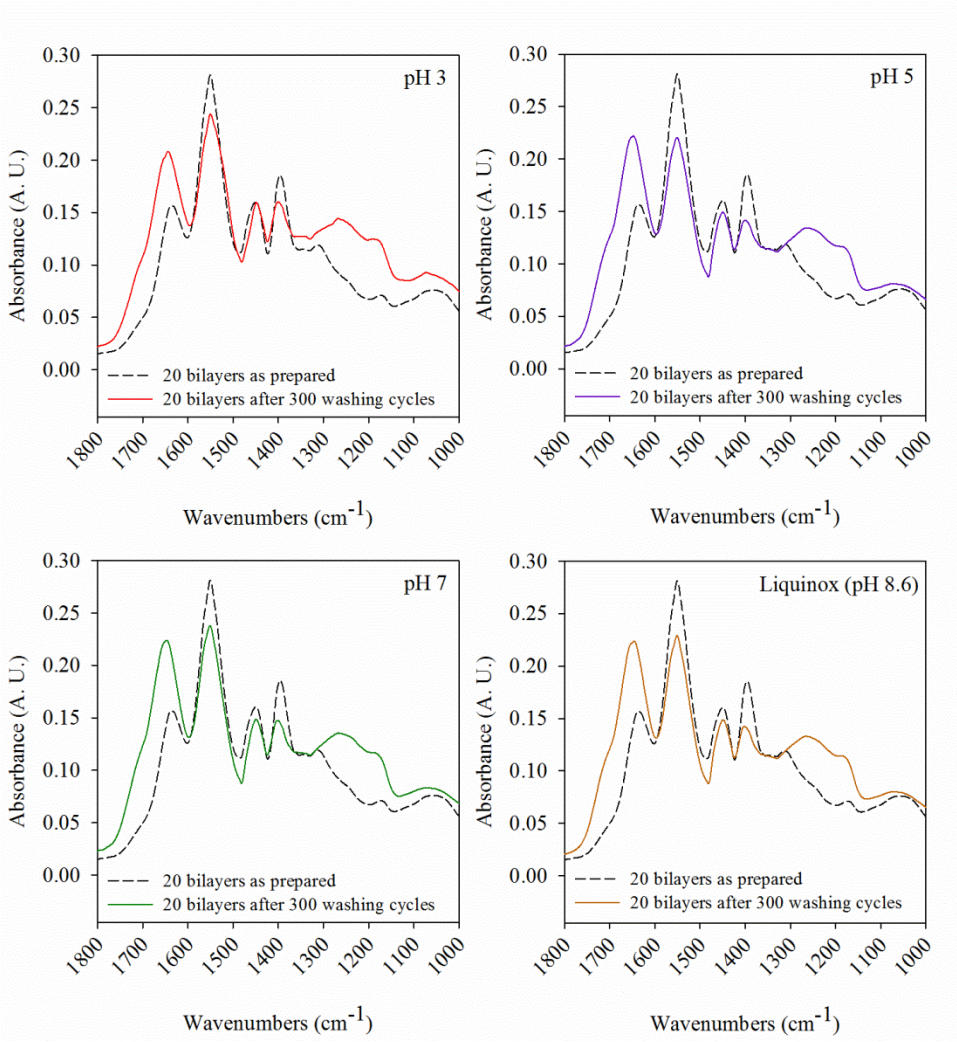

Figure 5.9 Representative ATR-FTIR spectra of 20 bilayers coupons as prepared (dashed line) and after exposure to 300 washing cycles of different solutions (solid line).

5.4.5 X-Ray Photoelectron Spectroscopy (XPS)

The surface chemistry of native (clean), UV-O_3 treated, and N-halamine modified PE was further characterized by XPS, a technique that probes only the top several nanometers of a surface, to better understand changes to specific chemical bonds in the coating during preparation (Table 5.2) and after exposure to repeated chlorination cycles

and various washing solutions (Tables 5.2, 5.3 and 5.4). The surface chemistry exhibited a change as the PE coupons were modified. The presence of oxygen and nitrogen indicated the presence of PEI and PAA, which supports the previously observed changes in surface chemistry confirmed through ATR-FTIR (Figure 2). Figure 9 shows the high resolution bands of carbon (C 1s), oxygen (O 1s) and Nitrogen (N 1s) with the deconvolution of the corresponding chemical bonds each element shares with other atoms in clean PE, UV-O3 treated PE, and 20 bilayers subjected to the regeneration and stability studies.

Table 5.2 Percentages of the atomic concentrations of all the treatments as determined by XPS.[a]

20 bilayers as prepared			
Treatment	C	O	N
Clean PE	100.00	-	-
UV-O_3 treated PE	82.6	17.4	-
5 bilayers	78.3	12.4	9.3
10 bilayers	73.6	15.4	11.0
15 bilayers	74.3	14.9	10.7
20 bilayers	73.5	15.6	10.9
20 bilayers subjected to the regeneration and stability studies[b]			
Treatment	C	O	N
100 rechlorinations	73.0	13.8	13.2
Liquinox	69.6	17.9	12.5
pH 3	76.1	13.4	10.6
pH 5	69.8	18.0	12.2
pH 7	70.7	19.1	11.5

[a]Results are representative values of at least 2 measurements.
[b]Results representative of 20 bilayers coupons subjected to 100 rechlorinations and 300 washing cycles with Liquinox, and pH 3, 5 and 7 buffers.

Table 5.3 Percentages of the different chemical bonds obtained from the deconvolution of C 1s.*

Treatment	C–C and C–H (285 – 284 eV)	C–O (287 – 286 eV)	C=O and O–C=O (289 – 288 eV)	N–C=O (288 – 287 eV)	C–N (286 – 285 eV)
20 bilayers (as prepared)	50.4	6.0	1.12	8.1	34.3
100 rechlorinations	41.6	8.2	1.3	8.0	40.8
Liquinox (pH 8.6)	53.5	2.1	2.1	15.1	27.4
pH 3	48.8	9.6	0.7	7.1	33.9
pH 5	45.8	5.9	3.7	15.5	29.1
pH 7	53.9	4.1	2.2	13.3	26.5

*Results are representative values of at least 2 measurements. Results are representative of modified PE coupons with 20 bilayers that were subjected to 100 rechlorinations and to 300 washing cycles with detergent Liquinox and with pH 3, 5 and 7 buffers.

Table 5.4 Percentages of the different chemical bonds obtained from the deconvolution of O 1s and N 1s.*

Treatment	O–C=O and N–C=O (531 – 530 eV)	C–O (533 – 532 eV)	N–C=O (401 – 400 eV)	$N–H_2$ (400 – 399 eV)
20 bilayers (as prepared)	79.1	20.9	27.5	72.5
100 rechlorinations	89.0	11.0	13.5	86.5
Liquinox (300 cycles)	72.9	27.1	18.8	81.2
pH 3 (300 cycles)	69.6	30.4	13.2	86.8
pH 5 (300 cycles)	77.4	22.6	8.9	91.2
pH 7 (300 cycles)	79.1	21.0	5.2	94.8

*Results are representative values of at least 2 measurements. Results are representative of modified PE coupons with 20 bilayers that were subjected to 100 rechlorinations and to 300 washing cycles with detergent Liquinox and with pH 3, 5 and 7 buffers.

After repeated rechlorinations or exposure to various wash solutions, there was no substantial change to the surface atomic concentrations of Carbon, Oxygen, and Nitrogen (Table 5.2, Figure 5.10). These results support that the antimicrobial coatings are stable after repeated use. While the overall atomic concentration remains unchanged, there are changes in specific chemical bonds after deconvolution of the high resolution spectra, most notably in the O 1s and N 1s spectra (Tables 5.3 and 5.4, Figure 5.10) (Lai and others 2009). Indeed, the analysis of N 1s and O 1s spectral deconvolution confirms the results of ATR-FTIR analysis: a rupture of amide bonds suggested by the reduction of the percentage corresponding to the N–C=O deconvolution peak and an increase in the percentages of C–O or N–C=O and O–C=O, indicating formation of carboxylic acids. A greater reduction in the percentage of N–C=O binding energy after exposure to pH 3 wash buffer was observed. This is expected as amide bonds hydrolyze more readily in acidic conditions (Smith and Hansen 1998). Overall, these results support the conclusions from the ATR-FTIR and N-halamine quantification analyses, that after extended exposure to chlorine, alkaline detergent, or wash buffers of neutral to acidic pH values, there are subtle changes in the specific nature of the N-halamine forming moieties, but the coating remains intact and able to form equivalent antimicrobial N-halamines compared to as prepared materials.

From the surface analysis results it becomes apparent that the main change in surface chemistry the N-Halamine modified undergoes is hydrolysis of amides (Figure 5.11), which may regenerate continuously as the coupons are used and exposed to deteriorating agents (bleach, detergents, etc.).

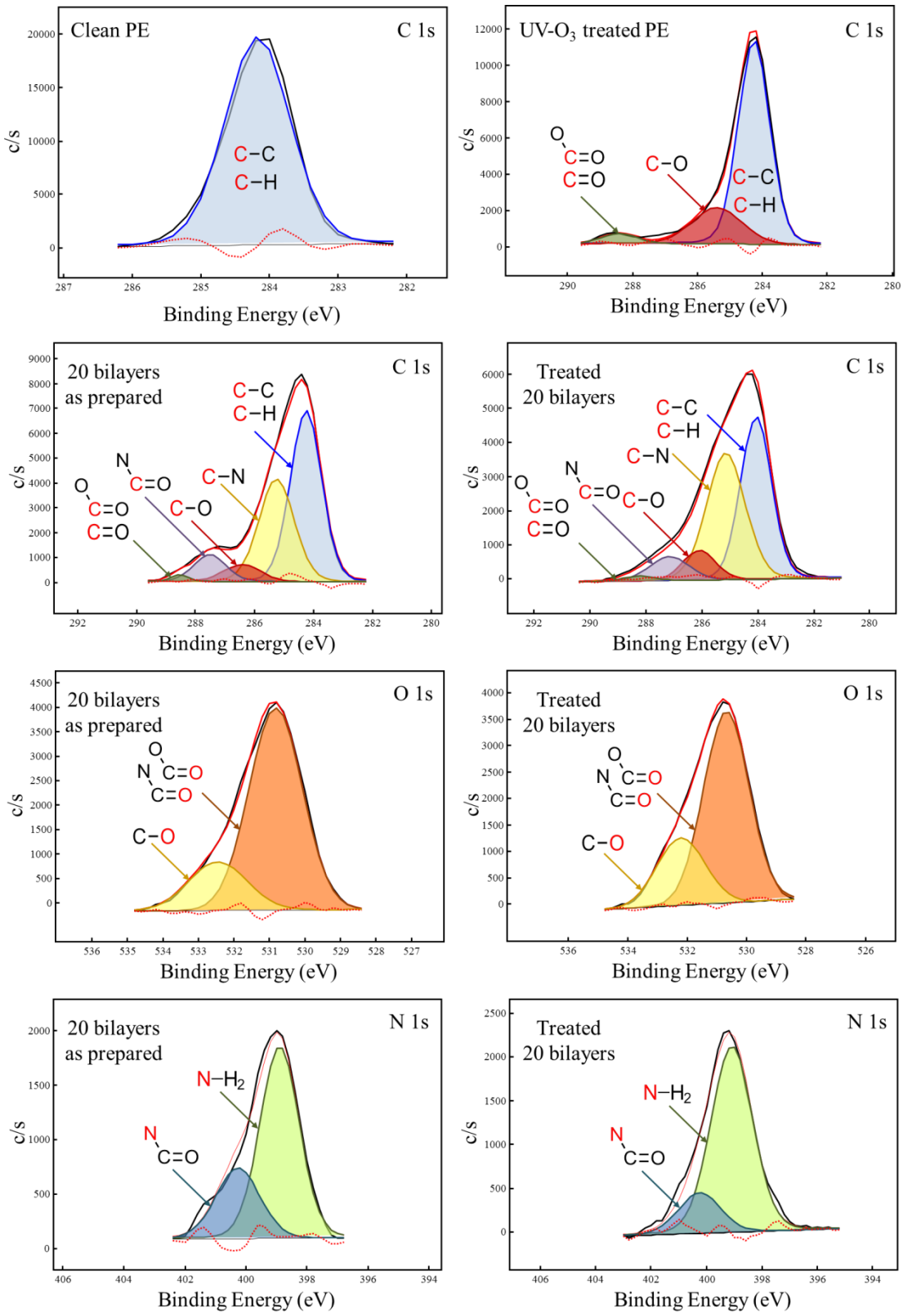

Figure 5.10 Representative high resolution bands from the XPS analysis.

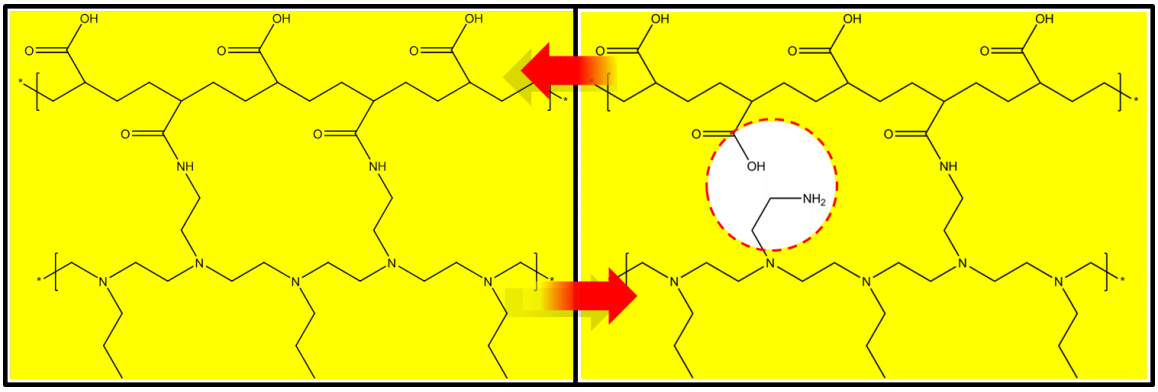

Figure 5.11 Possible mechanism behind the stability of the N-halamine coating applied on PE.

5.4.6 Storage study

Figure 5.12 shows the data fitted with Equation 2. The Weibull's model parameters (*k* and *n*) were (respectively) 0.008 and 0.97 (4 °C); 0.031 and 0.95 (20 °C); and 0.32 and 1.08 (37 °C). The values of R^2 were 0.94 (4 °C), 0.96 (20 °C) and 0.88 (37 °C). As expected, the speed at which chlorine is released increased with temperature. Comparable results have been obtained in previous works involving storage studies of N-halamine compounds (Worley and Williams 1988).

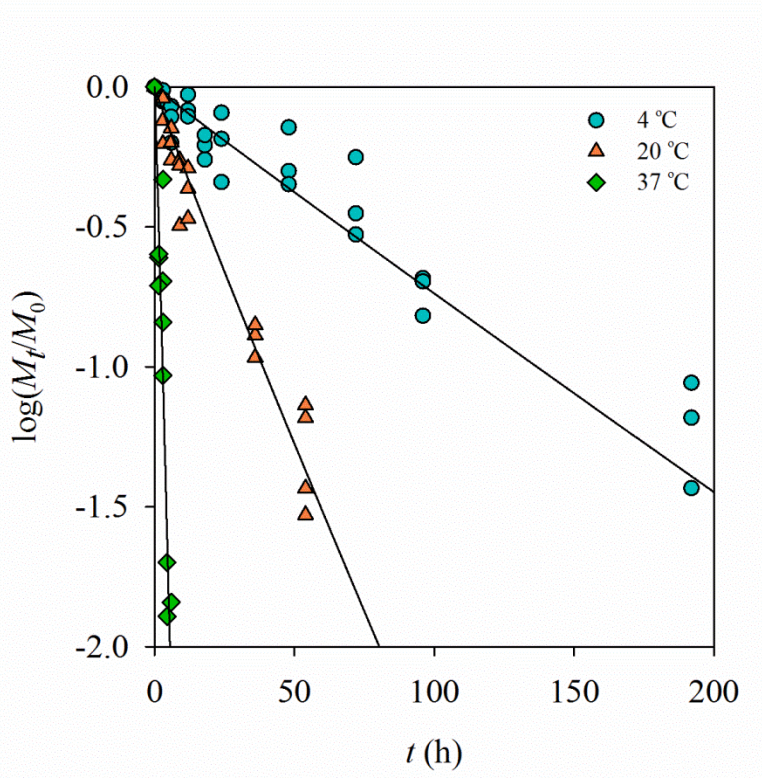

Figure 5.12 Data from the storage study fitted with Equation 2.

5.5 Conclusions

N-halamine forming moieties were introduced to the surface of PE via a facile layer-by-layer coating method. Materials were characterized by changes in surface chemistry, quantification of antimicrobial N-halamines, antimicrobial activity against *Listeria monocytogenes,* and stability after repeated rechlorinations and exposure to a range of acidic to alkaline washing solutions. Successful surface modification of PE was confirmed through ATR-FTIR and XPS. N-halamine chlorination followed the exponential association model, indicating similar levels of chlorination in materials coated with 10 to 20 bilayers and a plateau in chlorination after 10 minutes exposure to chlorine. N-halamine modified chlorinated PE was able to reduce the initial population of

L. monocytogenes in more than 5 logarithmic cycles. After exposure to up to 300 washing cycles with Liquinox and pH 3, 5 and 7 buffers, there was some change in the exact nature of N-halamine forming moieties (chemical bonds). However, the overall number of antimicrobial N-halamines was unchanged. The storage study conducted on 5 bilayers PE coupons revealed that the release of chlorine in water follows an almost linear behavior that can be characterized with the Weibull model. These results support that N-halamine coatings prepared by the layer-by-layer deposition method described herein result in robust antimicrobial materials, capable of repeated reuse in conditions typical of a food processing environment.

5.6 Acknowledgements

This material is based upon work supported by the National Institute of Food and Agriculture, U.S. Department of Agriculture under project number 2011-65210-20059 and in part by the Center for Hierarchical Manufacturing at The University of Massachusetts Amherst, an NSF Nanoscale Science & Engineering Center supported by the National Science Foundation under NSF Grant No. CMMI-0531171. The authors would like to thank Prof. Thomas J. McCarthy and Jacob Hirsh for assistance in the XPS analysis.

CHAPTER 6

LAYER-BY-LAYER ASSEMBLY OF ANTIMICROBIAL COATINGS WITH BOTH CATIONIC AND N-HALAMINE CHARACTER[5]

6.1 Abstract

A method to prepare an antimicrobial coating through layer-by-layer (LbL) assembly is reported. The surface modification was carried out by coating 2 alternating layers of branched polyethyleneimine (PEI) and styrene maleic anhydride copolymer (SMA) onto the surface of polypropylene (PP), followed by heating to promote covalent bond formation. The resulting coatings had low surface energy, equivalent to that of unmodified materials ($P > 0.05$), and presented enhanced antimicrobial character due to the presence of both cationic and N-halamine forming chemical structures. In its unchlorinated form, the coating was able to inactivate *Listeria monocytogenes* by ~ 3 logarithmic cycles (~ 99.9% reduction) as a result of its cationic nature. Chlorination of the N-halamines increased the antimicrobial activity of the coating to > 5 logarithmic cycles (> 99.999% reduction) in the same period. Microbial inactivation kinetics showed a Weibullian behavior when the coating was unchlorinated and a sigmoidal behavior when chlorinated, suggesting that cationic and N-halamine antimicrobial moieties presented different, but possibly synergistic, mechanisms of activity. Microscopy analysis confirmed that the reduction in the microbial load was a result of the biocidal effects of the coating and not due to bacterial adhesion onto the modified surface. Finally, the modified surface was able to be repeatedly rechlorinated. The reported antimicrobial

[5] Submitted to Langmuir.

coating can be prepared through layer-by-layer assembly and presents greater than 99.999% reduction of microorganisms in the form of N-halamine moieties and approximately 99.9% microbial reduction in the cationic form.

Keywords: Antimicrobials, surface modification, N-halamines, polycations, reusability.

6.2 Introduction

Contamination of materials used in healthcare and food processing industries by pathogenic microorganisms remains a significant challenge to public health (Jiang and others 2004; Cools and others 2005; Vorst and others 2006; Wilks and others 2006; Rodriguez and others 2007; Jampala and others 2008; Asri and others 2014). A number of antimicrobial coatings have therefore been proposed in an effort to reduce infections resulting from such cross-contamination (Jiang and others 2004; Jampala and others 2008; Hequet and others 2011; Chen and others 2012; Asri and others 2014). Incorporation of small molecule biocides (e.g. antibiotics, metal nanoparticles) into a coating is effective; however, reliance on migration of an antimicrobial agent for activity has two significant drawbacks. Materials inherently lose antimicrobial activity over time, and migration of small molecule antimicrobial agents may promote development of microbial resistance (Kocer and others 2010; Hequet and others 2011). Polycationic and N-halamine based coatings have been explored to overcome these challenges. N-halamines constitute a diverse class of antimicrobial compounds. They are generally organic substances characterized by the presence of nitrogen atoms which are normally in the form of amines, amides and imides. These nitrogenous functional groups are able to form covalent bonds with halogens (N–X) like bromine, iodine, and chlorine. N-halamines exert antimicrobial activity towards a wide range of microorganisms by releasing their halogen through a mechanism believed to include cell membrane disruption and inner cell molecules oxidation. The most remarkable characteristic of N-halamines is their ability to be recharged with halogens for many cycles, providing

continuous antimicrobial activity (Williams and others 1987; Worley and Williams 1988; Lauten and others 1992). Even though the effectiveness of N-halamine derived coatings has been extensively demonstrated, they are generally ineffective against microorganisms in their unchlorinated state, and their need for continuous rechlorination can affect their chemical integrity (Goddard and Hotchkiss 2008; Kocer and others 2010).

Cationic polymers represent another well-studied class of antimicrobial substances which include polylysine (Fang and others 2014), chitosan (Mansilla and others 2013), and polyamines (Wang and others 2010; Xia and others 2011). They are believed to impart antimicrobial activity by disrupting cell membrane functions mainly through ionic exchange (Kugler and others 2005; Lichter and Rubner 2009; Chakraborti and others 2013). A hurdle to utilization of cationic polymer based antimicrobial coatings is their risk of fouling by organic molecules (Onnis-Hayden and others 2011).

We hypothesized that incorporation of both cationic and N-halamine moieties within an antimicrobial coating would result in a material with constant antimicrobial activity which could be strengthened by exposure to a halogenated solution. To the best of our knowledge, no extensive studies have been made in which an antimicrobial coating integrates both cationic and N-halamine properties. To test our hypothesis, the objective of the present study was to create a coating with dual antimicrobial activity (cationic and N-halamine) through LbL deposition of branched polyethyleneimine (PEI) and styrene maleic anhydride copolymer (SMA), characterize it, and demonstrate its effectiveness after application onto polypropylene (PP) against the pathogen *Listeria monocytogenes*.

6.3 Materials and methods

6.3.1 Antimicrobial coating application onto PP coupons

Preparation of PP coupons. PP pellets (isotactic, Scientific Polymer Products, Ontario, NY) were cleaned by sonication first with isopropanol (Fisher Scientific, Pittsburgh, PA), then with acetone (Fisher Scientific, Pittsburgh, PA), and finally with DI water (2 cycles of 10 min were applied for each solvent). Cleaned PP pellets were left to dry overnight under anhydrous calcium sulfate (RH < 20%) and then hot pressed at 170 °C with a load force of 9,000 lbs (Tian and others 2013). Coupons of 2 × 2 cm were cut from the obtained films (thickness 0.5 ± 0.1 mm), and cleaned and dried under the same conditions applied to the PP pellets.

PP surface activation. The 2 × 2 cm coupons were UV-Ozone irradiated from one side with a Jelight Co. model 42 UVO Cleaner (Irvine, CA) for 15 min (Bastarrachea and others 2013; Bastarrachea and others 2014) (this step will be referred as UV-O_3). To create surface anhydride groups, UV-O_3 coupons were shaken for 2 h at room temperature in a 0.1 mM solution of 2-ethoxy-1-ethoxycarbonyl-1,2-dihydroquioline (EEDQ, MW 247.3, Sigma-Aldrich, St. Louis, MO) in 50 mM 2-(*N*-morpholino) ethanesulfonic acid (MES) sodium salt (GenScript Inc., Piscataway, NJ) buffer (pH 5.5) (Martin and others 1993). This step will be referred as EEDQ. EEDQ treated coupons were rinsed with 1:100 methanol:DI water solution and dried under an air gun.

Layer-by-layer assembly of antimicrobial coating. Branched polyethyleneimine (PEI, MW 25,000 Da, Sigma-Aldrich, St. Louis, MO) and styrene maleic anhydride copolymer

(SMA, MW 6,000 Da, Scientific Polymer Products, Ontario, NY) were dissolved in acetone (Karakus and others 2013b) at a concentration of 60 and 43.2 mg mL^{-1} (respectively) by sonication for 20 min or until completely dissolved. This proportion of PEI and SMA was chosen so that there would be approximately 3 polymer chains of SMA for every polymer chain of PEI. Alternating volumes of the PEI and SMA solutions were spin coated onto an anhydride activated PP coupon (EEDQ treated) for 1 min at 3000 rpm to produce two bilayers. After spin coating, a preheating step was applied to the coupons at 80 °C for 5 h in order to promote amide bond formation between the PEI and SMA layers (Berthier and others 2013; Karakus and others 2013a). This temperature was chosen because it is in the lower limit of the continuous service temperature range for PP (Müller and others 2010). Coupons were then subjected to an alkaline treatment (1 h at room temperature in a 50 mM pH 10 MES sodium salt buffer) to promote anhydride rings opening (Hermanson 2008). Coupons were then rinsed with DI water, dried under an air gun, and subjected to a final heating step of 12 h at 100 °C to promote imide ring closing (Song and Baker 1992; Scott and Macosko 1994; Schafer and others 1995; Liu and others 2010; Gule and others 2012; Li and others 2013) (Figure 6.1). Coupons were then kept in closed glass Petri dishes until usage.

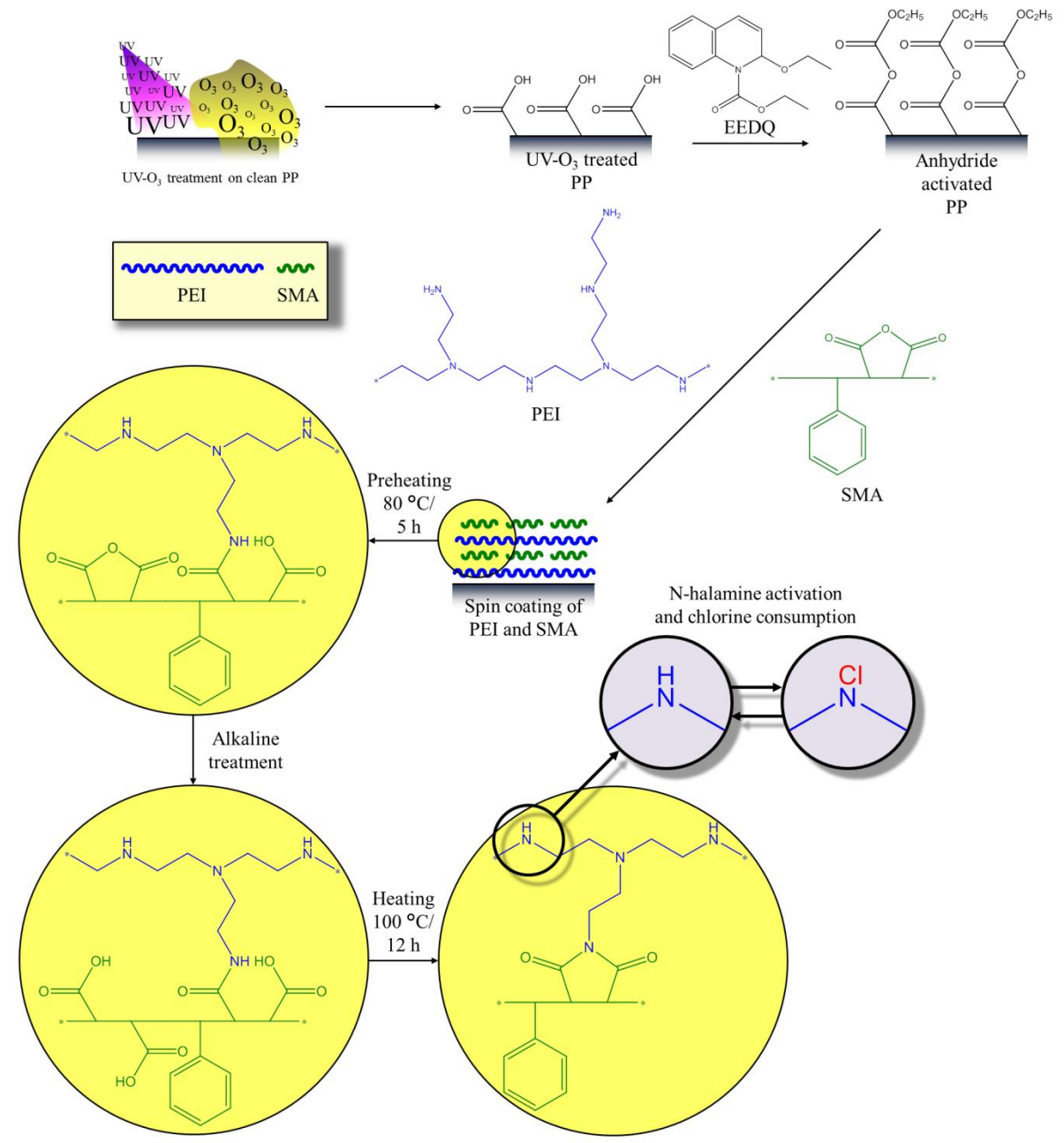

Figure 6.1 Antimicrobial coating preparation process.

6.3.2 Attenuated Total Reflectance Fourier Transform Infrarred Spectroscopy (ATR-FTIR)

Changes in surface chemistry were analyzed by ATR-FTIR after every step in the surface modification process with an IRPrestige 21 spectrometer (Shimadzu Corp., Tokyo, Japan). Coupons from 3 separately prepared sets were analyzed (3 replicates), with at least 1 randomly chosen coupon from each preparation step. Three spots were analyzed per coupon using Happ-Genzel apodization with a resolution of 4 cm^{-1}, capturing 32 scans per spot. Spectra were obtained with the IR-solution software (Shimadzu Corp., Tokyo, Japan) and interpreted with the KnowItAll software (Biorad Laboratories, Philadelphia, PA). Representative spectra from every step of the antimicrobial coating preparation were selected and combined for comparison. After the rechargeability evaluation (explained below), coupons were analyzed with the same criteria (Bastarrachea and others 2013; Bastarrachea and others 2014).

6.3.3 X-Ray Photoelectron Spectroscopy (XPS)

As a complementary source of coating characterization, a 0.5 × 0.5 cm piece of modified PP cut from a randomly selected coupon at every step of the antimicrobial coating preparation was analyzed using a Physical Electronics Quantum 2000 (Physical Electronics, Chanhassen, MN). A single 100 μm spot was analyzed from every coupon at an angle of 45° relative to the coupons' surface with Al Kα excitation. Survey scans were collected at a pass energy of 187.85 eV, and high resolution spectra of C 1s, O 1s and N 1s were collected at a pass energy of 46.95 eV. Atomic percentages and high resolution

spectra were analyzed with the Multipak software version 6.1A (Physical Electronics, Chanhassen, MN). High resolution bands of C 1s, O 1s and N 1s were fitted using the Gaussian-Lorentzian model with 90% Gaussian. Three coupons from every surface modification step were analyzed, each taken from separately prepared sets (3 replicates) (Bastarrachea and Goddard 2013; Bastarrachea and others 2014).

6.3.4 Atomic Force Microscopy (AFM)

Surface topographies were analyzed with a Dimension 3100 Atomic Force Microscope (Digital Instruments, Santa Barbara, CA) under tapping mode with a Si N-type tip (uncoated, f_0: 200 – 400 kHz, Applied NanoStructures, Inc., Mountain View, CA). Three measurements were taken from PP and as prepared modified PP coupons. The SPIP^{TM} software version 6.0.6 (Scanning Probe Image Processor, Image Metrology, Denmark) was used to calculate mean square roughness (S_q).

6.3.5 Primary amine quantification

The Acid Orange 7 (AO7) colorimetric assay (Uchida and others 1993) was followed to determine the primary amine content onthe antimicrobial coating. At least two 1 × 1 cm coupons were taken from each of 3 separately prepared sets of samples (3 replicates, at least 2 coupons per replicate) for analysis. PP and modified PP coupons were put in contact with a pH 3, 1 mM solution (1 mL cm^{-2} of modified surface) of AO7 dye (Orange (II) (Cert), Acros Organics, Fair Lawn, NJ) and shaken for 3 h. Then, coupons were rinsed with pH 3 DI water to remove not bound AO7 dye. Following

rinsing, coupons were immersed in 5 mL of pH 12 DI water and shaken for 15 min to desorb dye. Absorbances of the solutions containing desorbed dye were read at 455 nm and the concentrations were determined from a standard curve prepared with different AO7 concentrations in pH 12 DI water.

6.3.6 N-halamine quantification

To quantify the N-halamine content of the antimicrobial coating a colorimetric assay published earlier was followed (Bastarrachea and Goddard 2013; Bastarrachea and others 2013; Bastarrachea and others 2014). Coupons were first chlorinated by exposure to 200 ppm of chlorine prepared from a NaClO solution (Acros Organics, Fair Lawn, NJ), which chlorine content was previously confirmed through a standard procedure (American Society for Testing and Materials 2008). This chlorine concentration was chosen because it is the maximum chlorine concentration allowed for disinfection by federal agencies (Rutala and Weber 2008). During chlorination, coupons were randomly taken at different points in time and rinsed with copious DI water to remove unbound chlorine. To quantify N-halamine content of the chlorinated antimicrobial coatings, rinsed coupons were immersed in 2 mL of DI water, to which 50 μL of the DPD reagent were applied. DPD reagent was prepared by mixing 1 pack of N,N-diethyl-p-phenylenediamine DPD total chlorine reagent powder (Hach Co., Loveland, CO) with 1 mL of DI water. The solutions containing the coupons were shaken for 5 min for color formation and absorbances were read at 512 nm. N-halamine content was determined from a standard curve prepared with multiple chlorine concentrations. Chlorination kinetics (and time of chlorine saturation) was determined by fitting data with the

exponential association model using GraphPad Prism 5 version 5.04 (GraphPad Software Inc., La Jolla, CA):

$$NH = NH_{asympt}(1 - e^{-Kt}) \quad (1)$$

where NH is the N-halamine content in nmol cm^{-2}, NH_{asympt} is the asymptotic N-halamine content (in nmol cm^{-2}, theoretical amount of N-halamines at saturation), K is the exponential rate constant (min^{-1}) and t is the time (min).

6.3.7 Surface pK_a determination

Surface pK_a of the antimicrobial coating was quantified following a protocol reported in previous works (Holmes-Farley and others 1985; Van der Maaden and others 2012). Buffers (pH levels from 2 to 10) were prepared with 10 mM 4-(2-hydroxyethyl)-1-piper-azineethane-sulfonic acid (HEPES, Sigma-Aldrich, St. Louis, MO) solutions. For every pH level evaluated, a 5 μL HEPES buffer drop was applied in at least 2 spots of the surface of a previously cut 1 × 2 cm PP and modified PP coupon. After 15 s, the static contact angle θ_S was measured at room temperature with a drop shape analyzer DSA100 using its Drop Shape Analysis software version 1.91.0.2 (Krüss, Hamburg, Germany). Coupons from 3 sets prepared separately were analyzed (3 replicates), with at least one coupon per replicate. To calculate surface pK_a, data from each replicate were fitted with the sigmoidal dose-response model through non-linear regression using the GraphPad software:

$$\theta_S = \theta_{min} + \frac{\theta_{max} - \theta_{min}}{\left(1 + 10^{(\mathrm{p}K_a - pH)}\right)} \quad (2)$$

where θ_S is the static contact angle (in degrees), θ_{max} and θ_{min} are the maximum and minimum angles obtained from the sigmoidal curve (respectively), *pH* is the pH level of the buffer used.

6.3.8 Surface energy determination

The Zisman plot method was applied to calculate surface energy (Zisman 1964; Kabza and others 2000; Combe and others 2004) (surface tension, γ_{GS}, in mN m^{-1}) of the antimicrobial coating. Advancing contact angle (θ_A) was obtained with the same DSA100 Drop Shape Analyzer using liquids of different surface tensions (Howard and McAllister 1957; Costanzo and others 1990): DI water (72.8 mN m^{-1}), glycerol (63 mN m^{-1}, Fisher Scientific, Pittsburgh, PA), ethylene glycol (47.7 mN m^{-1}, Acros Organics, Fair Lawn, NJ) and acetone (25.8 mN m^{-1}, Fisher Scientific, Pittsburgh, PA). A 5 µL drop of each liquid was applied in at least 2 spots of the surface of 1 × 2 cm coupons of PP and modified PP. For each liquid and each type of PP, at least 1 coupon was analyzed from each of 3 separately prepared sets (3 replicates). The cosine of the values of θ_A (in radians) was plotted against the values of surface tension of the corresponding liquid (γ_{GL}) for each treatment (PP and modified PP). After applying linear regression analysis to the data with the GraphPad software, γ_{GS} values for PP and modified PP were obtained from the regression curves when Cos(θ_A) equals 1.

6.3.9 Antimicrobial evaluation

Antimicrobial activity of the coatings was studied following a protocol published earlier (Bastarrachea and others 2013; Bastarrachea and others 2014). Bacterial suspensions of *L. monocytogenes* Scott A (provided by Dr. Martin Wiedmann, Food Science Department, Cornell University, Ithaca, NY) were prepared by streaking a loopful of stock culture kept at – 80 °C in 25% glycerol onto Tryptic Soy Agar (TSA, Difco, Becton Dickinson, Sparks, MD), which was incubated at 37 °C for 24 h. Then, a single colony was inoculated in 9 mL of sterile Tryptic Soy Broth (TSB, Difco, Becton Dickinson, Sparks, MD) and incubated overnight for 14 h at the same temperature. A 1% dilution of this overnight broth was prepared with fresh and sterile TSB, and incubated for 4 h at 37 °C. The bacterial suspension with approximately 6 log(CFU mL^{-1}) was obtained by preparing a 0.01% dilution of the broth incubated for 4 h using DI water. To evaluate the antimicrobial effectiveness, PP, chlorinated PP, modified PP, chlorinated modified PP, bacterial suspension alone, and bacterial suspension with chlorine added were tested. PP and modified PP 1 × 1 cm coupons were chlorinated for 45 min with a solution having 200 ppm of chlorine following the same procedure explained before. The chlorination time was chosen because (as it will be explained later), that is the time required to reach chlorine saturation. A volume of 1 mL of bacterial suspension was put in contact with four 1 × 1 cm coupons of each treatment in individual test tubes and incubated for 2 h with rotation (60 rpm) at 32 °C. This temperature was selected because according to previous studies, it is within the range of maximum biocidal effectiveness of chlorine against *L. monocytogenes* (Elkest and Marth 1988a). For the case of bacterial

suspension with chlorine added, the amount of chlorine was adjusted to mimic the amount of chlorine given by the four 1 × 1 cm coupons of chlorinated modified PP. After the 2 h of incubation, serial 10% dilutions were prepared from the bacterial suspensions. For the first dilution, neutralizing buffer was used to quench chlorine (Difco, Becton Dickinson, Sparks, MD), and subsequent dilutions were prepared with 0.9 % saline water. A volume of 100 μL of each dilution was inoculated onto TSA plates using an automated spiral plater Autoplater 4000 (Spiral Biotech Inc., Norwood, MA) and incubated for 48 h at 37 °C. After incubation, colonies were counted with a plate reader Scan® 500 (Interscience, Saint-Non-la-Brèteche, France). In order to lower the detection limit to 1 log(CFU mL^{-1}), the whole volume of the first dilution after incubation was inoculated manually onto 3 TSA plates (333 μL per plate). This antimicrobial evaluation was repeated 3 times using coupons from separately prepared sets (3 replicates). For the chlorine rechargeability study (explained below) coupons were challenged against *L. monocytogenes* at the 10^{th} rechlorination under the same conditions explained for the antimicrobial evaluation.

The inactivation kinetics given by the antimicrobial coatings in cationic and N-halamine form was evaluated as follows (Bastarrachea and others 2013). Multiple test tubes with 1 mL of bacterial suspension with approximately 6 log(CFU mL^{-1}) containing four 1 × 1 cm coupons of the corresponding treatment were incubated for up to 2 h under the same conditions described above. Test tubes were taken randomly over time, the corresponding dilutions prepared in the same way explained before, and inoculated onto TSA plates to be incubated for 48 h at 37 °C. Number of survivors was quantified as in

the antimicrobial evaluation. Data were fitted with the following models (Peleg 2003; Peleg 2006) using non-linear regression with the software GraphPad:

$$\log\left(\frac{N}{N_0}\right) = -kt^n \quad (3)$$

$$\log\left(\frac{N}{N_0}\right) = -\frac{at}{(b+t)} - \frac{ct}{(d-t)} \quad (4)$$

Equation 3 corresponds to the Weibull model where $\log(N/N_0)$ is the survival ratio, k is the kinetic constant in min^{-1}, n is the shape factor, and t is the time in minutes. Equation 4 corresponds to a sigmoidal isothermal semi-logarithmic model, where a, b (min), c and d (min) are temperature dependent coefficients. Two replicates were performed for the inactivation kinetics evaluation.

6.3.10 Scanning Electron Microscopy (SEM)

In order to asses bacterial adhesion on the antimicrobial coatings, after the antimicrobial evaluation PP and modified PP coupons were rinsed 3 times with sterile DI water and then immersed for 45 s in absolute ethanol (Acros Organics, Fair Lawn, NJ) to fix any attached bacteria (Djordjevic and others 2002). Then, coupons were sputter coated with gold for 20 s under argon with a Cressington Sputter Coater 108 Auto (Ted Pella, Inc., Redding, CA). Surfaces of the coupons were extensively observed with a scanning electron microscope JCM-6000 NeoScope (JEOL, Japan) at 10 kV, and at least 10 images were taken from coupons of each treatment.

6.3.11 Chlorine rechargeability of the antimicrobial coating

Modified PP coupons were subjected to 10 rechlorination cycles in order to evaluate the ability of the antimicrobial coating to be rechlorinated. The same conditions explained earlier were applied for chlorination (200 ppm chlorine), and 45 min of chlorination were applied in every cycle. N-halamine content was quantified through the DPD assay. Coupons were analyzed through ATR-FTIR as described before to evaluate changes in surface chemistry after the 10 rechlorinations.

6.3.12 Statistical analysis

In addition to the regression analyses, significant differences between treatments were determined when appropriate through the general linear model followed by Tukey's pairwise comparisons with the software Minitab version 16.1.1 (Minitab Inc., State College, PA), using a confidence interval of 95%.

6.4 Results and discussion

6.4.1 Surface characterization

An antimicrobial coating has been prepared via layer-by-layer assembly which exhibits dual antimicrobial functionality by presence of both cationic and N-halamine moieties (Figure 6.1). ATR-FTIR spectroscopy was performed at each step of the antimicrobial coating preparation to characterize changes in surface chemistry (Figure

6.2) (Smith 1999). Figure 6.2 contains different regions of the infrared range in which the spectra corresponding to every step of the antimicrobial coating application are displayed: (a) PP, (b) UV-O_3, (c) EEDQ, (d) spin coating, (e) preheating, (f) alkaline treatment, and (g) heating. The presence of the carbonyl group (C=O) from carboxylic acids can be observed in the 1740 – 1720 cm^{-1} range, and confirms activation by the UV-O_3 and EEDQ treatments (Figure 6.2, spectra b and c). After spin coating, an increase of the carbonyl group of carboxylic acids is observed, as well as the formation of a band at ~ 1650 cm^{-1} that corresponds to the carbonyl group of amides, (Figure 6.2, spectrum d). It can be observed from the increment in absorbance at ~ 1650 cm^{-1} and the decrease in the carbonyl group of carboxylic acids (1740 – 1720 cm^{-1}) that the amide bond formation increases during the preheating step (Figure 6.2, spectra e), which confirms crosslinking between PEI and SMA. After the alkaline treatment, the bands at ~ 1780 and ~ 1850 cm^{-1} that correspond to the vibration of C=O from anhydrides disappear (Figure 2, spectra d and e), which confirms the opening of the anhydride rings of SMA. Finally, after the heating step, the increase in absorbance from the carbonyl group of amides at ~ 1650 cm^{-1} (Figure 6.2, spectrum g) as well as the decrease in the absorbance of the O–H vibration from carboxylic acids in the 3400 – 3200 cm^{-1} range (Figure 2, spectra g), and the decrease in absorbance at ~ 1550 cm^{-1}, which belongs to the N–H bond in plane bend of secondary amines (Figure 2, spectrum g) confirm the closing of the ring that results in imide formation (Figure 6.1).

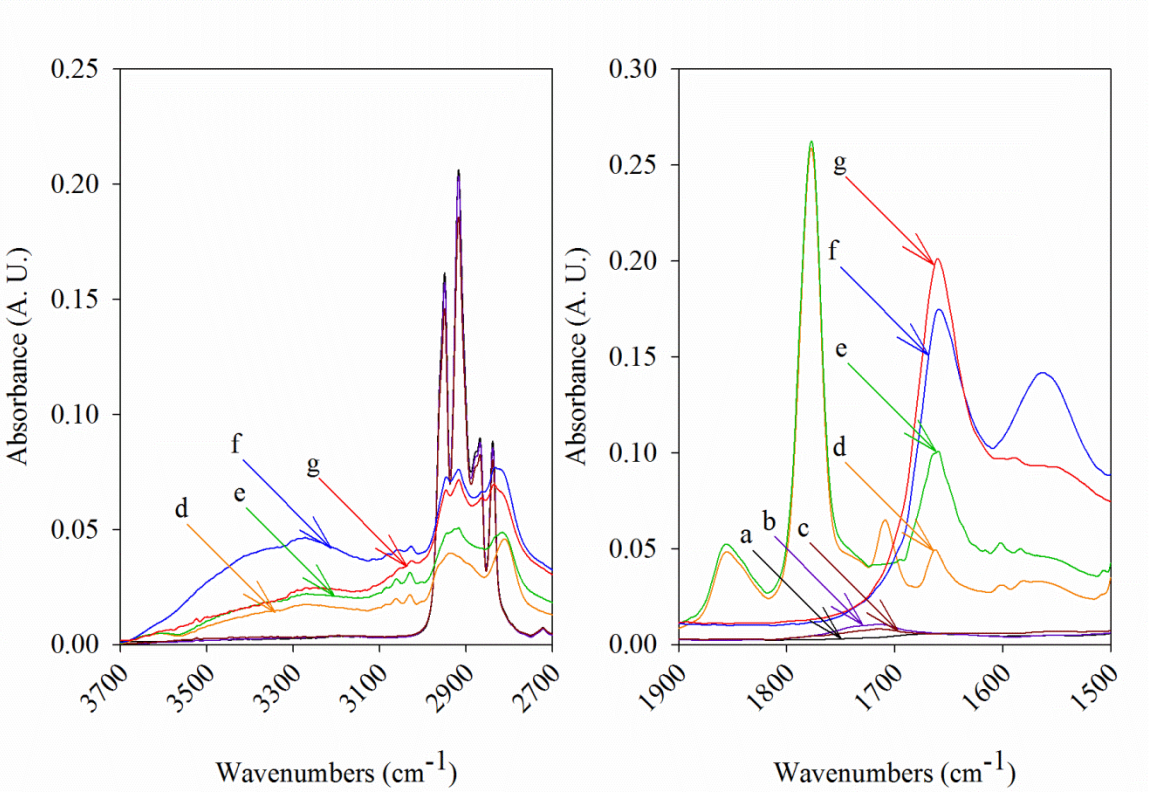

Figure 6.2 ATR-FTIR results showing characteristic bands throughout the antimicrobial coating preparation: PP (a), UV-O_3 (b), EEDQ (c), spin coating (d), preheating (e), alkaline treatment (f), and heating (g).

Table 6.1 shows the atomic percentages and the functional groups percentages from the deconvolution of the high resolution bands of C 1s, O 1s and N 1s at every step of the antimicrobial coating preparation. XPS confirmed the anhydride surface activation of PP after the EEDQ treatment, as noted by the increase in the O–C=O deconvolution band from O 1s (Figure 6.3). The effect given by the preheating and heating steps was also confirmed from the increase in the amide bond formation exhibited by the increase in the N–C=O deconvolution band from O 1s and N 1s (Figures 6.3 and 6.4). A decrease in the band that englobes both O–C=O and N–C=O in O 1s (Lai and others 2009) after the alkaline treatment and an increase in the deconvolution band characteristic of the C–O bond confirms the resulting anhydride ring opening.

Table 6.1 XPS analysis results. Results are average values of 3 replicates ± 1 standard deviation, treatments followed by the same letter within the same column are not significantly different ($P > 0.05$).

Atomic percentages			
Preparation step	C	O	N
Clean PP	97.9 ± 2.3[a]	2.1 ± 2.3[a]	0.0 ± 0.0[a]
UV-O_3	85.6 ± 0.8[b]	14.4 ± 0.8[b]	0.0 ± 0.0[a]
EEDQ	87.6 ± 1.2[b]	12.4 ± 1.2[b]	0.0 ± 0.0[a]
Spin coating	75.6 ± 0.3[c]	15.1 ± 0.6[b]	9.3 ± 0.9[b]
Preheating	73.3 ± 1.2[c]	12.5 ± 1.5[b]	14.2 ± 0.7[c]
Alkaline treatment	74.4 ± 1.0[c]	14.6 ± 1.5[b]	11.0 ± 2.0[b]
Heating	75.8 ± 2.4[c]	12.7 ± 1.4[b]	11.4 ± 1.2[b]

High resolution bands of C 1s					
Preparation step	C–C and C–H (285 – 284 eV)	C–O (287 – 286 eV)	C=O and O–C=O (288 – 287 eV)	C–O and C–N (286 – 285 eV)	N–C=O and O–C=O (288 – 287 eV)
Clean PP	100.0 ± 0.0[a]				
UV-O_3	73.2 ± 9.9[b]	22.6 ± 9.3[a]	4.3 ± 0.6[a]		
EEDQ	60.3 ± 10.7[bcd]	37.0 ± 11.2[a]	2.7 ± 0.8[b]		
Spin coating	63.8 ± 6.0[bc]			27.8 ± 6.0[a]	8.4 ± 0.1[a]
Preheating	45.2 ± 4.7[d]			43.0 ± 4.4[b]	11.8 ± 0.3[b]
Alkaline treatment	49.6 ± 1.7[cd]			39.4 ± 1.0[b]	11.1 ± 0.9[b]

High resolution bands of O 1s and N 1s				
Preparation step	C–O (533 – 532 eV)	N–C=O and/or O–C=O (531 – 530 eV)	N–C=O (401 – 400 eV)	N–H_2 (400 – 399 eV)
UV-O_3	24.8 ± 8.8[ab]	75.2 ± 8.8[ab]		
EEDQ	14.0 ± 0.5[bc]	86.0 ± 0.5[ac]		
Spin coating	29.1 ± 2.9[a]	71.1 ± 3.2[b]	23.5 ± 11.0[a]	76.5 ± 11.0[a]
Preheating	10.0 ± 3.6[c]	90.0 ± 3.6[c]	26.8 ± 4.2[ab]	73.2 ± 4.2[ab]
Alkaline treatment	17.9 ± 3.4[abc]	82.1 ± 3.4[abc]	24.0 ± 1.4[a]	76.0 ± 1.4[a]
Heating	8.6 ± 3.1[c]	91.4 ± 3.1[c]	43.7 ± 6.8[b]	56.3 ± 6.8[b]

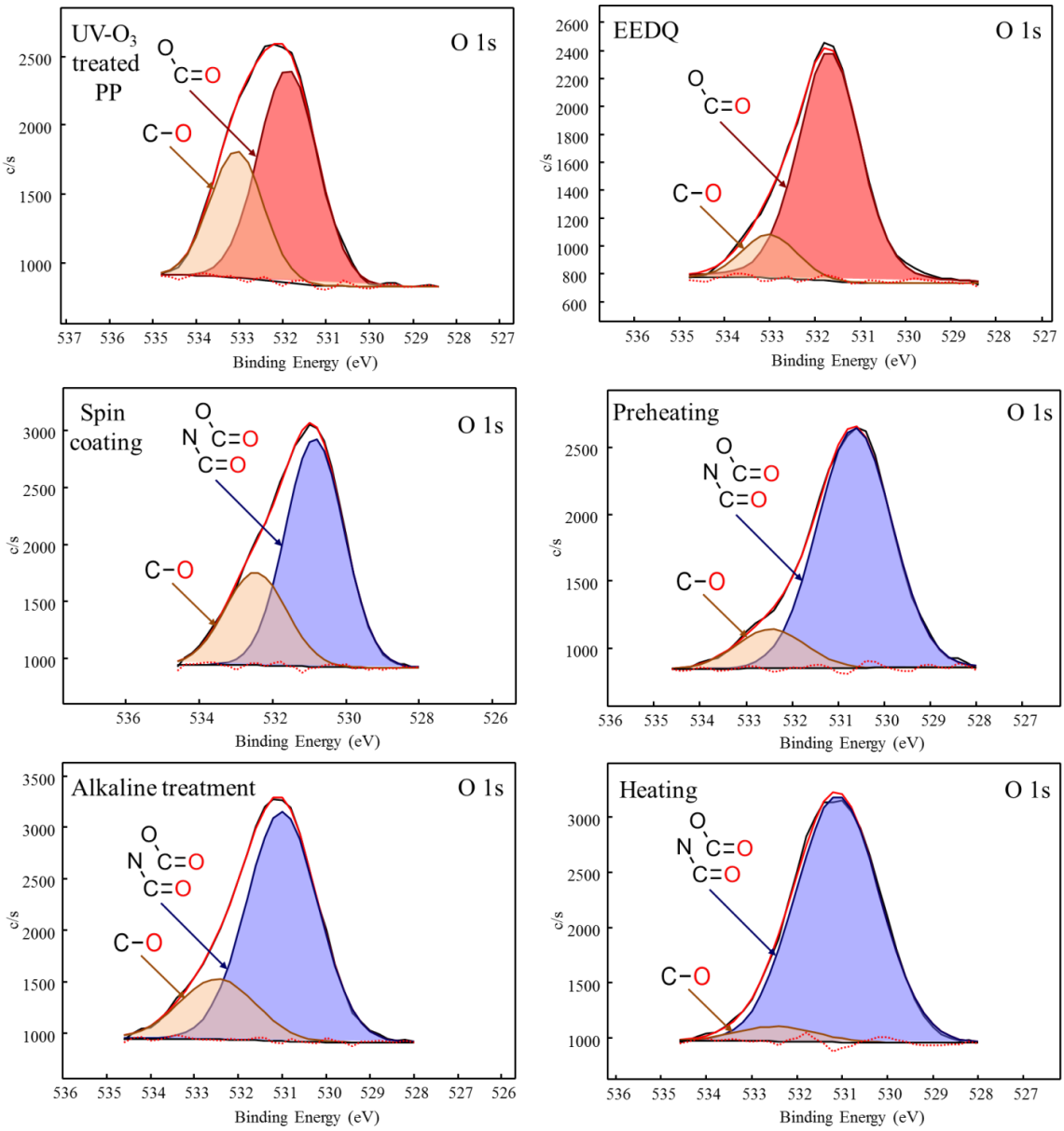

Figure 6.3 XPS high resolution bands of O 1s.

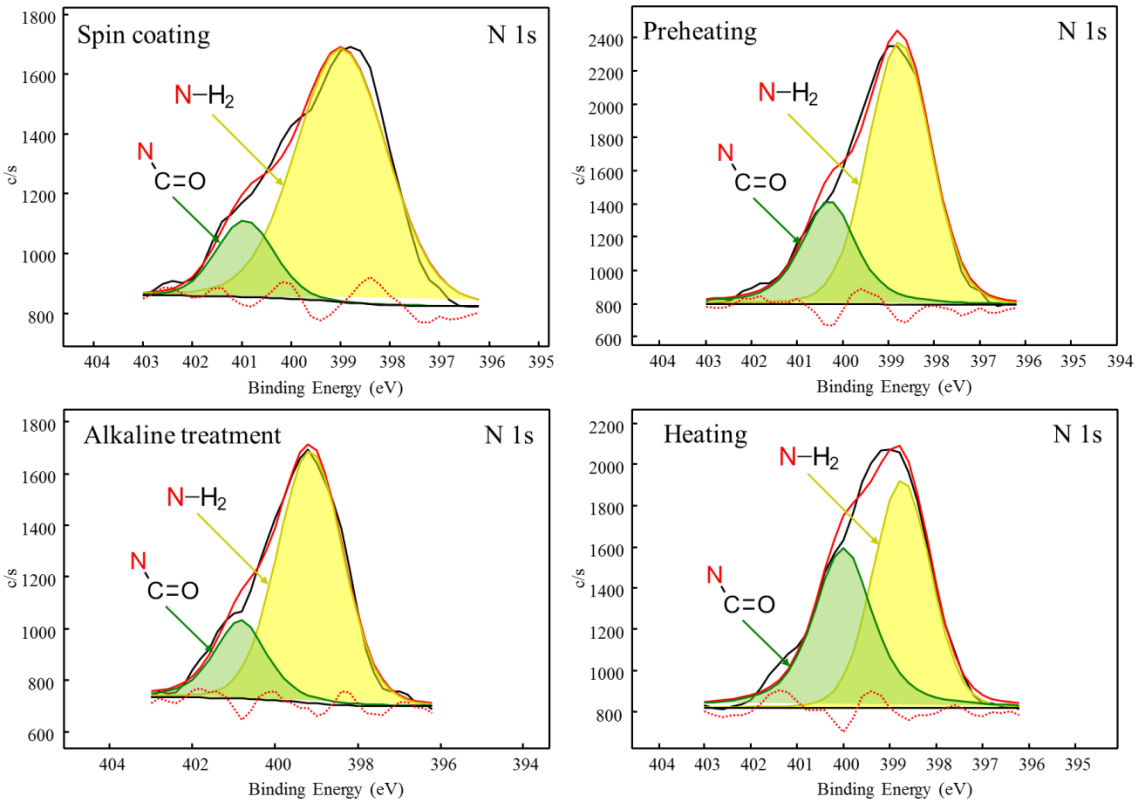

Figure 6.4 XPS high resolution bands of N 1s.

Figure 6.5 shows the AFM images obtained. A significant ($P < 0.05$) increase in *Sq* was obtained after the application of the antimicrobial coating over PP, going from 8.8 ± 2.6 to 18.3 ± 1.1 nm. A porous surface was observed from modified PP. This effect may be created by the evaporation of the solvent that contains PEI and SMA (acetone) during spin coating and when heating is applied.

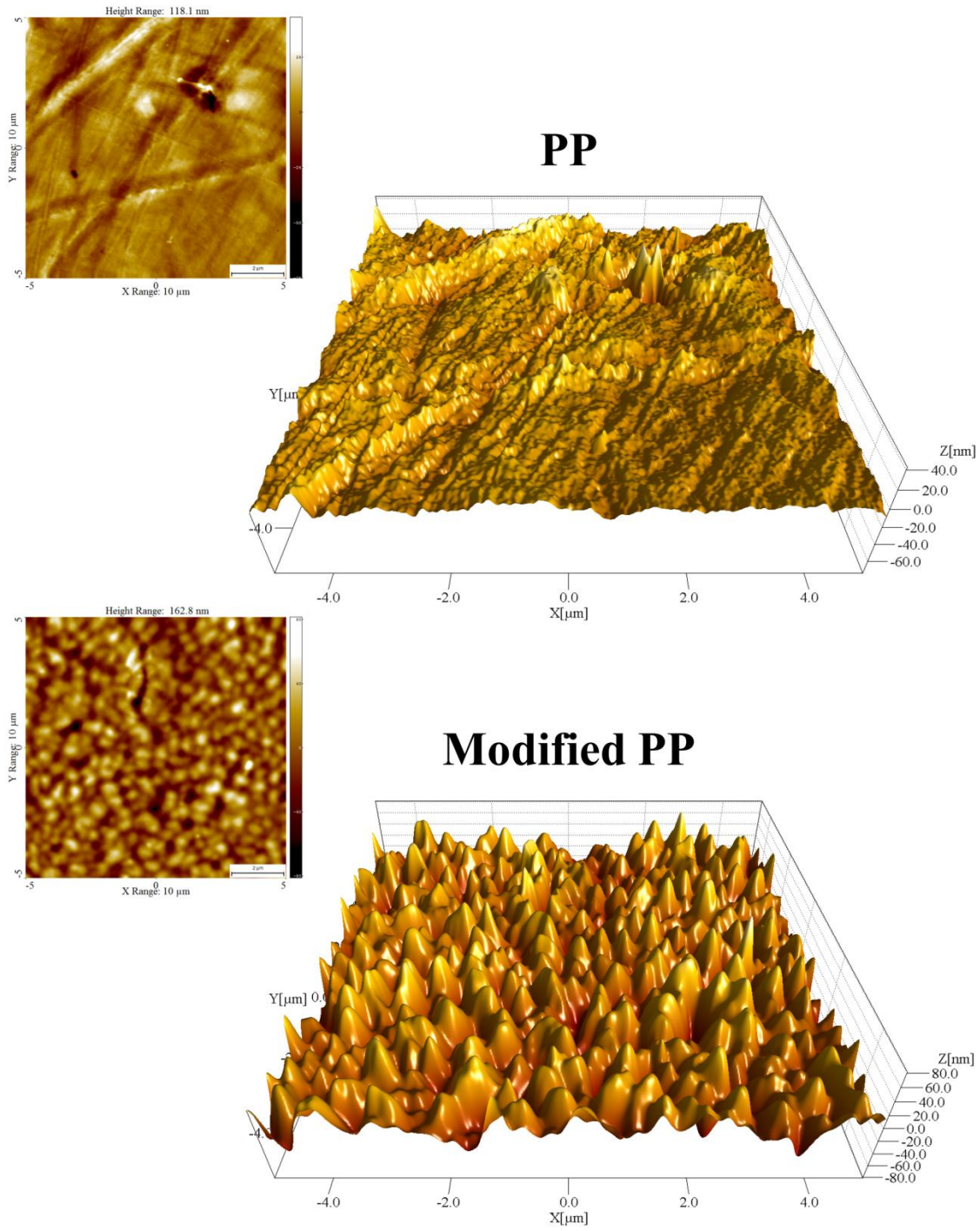

Figure 6.5 AFM results of PP and modified PP as prepared.

The primary amine content of PP and modified PP was 0.0 ± 0.0 and 503 ± 65 nmol cm^{-2}, respectively ($P < 0.05$). Figure 6.6-A shows the N-halamine content of the antimicrobial coating as a function of time according to Equation 1 (NH_{asympt} = 151 ± 22 nmol cm^{-2}, K = 0.03 ± 0.01 min^{-1}, R^2 = 0.88 ± 0.1). As it can be observed, chlorine saturation starts to be reached at 45 min. Figure 6.6-B shows the data from the pK_a determination of the as prepared antimicrobial coating fitted with Equation 2 (bold line, R^2 = 0.83 ± 0.04) and the data obtained from PP (dashed line represents the average θ_S value of PP in all the pH range evaluated). The shape of the sigmoidal curve obtained corresponds to that of a cationic surface (character given by the high amount of primary amines), and the obtained pK_a value (4.6 ± 1.4) is comparable to the ones reported in previous works involving similar surface chemistries (Vezenov and others 1997; Van der Maaden and others 2012). Even though amines exhibit a basic nature, it has been reported in previous works that molecules possessing amines present a shift in pK_a values when they are covalently coated onto a different substrate. Such reduction in pK_a can fall into acidic ranges. This phenomenon has been explained from the influence the corresponding substrates to which these molecules are attached impart to them, leaving fewer amine groups available as compared to the molecules when they are free in solution (Abiman and others 2007). Even though a higher hydrophilicity was observed from modified PP brought by the antimicrobial coating, there was no significant difference ($P > 0.05$) in surface energy. Values of γ_{GS} of PP and modified PP were 22.5 ± 0.5 and 23.9 ± 2.3 mN m^{-1}, respectively. For both PP and modified PP, a good linear correlation was gotten (Figure 6.6-C, R^2 values of 0.97 ± 0.01 and 0.88 ± 0.06, respectively). Comparable results

of surface energy for PP have been reported (Tsutsui and others 1989; Farris and others 2014).

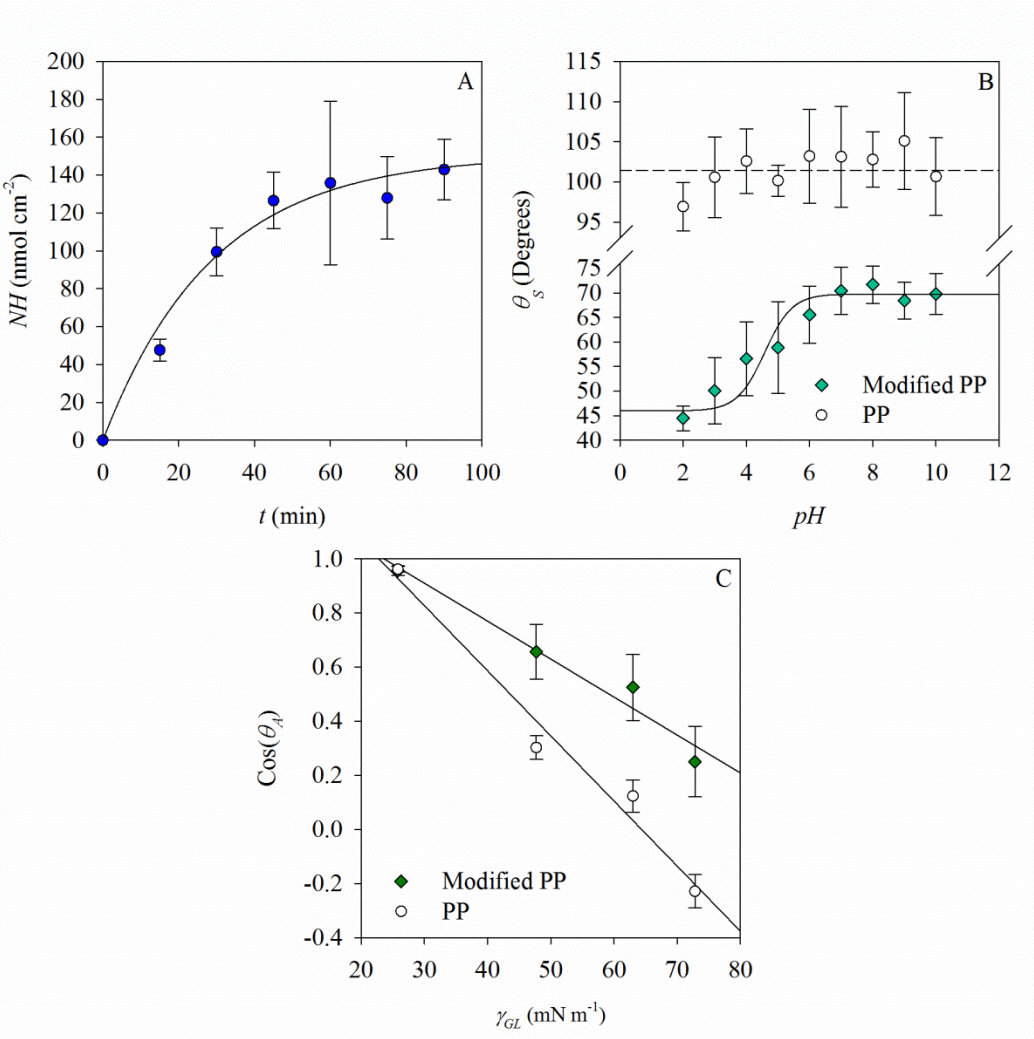

Figure 6.6 N-halamine content determination (A), surface pK_a (B), and surface energy (C). Results are the average value of 3 replicates ± 1 standard deviation.

6.4.2 Antimicrobial evaluation

As expected, no antimicrobial effect was observed from either PP or chlorinated PP, and after 2 h of incubation, approximately 3 logarithmic reductions were given by

modified PP and > 5 by chlorinated modified PP (Figure 6.7-A and Figure 6.8). In addition, antimicrobial activity was preserved from modified PP coupons that had been subjected to 10 rechlorination cycles, providing also > 5 logarithmic reductions (Figure 6.7-A). The inactivation kinetics showed a different behavior between modified PP and chlorinated modified PP (Figure 6.7-B). When not chlorinated (cationic form), modified PP showed agreement with Equation 3 (R^2 = 0.84), and when chlorinated (N-halamine form) it did it with Equation 4 (R^2 = 0.84). Cationic polymers have been reported to inactivate microorganisms in previous studies, and the possible explanations provided for their action have been an ion exchange process between the positive charges of the polymers and the cells membrane (causing its deterioration), the generation of reactive oxygen species that can provoke oxidative stress and damage on genetic information and other biomolecules, and interruption of the electron transport chain, vital for energy generation (Kugler and others 2005; Lichter and Rubner 2009; Chakraborti and others 2013). Similar behaviors have been observed in previous studies involving kinetics of inactivation of cationic polymers (Milovic and others 2005) and N-halamines (Williams and others 1987; Bastarrachea and others 2013). A possible reason behind the initially slow speed of inactivation given by chlorinated modified PP as compared to modified PP may be a charge neutralization effect imparted by the absorption of chlorine. The limited (although fast) level of inactivation given by modified chlorine (reducing the microbial load in approximately 3 logarithmic cycles) may be explained by the fact that the bacterial suspension had a level of pH of 6.1 ± 0.1, which is closed to the upper limit of the surface pK_a reported (4.6 ± 1.4), and suggests the coating was protonated.

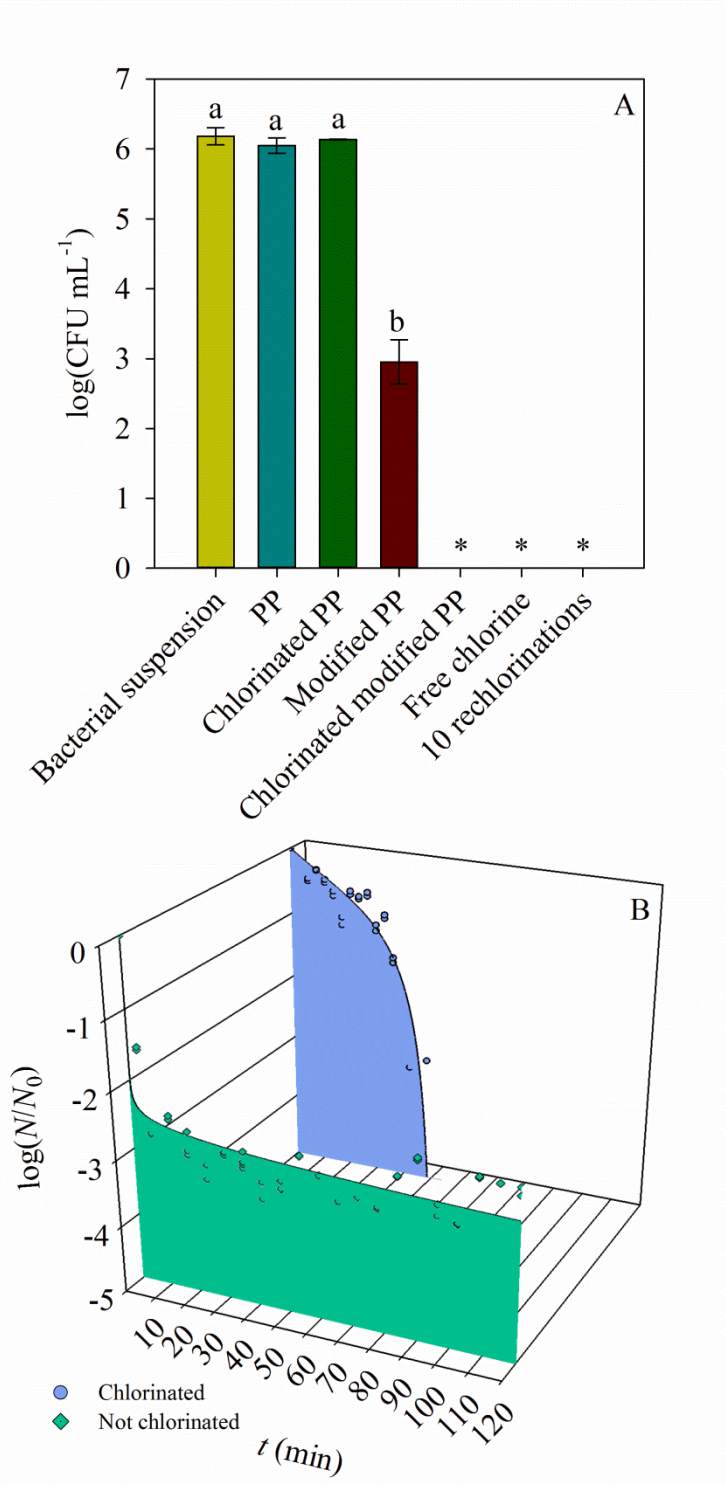

Figure 6.7 Antimicrobial evaluation (A, treatments followed by the same letter are not significantly different $P > 0.05$) and inactivation kinetics of modified PP and chlorinated modified PP (B), * indicates inactivation below the limit of detection (< 1 log(CFU mL^{-1})).

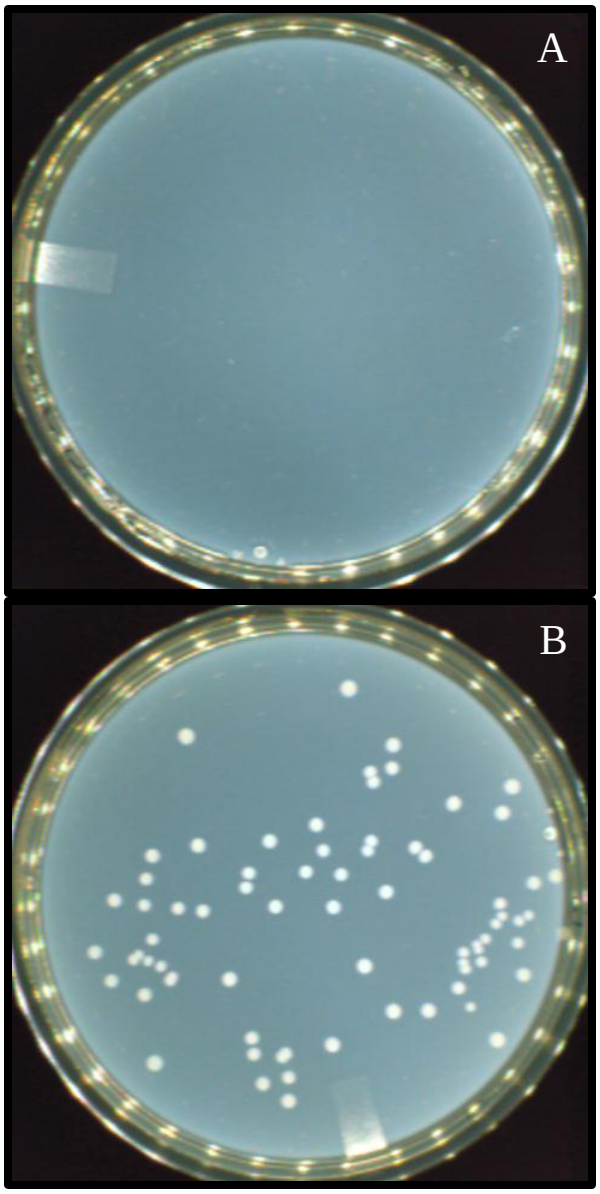

Figure 6.8 Petri dishes showing the dilutions plated as 10^{-1} from the antimicrobial evaluation of fully chlorinated modified PP (A) and modified PP (B) (dilutions plated as 10^{-1}).

6.4.3 Scanning Electron Microscopy (SEM)

Figure 6.9 shows representative images of the coupons' surfaces after the antimicrobial evaluation (2 h of incubation at 32 °C). No visual evidence of attached bacteria was found. Previous works have shown that PP exhibits a low level of surface

attachment of *L. monocytogenes* as compared to other materials' surfaces. In the same mentioned studies, adhesion of *L. monocytogenes* cells on surfaces has not been possible to link with materials properties such as roughness and hydrophobicity (Silva and others 2008), which makes this phenomenon unpredictable on the basis of surface properties. The results obtained confirm that, under the test conditions and at the inoculum level used the reduction in microbial load exerted by modified PP and chlorinated modified PP is not caused by cell adhesion on the coupons' surfaces.

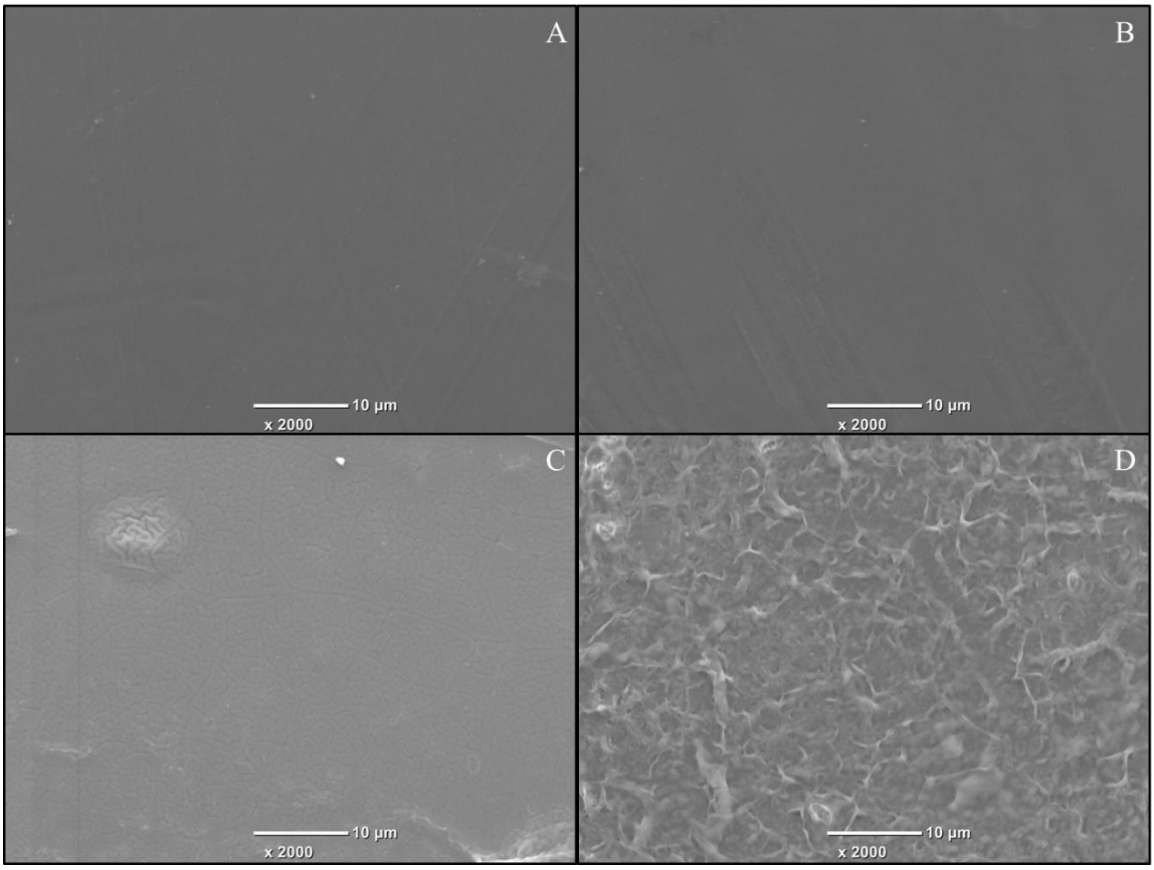

Figure 6.9 SEM images showing surfaces of PP (A), chlorinated PP (B), modified PP (C), and chlorinated modified PP (D) after the antimicrobial evaluation.

6.4.4 Chlorine rechargeability of the antimicrobial coating

Figure 6.10 shows the N-halamine content during the 10 rechlorination cycles applied. According to the ATR-FTIR results, some hydrolysis of amide bonds seem to occur from the absorbance increase in the 3400 – 3200 cm^{-1} (Figure 6.10-A) and 1740 – 1720 cm^{-1} (Figure 10-B) ranges characteristic of the C–O and C=O vibrations of carboxylic acids, respectively, and an absorbance reduction at ~ 1650 cm^{-1} (Figure 6.10-B, C=O vibration of amides). As it can be observed (Figure 6.10-C), an initial increase in chlorine absorption is exhibited, followed by stabilization. From Figure 6.9-D, it can be seen that a single chlorination causes a change in the surface pattern. Similar results have been reported in studies involving rechlorination of polymeric N-halamines (Bastarrachea and others 2014).

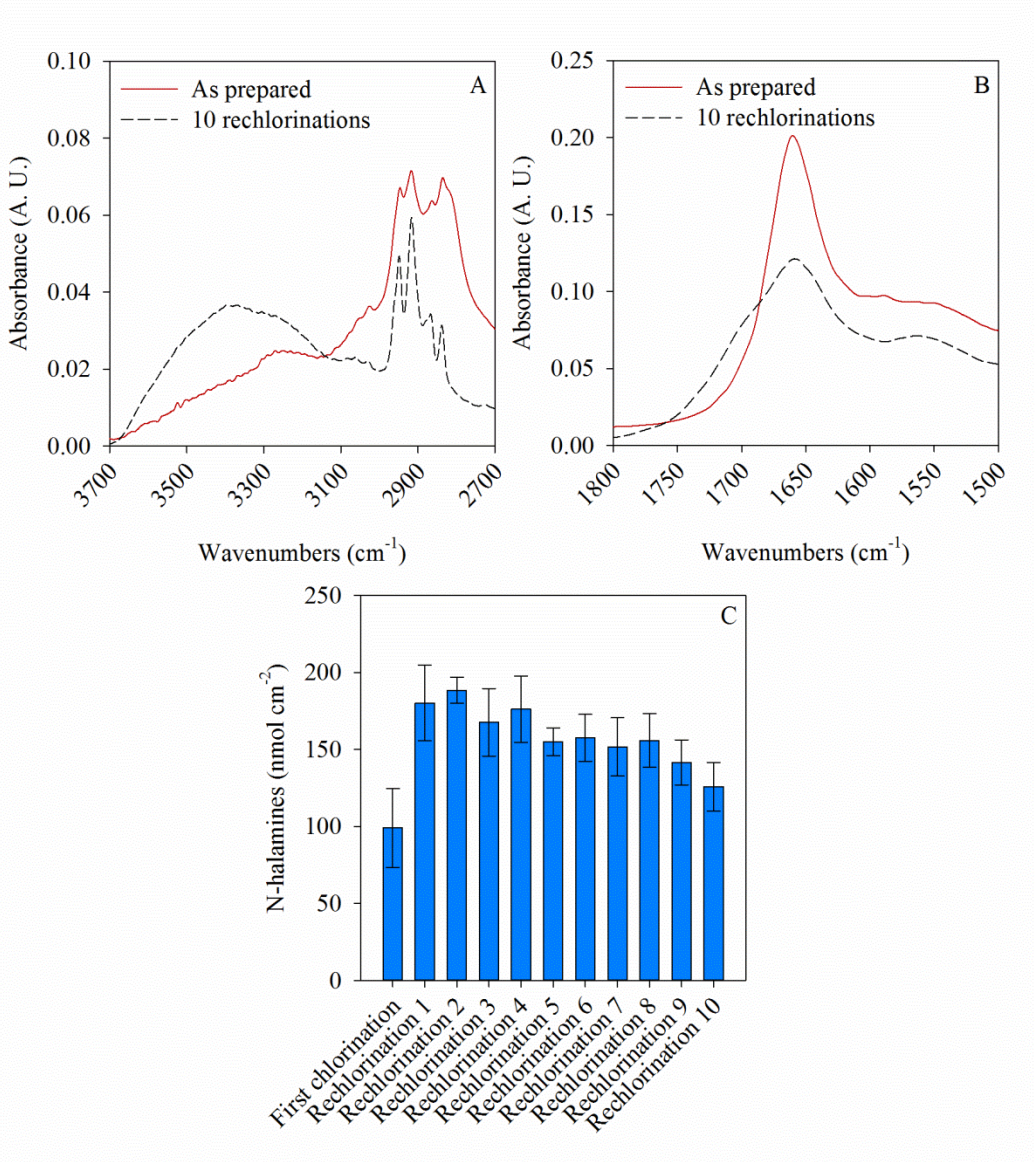

Figure 6.10 ATR-FTIR results (A and B) after the chlorine rechargeability study (C) of modified PP.

6.5 Conclusions

Polyethylenimine and styrene maleic anhydride copolymer were alternately deposited onto anhydride functionalized polypropylene coupons to synthesize a coating with both cationic and N-halamine antimicrobial moieties. Antimicrobial efficacy was

achieved after application of just two bilayers. Prior to chlorination by dilute bleach the coatings were able to inactivate *L. monocytogenes* by ~ 3 logarithmic cycles. Chlorination increased the antimicrobial efficacy to greater than 5 logarithmic cycles (> 99.999% reduction in microbial population). Inactivation kinetics shifted from a Weibullian to sigmoidal behavior following chlorination. The reported surface modification procedure resulted in an antimicrobial coating with no significant difference in surface energy ($P > 0.05$) as compared to PP. Electron microscopy confirmed that the biocidal effect was due to the antimicrobial nature of the coating and not a result of bacterial adhesion. The antimicrobial surface also exhibited capability to be rechlorinated multiple times, with full retention of antimicrobial properties.

6.6 Acknowledgements

Authors would like to thank Prof. D. Julian McClements for the use of his Drop Shape Analyzer DSA100; Prof. Thomas McCarthy and Jacob Hirsch for use of their Physical Electronics Quantum 2000; Dr. Sekar T. Dhanasekaran for training and assistance in the AFM analysis.

CHAPTER 7

CONCLUSIONS

Stainless steel was successfully surface-modified with PEI and PAA to make it able to harbor antimicrobial N-halamines. The available number of N-halamines ranged from 0.30 ± 0.5 to 36.8 ± 5.0 nmol cm^{-2} (from 1 to 6 bilayers). Changes in surface chemistry were confirmed with FTIR and XPS. Ellipsometry and AFM showed that the deposition of the bilayers was not uniform, given the bilayers' equivalence thickness that ranged from 1.1 ± 0.3 nm (1 bilayer) to 78.6 ± 1.2 nm (6 bilayers). N-halamine surface-modified stainless steel was challenged against *L. monocytogenes*, and only coupons having 6 bilayers were able to inactivate the pathogen in more than 3 logarithmic cycles (> 99.9%).

LDPE was surface-modified using a similar approach to the one followed with stainless steel. Up to five bilayers of PEI and PAA were applied on LDPE coupons, making them able to harbor from 3.4 ± 1.2 nmol cm^{-2} (1 bilayer) to 27.3 ± 3.5 nmol cm^{-2} (5 bilayers). Changes in surface chemistry were confirmed through ATR-FTIR, and exhibited a high degree of crosslinking between PEI and PAA. The antimicrobial evaluation indicated that (under the experimental conditions) modified LDPE coupons having from 2 to 5 bilayers were able to inactivate *L. monocytogenes* in more than 5 logarithmic cycles (> 99.999%). Kinetics of inactivation showed a sigmoidal behavior by coupons having from 2 to 5 bilayers. The inactivation kinetics results showed that, in contrast to free chlorine in solution, the equivalent amount of chlorine from the N-

halamine modified LDPE coupons inactivates *L. monocytogenes* at a slow rate. Inactivation below the limit of detection was reached after approximately 48 min (5 bilayers), 54 min (4 bilayers), 65 min (3 bilayers), and 91 min (2 bilayers). In contrast, the equivalent amount of free chlorine in solution for each level of surface modification inactivated *L. monocytogenes* in less than 6 min. Even though biocidal efficacy was demonstrated, the coating was not stable. After 3 reuses against *L. monocytogenes*, the coating had delaminated, leaving LDPE with no antimicrobial property.

In order to improve the stability of the N-halamine coating consisting of PEI and PAA, the number of bilayers applied was increased (5, 10, 15 and 20 bilayers) and the surface modification method of PE was changed. Changes in surface chemistry were confirmed through ATR-FTIR and XPS. N-halamine content ranged from 49.3 nmol cm^{-2} (5 bilayers) to 293.5 nmol cm^{-2} (20 bilayers). N-halamine modified PE coupons were able to inactivate *L. monocytogenes* in more than 5 logarithmic cycles (> 99.999%) at every level of surface modification (from 5 to 20 bilayers). Evaluations were conducted to assess the stability of the coating consisting of PEI and PAA. After 100 rechlorinations, coupons containing 20 bilayers exhibited minor changes in surface chemistry confirmed through ATR-FTIR and ability to harbor a substantial number of N-halamines. Coupons with 20 bilayers subjected to up to 300 washing cycles with buffers of pH levels of 3, 5 and 7, and a commercial detergent, exhibited also minor changes in surface chemistry confirmed through ATR-FTIR, and statistically the same number of N-halamines the as prepared 20 bilayers coupons contained ($P > 0.05$). The results of the evaluation study with the multiple washing cycles also showed that the stability of the bound chlorine on the coating increases as the coupons are continuously used, and that stability is more

evident at low levels of pH. XPS analysis was done to 20 bilayers coupons after the 100 rechlorinations and the washing cycles. Both XPS and ATR-FTIR showed that minor changes occurred on the surface chemistry, which consisted in rupture of the amide bonds that hold together PEI and PAA.

As an alternative method for surface modification with N-halamines, PP was studied with the polymers PEI and SMA. Unlike the previous surface modification methods used with PEI and PAA that involved carbodiimide chemistry crosslinkers, the reactivity of the anhydrides contained in SMA made it unnecessary to use any catalyst for the application of the polymer layers. The modified PP was able to harbor an amount of N-halamines of 151 ± 22 nmol cm^{-2}. The modified material also exhibited a cationic nature given the high presence of primary amines (503 ± 65 nmol cm^{-2}). A sigmoidal contact angle titration curve characteristic of cationic surfaces was also obtained (pK_a = 4.6 ± 1.4), and modified PP didn't experience a significant change in surface energy (P > 0.05). AFM analysis revealed that modified PP possesses a porous surface with a significantly different value of roughness (8.8 ± 2.6 nm for PP and 18.3 ± 1.1 nm for modified PP). Surface chemistry was characterized through ATR-FTIR and XPS, and the analysis confirmed successful surface modification. When not chlorinated, modified PP was able to inactivate *L. monocytogenes* in approximately 3 logarithmic cycles, and the inactivation kinetics agreed with the Weibull model. When chlorinated, modified PP was able to inactivate *L. monocytogenes* in more than five logarithmic cycles (> 99.999%) and the inactivation kinetics agreed with the sigmoidal isothermal model. Modified PP was also able to be rechlorinated for 10 cycles, and the ATR-FTIR results after these

cycles of rechlorination confirmed hydrolysis of the PEI and SMA layers, but an overall stable coating.

Overall, it was possible to create N-halamine antimicrobial surfaces that are robust towards continuous usage. However, the applied coatings are prone to hydrolysis and delamination due to continuous chlorination. More research is necessary to maximize stability and applicability.

CHAPTER 8

RECOMMENDATIONS FOR FUTURE WORK

As it was confirmed throughout the present research work, antimicrobial coatings in general, and N-halamine coatings in particular, represent a promising tool that can diminish the constant risk of microbial contamination of products during food processing. However, more research is needed in order to overcome the challenges that these technologies still face, which deal mainly with durability for long term usage, improvement of the efficiency of the preparation methods, scalability for industrial application and implementation, versatility towards the conditions present in the food facilities environments, assurance of safety towards the public and the environment, and development of reliable standard methods to assess antimicrobial activity.

The long-term objective of this research is to develop antimicrobial food-contact materials that can help prevent microbial contamination during food processing that can affect public health. In order to achieve this research goal, the following directions can be followed.

8.1 Technology improvement

As it was mentioned, one of the main drawbacks of the antimicrobial technologies studied in this research deals with stability. As it was confirmed from the results obtained, the stability against deteriorating agents (continuous usage, extreme levels of

pH, etc.) of a coating applied onto a substrate of different chemical composition and physical properties is a multifactorial phenomenon. In general, the higher the molecular weight of its components, the more stable the coating may become. This can be explained from the fact that a higher molecular weight implies more numerous sites for reaction between the substrate and the polymer. If the molecular weight is high enough, the polymer chains that couldn't interact with the substrate will be able to react with subsequent layers, like in a LbL process. A big molecule with multiple points of interaction (covalent bonds) with other molecules will resist more efficiently delamination caused by hydrolysis, like when an amide bond is attacked by extreme levels of pH. Further, if it is possible for those covalent bonds to regenerate, the long length of the polymer chains will ensure there is no separation from the substrate and adjacent polymer layers. However, as it was also confirmed, molecular weight is not the only factor that influences coating stability. For instance, a higher presence of amides as compared to amines may compromise stability towards chlorination, given the fact that amides are prone to hydrolysis. In contrast, amines exhibit a higher affinity to bind with chlorine and don't experience hydrolysis, which results in a more stable N-halamine coating upon chlorination. Hence, the likelihood of the bonds that hold together the polymer chains in a coating towards breaking under deteriorating conditions can be more important than molecular weight. In addition, the affinity of the components of the coating in terms of hydrogen bonds, and hydrophilic, hydrophobic and electrostatic interactions also dictates coating stability (Haynie and others 2005). A direction to follow for improvement of the antimicrobial technology will have to be related with finding the most efficient combination of constituents that will result in a maximized stability

towards the environmental conditions food contact materials in general, and N-halamines in particular, experience (washing agents, chlorination, presence of organic matter, etc.).

Another drawback some of the technologies studied exhibit deals with the preparation method, that may be time consuming and/or involve expensive and toxic catalysts, like those used in carbodiimide chemistry, and which application at an industrial scale could be unrealistic. Based on this disadvantage, a polymeric anhydride (SMA, with high reactivity towards primary amines) was tested for preparation of an N-halamine antimicrobial coating, with promising results. Another direction to follow could involve the use of polymeric anhydrides of different chemical composition and molecular weights. These polymers have been used extensively, and their diversity, availability and safety (Kumar and others 2002; Jain and others 2008) are characteristics that could be exploited to develop stable antimicrobial N-halamine coatings.

8.2 Technology diversification

As it was mentioned earlier, surface modification offers the advantage of keeping the bulk properties of the modified substrates intact (Ratner 1995). However, coatings may have short durability. To overcome this, bulk modifications or development of new materials could represent an effective solution. An alternative method to develop antimicrobial food contact materials could be the preparation of polymer blends and composites (Denchev and Dencheva 2008; Blaiszik and others 2010; Liu and others 2014). Polymeric anhydrides have already been used to prepare polymer blends through extrusion (Denchev and Dencheva 2008). As it was confirmed in this research,

anhydrides form stable bonds with primary amines at high temperatures. Heat transfer operations like extrusion could represent an efficient and fast way to prepare antimicrobial N-halamine materials. A number of polymer combinations could be studied with a variety of final properties (wettability, surface energy, tensile properties, etc.). The process parameters could be set in a way that allows the presence of nitrogen-containing functional groups able to bind chlorine. The most commonly used polymers to fabricate the accessories and utensils found in food processing facilities could be selected to prepare the new antimicrobial blends and composites. Their application could be extended to health services facilities and materials used for housing.

8.3 Technology evaluation and application

Once new and improved antimicrobial coatings or materials haven been developed, they will have to be subjected to evaluations that challenge their ability to be reused constantly to inactivate microorganisms. A wide range of microorganisms would need to be studied, including bacteria (Gram (+), Gram (-), spore forming, etc.), yeasts and fungi.

As it was mentioned before, N-halamines lose effectiveness in the presence of organic matter. Antimicrobial evaluations should also involve as a factor increasing levels of organic matter (increasing concentrations of polysaccharides, proteins, monosaccharides, etc.).

Extensive evaluations to assess chemical integrity and robustness of the antimicrobial material would be necessary. They could include exposure to corrosive cleaning agents, physical abrasion, etc.

Finally, once the antimicrobial materials have been tested and perfected at a laboratory scale, evaluations of real applications could be conducted in pilot plants, or in small food processing facilities where microbial contamination has taken place (using nonpathogenic surrogates like *Listeria innocua* or *Escherichia coli* K12). Accessories made with the new materials (plastic containers, gaskets, conveyor belts, curtains, etc.) would be tested and compared with non antimicrobial ones under normal conditions of use, and under different levels of microbial contamination using the nonpathogenic surrogates.

REFERENCES

Abiman P, Wildgoose G, Crossley A, Jones J, Compton R. 2007. Contrasting pK_a of protonated bis(3-aminopropyl)-terminated polyethylene glycol "Jeffamine" and the associated thermodynamic parameters in solution and covalently attached to graphite surfaces. Chem.-Eur.J. 13(34):9663-7.

Adamson AW GA. 1997. *Physical Chemistry of Surfaces*. 6th ed. New York, NY: John Wiley & Sons Inc. 808 p.

Ahmed AEI, Cavalli G, Bushell ME, Wardell JN, Pedley S, Charles K, Hay JN. 2011. New Approach To Produce Water Free of Bacteria, Viruses, and Halogens in a Recyclable System. Appl.Environ.Microbiol. 77(3):847-53.

Alf ME, Asatekin A, Barr MC, Baxamusa SH, Chelawat H, Ozaydin-Ince G, Petruczok CD, Sreenivasan R, Tenhaeff WE, Trujillo NJ, Vaddiraju S, Xu J, Gleason KK. 2010. Chemical Vapor Deposition of Conformal, Functional, and Responsive Polymer Films. Adv Mater 22(18):1993-2027.

American Society for Testing and Materials. 2008. Standard Test Methods of Sampling and Chemical Analysis of Chlorine-Containing Bleaches. D 2022 – 89. Philadelphia, PA: ASTM.

Amiri F, Mesquita MMF, Andrews SA. 2010. Disinfection effectiveness of organic chloramines, investigating the effect of pH. Water Res. 44(3):845-53.

Araújo EA, de Andrade NJ, Mendes da Silva LH, de Carvalho AF, de Sá Silva CA, Ramos AM. 2010. Control of Microbial Adhesion as a Strategy for Food and Bioprocess Technology. Food Bioprocess Technol. 3(3):321-32.

Asri LATW, Crismaru M, Roest S, Chen Y, Ivashenko O, Rudolf P, Tiller JC, van der Mei HC, Loontjens TJA, Busscher HJ. 2014. A Shape- Adaptive, Antibacterial-Coating of Immobilized Quaternary- Ammonium Compounds Tethered on Hyperbranched Polyurea and its Mechanism of Action. Adv.Funct.Mater. 24(3):346-55.

Avila-Sosa R, Palou E, Jimenez Munguia MT, Nevarez-Moorillon GV, Navarro Cruz AR, Lopez-Malo A. 2012. Antifungal activity by vapor contact of essential oils added to amaranth, chitosan, or starch edible films. Int.J.Food Microbiol. 153(1-2):66-72.

Avila-Sosa R, Hernandez-Zamoran E, Lopez-Mendoza I, Palou E, Jimenez Munguia MT, Virginia Nevarez-Moorillon G, Lopez-Malo A. 2010. Fungal Inactivation by Mexican Oregano (*Lippia berlandieri Schauer*) Essential Oil Added to Amaranth, Chitosan, or Starch Edible Films. J.Food Sci. 75(3):M127-33.

Bakkali F, Averbeck S, Averbeck D, Waomar M. 2008. Biological effects of essential oils - A review. Food Chem.Toxicol. 46(2):446-75.

Barish JA, Goddard JM. 2013. Anti-fouling surface modified stainless steel for food processing. Food Bioprod.Process. 91(C4):352-61.

Bastarrachea L, Dhawan S, Sablani SS. 2011. Engineering Properties of Polymeric-Based Antimicrobial Films for Food Packaging. Food Eng.Rev. 3(2):79-93.

Bastarrachea L, Dhawan S, Sablani SS, Mah J, Kang D, Zhang J, Tang J. 2010. Biodegradable Poly(butylene adipate-*co*-terephthalate) Films Incorporated with Nisin: Characterization and Effectiveness against *Listeria innocua*. J.Food Sci. 75(4):E215-24.

Bastarrachea LJ, Goddard JM. 2013. Development of antimicrobial stainless steel via surface modification with N-halamines: Characterization of surface chemistry and N-halamine chlorination. J Appl Polym Sci 127(1):821-31.

Bastarrachea LJ, McLandsborough LA, Peleg M, Goddard JM. 2014. Antimicrobial N-halamine Modified Polyethylene: Characterization, Biocidal Efficacy, Regeneration, and Stability. J.Food Sci. 79(5):E887-97.

Bastarrachea LJ, Peleg M, McLandsborough LA, Goddard JM. 2013. Inactivation of*Listeria monocytogenes*on a polyethylene surface modified by layer-by-layer deposition of the antimicrobial N-halamine. J.Food Eng. 117(1):52-8.

Berthier DL, Paret N, Trachsel A, Fieber W, Herrmann A. 2013. Controlled Release of Damascone from Poly(styrene-*co*-maleic anhydride)-based Bioconjugates in Functional Perfumery. Polymers 5(1):234-53.

Beyth N, Yudovin-Farber I, Perez-Davidi M, Domb AJ, Weiss EI. 2010. Polyethyleneimine nanoparticles incorporated into resin composite cause cell death and trigger biofilm stress in vivo. Proc.Natl.Acad.Sci.U.S.A. 107(51):22038-43.

Bhattacharya A, Rawlins J, Ray P. 2009. Polymer grafting and crosslinking. 1st ed. Hoboken, N.J.: John Wiley. 341 p.

Blaiszik BJ, Kramer SLB, Olugebefola SC, Moore JS, Sottos NR, White SR. 2010. Self-Healing Polymers and Composites. Ann.Rev.Mater.Res. 40:179-211.

Bratskaya S, Marinin D, Simon F, Synytska A, Zschoche S, Busscher HJ, Jager D, van der Mei HC. 2007. Adhesion and viability of two enterococcal strains on covalently grafted chitosan and chitosan/κ-carrageenan multilayers. Biomacromolecules 8(9):2960-8.

Brooks JD, Flint SH. 2008. Biofilms in the food industry: problems and potential solutions. Int.J.Food Sci.Technol. 43(12):2163-76.

Buffet-Bataillon S, Tattevin P, Bonnaure-Mallet M, Jolivet-Gougeon A. 2012. Emergence of resistance to antibacterial agents: the role of quaternary ammonium compounds-a critical review. Int.J.Antimicrob.Agents 39(5):381-9.

Cao Z, Sun Y. 2009. Polymeric N-Halamine Latex Emulsions for Use in Antimicrobial Paints. ACS Appl.Mater.Interfaces 1(2):494-504.

Carraher CE. 2010. Introduction to polymer chemistry. 2nd ed. Boca Raton, FL: CRC Press. 510 p.

Centers for Disease Control and Prevention. 2013. Foodborne diseases active surveillance network (FoodNet). [serial online]. 2014. Available from http://www.cdc.gov/foodnet. Posted 2013.

Centers for Disease Control and Prevention. 2004. Preliminary FoodNet data on the incidence of infection with pathogens transmitted commonly through food–selected sites, United States, 2003. MMWR: Morbidity and Mortality Weekly Report 53(16):338-46.

Centers for Disease Control and Prevention. 2003. Multistate outbreak of*Salmonella*serotype*Typhimurium*infections associated with drinking unpasteurized milk–Illinois, Indiana, Ohio, and Tennessee, 2002–2003. MMWR: Morbidity and Mortality Weekly Report 52(26):613-5.

Cerkez I, Worley SD, Broughton RM, Huang TS. 2013. Rechargeable antimicrobial coatings for poly(lactic acid) nonwoven fabrics. Polymer 54(2):536-41.

Cerkez I, Kocer HB, Worley SD, Broughton RM, Huang TS. 2011. N-Halamine Biocidal Coatings via a Layer-by-Layer Assembly Technique. Langmuir 27(7):4091-7.

Chakraborti S, Bhattacharya S, Chowdhury R, Chakrabarti P. 2013. The Molecular Basis of Inactivation of Metronidazole-Resistant*Helicobacter pylori*Using Polyethyleneimine Functionalized Zinc Oxide Nanoparticles. PLoS One 8(8):e70776.

Chan C. 1993. Polymer surface modification and characterization. New York, NY: Hanser/Gardner. 285 p.

Chen N, Chung C, Chiang C, Chen K, He J. 2013. Antimicrobial and decorative ion-plated copper-containing ceramic coatings. Surf.Coat.Technol. 236:29-35.

Chen R, Willcox MDP, Cole N, Ho KKK, Rasul R, Denman JA, Kumar N. 2012. Characterization of chemoselective surface attachment of the cationic peptide melimine and its effects on antimicrobial activity. Acta Biomater. 8(12):4371-9.

Cheshmedzhieva D, Ilieva S, Hadjieva B, Galabov B. 2009. The mechanism of alkaline hydrolysis of amides: a comparative computational and experimental study of the hydrolysis of N-methylacetamide, N-methylbenzamide, and acetanilide. J.Phys.Org.Chem. 22(6):619-31.

Chrzanowski W, Valappil SP, Dunnill CW, Abou Neel EA, Lee K, Parkin IP, Wilson M, Armitage DA, Knowles JC. 2010. Impaired bacterial attachment to light activated Ni-Ti alloy. Mater.Sci.Eng.C-Mater.Biol.Appl. 30(2):225-34.

Chua PH, Neoh KG, Shi Z, Kang ET. 2008. Structural stability and bioapplicability assessment of hyaluronic acid-chitosan polyelectrolyte multilayers on titanium substrates. J.Biomed.Mater.Res.Part A 87A(4):1061-74.

Chung C, Chiang C, Chen C, Hsiao C, Lin H, Hsieh P, He J. 2008. Photocatalytic TiO_2 on copper alloy for antimicrobial purposes. Appl.Catal.B-Environ. 85(1-2):103-8.

Cleland M, Singh A, Silverman J. 1992. Radiation processing of polymers. New York, NY: Hanser Publishers. 377 p.

Cloete T, Jacobs L. 2001. Surfactants and the attachment of *Pseudomonas aeruginosa* to 3CR12 stainless steel and glass. Water Sa 27(1):21-6.

Combe E, Owen B, Hodges J. 2004. A protocol for determining the surface free energy of dental materials. Dent.Mater. 20(3):262-8.

Cools I, Uyttendaele M, Cerpentier J, D'Haese E, Nelis HJ, Debevere J. 2005. Persistence of *Campylobacter jejuni* on surfaces in a processing environment and on cutting boards. Lett.Appl.Microbiol. 40(6):418-23.

Costanzo P, Giese R, Vanoss C. 1990. Determination of the Acid-Base Characteristics of Clay Mineral Surfaces by Contact-Angle Measurements Implications for the Adsorption of Organic Solutes from Aqueous-Media. J.Adhes.Sci.Technol. 4(4):267-75.

Da Rocha M, Loiko M, Tondo E, Prentice C. 2014. Physical, mechanical and antimicrobial properties of Argentine anchovy (*Engraulis anchoita*) protein films incorporated with organic acids. Food Hydrocoll. (37):213-20.

Dargaville T, George G, Hill D, Whittaker A. 2003. High energy radiation grafting of fluoropolymers. Prog.Polym.Sci. 28(9):1355-76.

Das M, Saxena N, Dwivedi PD. 2009. Emerging trends of nanoparticles application in food technology: Safety paradigms. Nanotoxicology 3(1):10-8.

Decher G. 1997. Fuzzy nanoassemblies: Toward layered polymeric multicomposites. Science 277(5330):1232-7.

Decher G, Eckle M, Schmitt J, Struth B. 1998. Layer-by-layer assembled multicomposite films. Curr.Opin.Colloid Interface Sci. 3(1):32-9.

Decraene V, Pratten J, Wilson M. 2008a. Novel light-activated antimicrobial coatings are effective against surface-deposited*Staphylococcus aureus*. Curr.Microbiol. 57(4):269-73.

Decraene V, Pratten J, Wilson M. 2008b. Assessment of the Activity of a Novel Light-Activated Antimicrobial Coating in a Clinical Environment. Infect.Control Hosp.Epidemiol. 29(12):1181-4.

Denchev ZZ, Dencheva NV. 2008. Transforming polymer blends into composites: a pathway towards nanostructured materials. Polym.Int. 57(1):11-22.

Djordjevic D, Wiedmann M, McLandsborough L. 2002. Microtiter plate assay for assessment of*Listeria monocytogenes*biofilm formation. Appl.Environ.Microbiol. 68(6):2950-8.

Dong A, Huang J, Lan S, Wang T, Xiao L, Wang W, Zhao T, Zheng X, Liu F, Gao G, Chen Y. 2011. Synthesis of N-halamine-functionalized silica-polymer core-shell nanoparticles and their enhanced antibacterial activity. Nanotechnology 22(29):295602.

Drelich J, Chibowski E, Meng DD, Terpilowski K. 2011. Hydrophilic and superhydrophilic surfaces and materials. Soft Matter 7(21):9804-28.

Dubas ST, Kumlangdudsana P, Potiyaraj P. 2006. Layer-by-layer deposition of antimicrobial silver nanoparticles on textile fibers. Colloid Surf.A-Physicochem.Eng.Asp. 289(1-3):105-9.

Dvoracek CM, Sukhonosova G, Benedik MJ, Grunlan JC. 2009. Antimicrobial Behavior of Polyelectrolyte-Surfactant Thin Film Assemblies. Langmuir 25(17):10322-8.

Eknoian M, Worley S, Harris J. 1998. New biocidal N-halamine-PEG polymers. J.Bioact.Compatible Polym. 13(2):136-45.

El Achari A, Coqueret X, Lablachecombier A, Loucheux C. 1993. Preparation of Polyvinylamine from Polyacrylamide - a Reinvestigation of the Hofmann Reaction. Makromolekulare Chemie-Macromolecular Chemistry and Physics 194(7):1879-91.

Elkest S, Marth E. 1988a. *Listeria monocytogenes*and its Inactivation by Chlorine - a Review. Lebensmittel-Wissenschaft & Technologie 21(6):346-51.

Elkest S, Marth E. 1988b. Inactivation of *Listeria monocytogenes* by Chlorine. J.Food Prot. 51(7):520-4.

Elsabee MZ, Abdou ES, Nagy KSA, Eweis M. 2008. Surface modification of polypropylene films by chitosan and chitosan/pectin multilayer. Carbohydr.Polym. 71(2):187-95.

Environmental Protection Agency. 2014. EPA Takes Action to Protect Public from an Illegal Nano Silver Pesticide in Food Containers; Cites NJ Company for Selling Food Containers with an Unregistered Pesticide Warns Large Retailers Not to Sell These Products. States News Service [serial online]. 2014. Available from http://yosemite.epa.gov/opa/admpress.nsf/0/6469952CDBC19A4585257CAC0053E637. Posted 2014.

Fang B, Jiang Y, Rotello VM, Nuesslein K, Santore MM. 2014. Easy Come Easy Go: Surfaces Containing Immobilized Nanoparticles or Isolated Polycation Chains Facilitate Removal of Captured *Staphylococcus aureus* by Retarding Bacterial Bond Maturation. ACS Nano 8(2):1180-90.

Farris S, Pozzoli S, La Vecchia S, Biagioni P, Bianchi CL, Piergiovanni L. 2014. Mapping physicochemical surface modifications of flame-treated polypropylene. Express Polym.Lett. 8(4):256-66.

Fayyad M, Al-Sheikh A. 2001. Determination of N-chloramines in As-samra chlorinated wastewater and their effect on the disinfection process. Water Res. 35(5):1304-10.

Feng Y, Han Z, Peng J, Lu J, Xue B, Li L, Ma H, Wang E. 2006. Fabrication and characterization of multilayer films based on Keggin-type polyoxometalate and chitosan. Mater Lett 60(13-14):1588-93.

Food and Drug Administration. 2014. Inventory of effective food contact substance (FCS) notifications. U S Department of Health & Human Services [serial online]. 2014. Available from http://www.accessdata.fda.gov/scripts/fdcc/?set=FCN. Posted 2014.

Food and Drug Administration. 2000. Report of the FDA Retail Food Program Database of Foodborne Illness Risk Factors. [serial online]. 2014. Available from http://www.fda.gov/Food/GuidanceRegulation/RetailFoodProtection/FoodborneIllnessRiskFactorReduction/ucm123544.htm. Posted 2000.

Gao G, Yu K, Kindrachuk J, Brooks DE, Hancock REW, Kizhakkedathu JN. 2011. Antibacterial Surfaces Based on Polymer Brushes: Investigation on the Influence of Brush Properties on Antimicrobial Peptide Immobilization and Antimicrobial Activity. Biomacromolecules 12(10):3715-27.

Ghodssi R, Lin P. 2011. MEMS Materials and Processes Handbook. New York, NY: Springer Science. 1187 p.

Gilbert P, Moore L. 2005. Cationic antiseptics: diversity of action under a common epithet. J.Appl.Microbiol. 99(4):703-15.

Glinel K, Thebault P, Humblot V, Pradier CM, Jouenne T. 2012. Antibacterial surfaces developed from bio-inspired approaches. Acta Biomater. 8(5):1670-84.

Goddard JM, Hotchkiss JH. 2008. Rechargeable Antimicrobial Surface Modification of Polyethylene. J.Food Prot. 71(10):2042-7.

Goldschmidt A, Streitberger H. 2003. BASF handbook on basics of coating technology. Hannover, Germany: Vincentz Network. 792 p.

Gomes AP, Mano JF, Queiroz JA, Gouveia IC. 2013. Layer-by-layer deposition of antimicrobial polymers on cellulosic fibers: a new strategy to develop bioactive textiles. Polym.Adv.Technol. 24(11):1005-10.

Gray J, Norton P, Alnouno R, Marolda C, Valvano M, Griffiths K. 2003. Biological efficacy of electroless-deposited silver on plasma activated polyurethane. Biomaterials 24(16):2759-65.

Grunlan J, Choi J, Lin A. 2005. Antimicrobial behavior of polyelectrolyte multilayer films containing cetrimide and silver. Biomacromolecules 6(2):1149-53.

Guarda A, Rubilar JF, Miltz J, Jose Galotto M. 2011. The antimicrobial activity of microencapsulated thymol and carvacrol. Int.J.Food Microbiol. 146(2):144-50.

Gule NP, Bshena O, de Kwaadsteniet M, Cloete TE, Klumperman B. 2012. Immobilized Furanone Derivatives as Inhibitors for Adhesion of Bacteria on Modified Poly(styrene-*co*-maleic anhydride). Biomacromolecules 13(10):3138-50.

Gupta R, Kumar A. 2008. Bioactive materials for biomedical applications using sol-gel technology. Biomed.Mater. 3(3):034005.

Guzman E, Cavallo JA, Chulia-Jordan R, Gomez C, Strumia MC, Ortega F, Rubio RG. 2011a. pH-Induced Changes in the Fabrication of Multilayers of Poly(acrylic acid) and Chitosan: Fabrication, Properties, and Tests as a Drug Storage and Delivery System. Langmuir 27(11):6836-45.

Guzman E, Chulia-Jordan R, Ortega F, Rubio RG. 2011b. Influence of the percentage of acetylation on the assembly of LbL multilayers of poly(acrylic acid) and chitosan. Phys.Chem.Chem.Phys. 13(40):18200-7.

Han X, Soblosky L, Slutsky M, Mello CM, Chen Z. 2011. Solvent Effect and Time-Dependent Behavior of C-Terminus-Cysteine-Modified Cecropin P1 Chemically Immobilized on a Polymer Surface. Langmuir 27(11):7042-51.

Haynie D, Zhang L, Rudra J, Zhao W, Zhong Y, Palath N. 2005. Polypeptide multilayer films. Biomacromolecules 6(6):2895-913.

Hazell L, Vandenberg J, Stocker R. 1994. Oxidation of Low-Density-Lipoprotein by Hypochlorite Causes Aggregation that is Mediated by Modification of Lysine Residues rather than Lipid Oxidation. Biochem.J. (302):297-304.

Hazen S, d'Avignon A, Anderson M, Hsu F, Heinecke J. 1998. Human neutrophils employ the myeloperoxidase hydrogen peroxide chloride system to oxidize α-amino acids to a family of reactive aldehydes - Mechanistic studies identifying labile intermediates along the reaction pathway. J.Biol.Chem. 273(9):4997-5005.

He T, Chan V. 2010. Covalent layer-by-layer assembly of polyethyleneimine multilayer for antibacterial applications. J.Biomed.Mater.Res.Part A 95A(2):454-64.

Hequet A, Humblot V, Berjeaud J, Pradier C. 2011. Optimized grafting of antimicrobial peptides on stainless steel surface and biofilm resistance tests. Colloid Surf.B-Biointerfaces 84(2):301-9.

Hermanson G. 2008. Bioconjugate Techniques. 2nd ed. Boston, MA: Academic Press. 1202 p.

Holmes-Farley S, Reamey R, McCarthy T, Deuth J, Whitesides G. 1985. Acid-Base Behavior of Carboxylic-Acid Groups Covalently Attached at the Surface of Polyethylene - the Usefulness of Contact-Angle in Following the Ionization of Surface Functionality. Langmuir 1(6):725-40.

Howard K, McAllister R. 1957. Surface Tension of Acetone-Water Solutions Up to their Normal Boiling Points. AIChE J. 3(3):325-9.

Huang Z. 2005. A review of progress in clinical photodynamic therapy. Technol.Cancer Res.Treat. 4(3):283-93.

Huemer I, Klijn N, Vogelsang H, Langeveld L. 1998. Thermal death kinetics of spores of *Bacillus sporothermodurans* isolated from UHT milk. Int.Dairy J. 8(10-11):851-5.

Humblot V, Yala J, Thebault P, Boukerma K, Hequet A, Berjeaud J, Pradier C. 2009. The antibacterial activity of Magainin I immobilized onto mixed thiols Self-Assembled Monolayers. Biomaterials 30(21):3503-12.

Ikeda T, Hirayama H, Yamaguchi H, Tazuke S, Watanabe M. 1986. Polycationic Biocides with Pendant Active Groups - Molecular-Weight Dependence of Antibacterial Activity. Antimicrob.Agents Chemother. 30(1):132-6.

Ingham S, Uljas H. 1998. Prior storage conditions influence the destruction of *Escherichia coli* O157 : H7 during heating of apple cider and juice. J.Food Prot. 61(4):390-4.

Irikura H, Hasegawa Y, Takahashi Y. 2003. Preparation of antibacterial polyimide film by vapor deposition polymerization. J.Photopolym Sci.Technol. 16(2):273-6.

Ismail S, Perni S, Pratten J, Parkin I, Wilson M. 2011. Efficacy of a Novel Light-Activated Antimicrobial Coating for Disinfecting Hospital Surfaces. Infect.Control Hosp.Epidemiol. 32(11):1130-2.

Izquierdo A, Ono S, Voegel J, Schaaf P, Decher G. 2005. Dipping versus spraying: Exploring the deposition conditions for speeding up layer-by-layer assembly. Langmuir 21(16):7558-67.

Jain JP, Chitkara D, Kumar N. 2008. Polyanhydrides as localized drug delivery carrier: an update. Expert Opin.Drug Deliv. 5(8):889-907.

Jampala SN, Sarmadi M, Somers EB, Wong ACL, Denes FS. 2008. Plasma-enhanced synthesis of bactericidal quaternary ammonium thin layers on stainless steel and cellulose surfaces. Langmuir 24(16):8583-91.

Jiang H, Manolache S, Wong A, Denes F. 2004. Plasma-enhanced deposition of silver nanoparticles onto polymer and metal surfaces for the generation of antimicrobial characteristics. J Appl Polym Sci 93(3):1411-22.

Juneja V, Snyder O, Marmer B. 1997. Thermal destruction of *Escherichia coli* O157:H7 in beef and chicken: Determination of *D*- and *z*-values. Int.J.Food Microbiol. 35(3):231-7.

Kabza K, Gestwicki J, McGrath J. 2000. Contact angle goniometry as a tool for surface tension measurements of solids, using Zisman plot method - A physical chemistry experiment. J.Chem.Educ. 77(1):63-5.

Karakus G, Polat ZA, Yaglioglu AS, Karahan M, Yenidunya AF. 2013a. Synthesis, characterization, and assessment of cytotoxic, antiproliferative, and antiangiogenic effects of a novel procainamide hydrochloride-poly(maleic anhydride-*co*-styrene) conjugate. J.Biomater.Sci.-Polym.Ed. 24(10):1260-76.

Karakus G, Zengin HB, Polat ZA, Yenidunya AF, Aydin S. 2013b. Cytotoxicity of three maleic anhydride copolymers and common solvents used for polymer solvation. Polym.Bull. 70(5):1591-612.

Kenawy E, Worley SD, Broughton R. 2007. The chemistry and applications of antimicrobial polymers: A state-of-the-art review. Biomacromolecules 8(5):1359-84.

Khalil RKS. 2013. Selective removal and inactivation of bacteria by nanoparticle composites prepared by surface modification of montmorillonite with quaternary ammonium compounds. World J.Microbiol.Biotechnol. 29(10):1839-50.

Kim B, Park S. 2008. Antibacterial behavior of transition-metals-decorated activated carbon fibers. J.Colloid Interface Sci. 325(1):297-9.

Kim YS, Davis R, Cain AA, Grunlan JC. 2011. Development of layer-by-layer assembled carbon nanofiber-filled coatings to reduce polyurethane foam flammability. Polymer 52(13):2847-55.

Kocer HB. 2012. Residual disinfection with N-halamine based antimicrobial paints. Prog.Org.Coat. 74(1):100-5.

Kocer HB, Worley SD, Broughton RM, Huang TS. 2011a. A novel N-halamine acrylamide monomer and its copolymers for antimicrobial coatings. React Funct Polym 71(5):561-8.

Kocer HB, Cerkez I, Worley SD, Broughton RM, Huang TS. 2011b. Polymeric Antimicrobial N-Halamine Epoxides. ACS Appl.Mater.Interfaces 3(8):2845-50.

Kocer HB, Akdag A, Worley SD, Acevedo O, Broughton RM, Wu Y. 2010. Mechanism of Photolytic Decomposition of N-Halamine Antimicrobial Siloxane Coatings. Acs Applied Materials & Interfaces 2(8):2456-64.

Kou L, Liang J, Ren X, Kocer HB, Worley SD, Broughton RM, Huang TS. 2009. Novel N-halamine silanes. Colloid Surf.A-Physicochem.Eng.Asp. 345(1-3):88-94.

Kreske AC, Ryu J, Pettigrew CA, Beuchat LR. 2006. Lethality of chlorine, chlorine dioxide, and a commercial produce sanitizer to *Bacillus cereu s*and *Pseudomonas* in a liquid detergent, on stainless steel, and in biofilm. J.Food Prot. 69(11):2621-34.

Kugler R, Bouloussa O, Rondelez F. 2005. Evidence of a charge-density threshold for optimum efficiency of biocidal cationic surfaces. Microbiology-Sgm 151(5):1341-8.

Kumar N, Langer R, Domb A. 2002. Polyanhydrides: an overview. Adv.Drug Deliv.Rev. 54(7):889-910.

Lai L, Yang Y, Lin Y, Huang L, Hsieh Y. 2009. Surface characterization of immunosensor conjugated with gold nanoparticles based on cyclic voltammetry and X-ray photoelectron spectroscopy. Colloid Surf.B-Biointerfaces 68(2):130-5.

Lauten S, Sarvis H, Wheatley W, Williams D, Mora E, Worley S. 1992. Efficacies of Novel N-Halamine Disinfectants Against *Salmonella* and *Pseudomonas* Species. Appl.Environ.Microbiol. 58(4):1240-3.

Lee HJ, Lee SG, Oh EJ, Chung HY, Han SI, Kim EJ, Seo SY, Do Ghim H, Yeum JH, Choi JH. 2011. Antimicrobial polyethyleneimine-silver nanoparticles in a stable colloidal dispersion. Colloid Surf.B-Biointerfaces 88(1):505-11.

Lee J, Whang HS. 2011. Poly(vinyl alcohol) Blend Film with m-Aramid as an N-halamine Precursor for Antimicrobial Activity. J Appl Polym Sci 122(4):2345-50.

Lemire JA, Harrison JJ, Turner RJ. 2013. Antimicrobial activity of metals: mechanisms, molecular targets and applications. Nat.Rev.Microbiol. 11(6):371-84.

Li Y, Yao Z, Chen Z, Qiu S, Zeng C, Cao K. 2013. Rheological Evidence of Physical Cross-Links and Their Impact in Modified Polypropylene. Ind Eng Chem Res 52(23):7758-67.

Li Y, Schulz J, Grunlan JC. 2009. Polyelectrolyte/Nanosilicate Thin-Film Assemblies: Influence of pH on Growth, Mechanical Behavior, and Flammability. Acs Applied Materials & Interfaces 1(10):2338-47.

Liang J, Wu R, Wang J-, Barnes K, Worley SD, Cho U, Lee J, Broughton RM, Huang T-. 2007. N-halamine biocidal coatings. J.Ind.Microbiol.Biotechnol. 34(2):157-63.

Lichter JA, Rubner MF. 2009. Polyelectrolyte Multilayers with Intrinsic Antimicrobial Functionality: The Importance of Mobile Polycations. Langmuir 25(13):7686-94.

Lichter JA, Van Vliet KJ, Rubner MF. 2009. Design of Antibacterial Surfaces and Interfaces: Polyelectrolyte Multilayers as a Multifunctional Platform. Macromolecules 42(22):8573-86.

Linton R, Carter W, Pierson M, Hackney C, Eifert J. 1996. Use of a modified Gompertz equation to predict the effects of temperature, pH, and NaCl on the inactivation of *Listeria monocytogenes* Scott A heated in infant formula. J.Food Prot. 59(1):16-23.

Liu H, Yao Z, Cao K, Li B. 2010. Kinetic Analysis of the Imidization of Poly(styrene-*co*-maleic anhydride) with Aniline in the Melt. J Appl Polym Sci 116(5):2951-7.

Liu Y, Du H, Liu L, Leng J. 2014. Shape memory polymers and their composites in aerospace applications: a review. Smart Mater.Struct. 23(2):023001.

Liu Y, Zheng Z, Zara JN, Hsu C, Soofer DE, Lee KS, Siu RK, Miller LS, Zhang X, Carpenter D, Wang C, Ting K, Soo C. 2012. The antimicrobial and osteoinductive properties of silver nanoparticle/poly(DL-lactic-*co*-glycolic acid)-coated stainless steel. Biomaterials 33(34):8745-56.

Llorens A, Lloret E, Picouet PA, Trbojevich R, Fernandez A. 2012. Metallic-based micro and nanocomposites in food contact materials and active food packaging. Trends Food Sci.Technol. 24(1):19-29.

Long J, Chen P. 2006. On the role of energy barriers in determining contact angle hysteresis. Adv.Colloid Interface Sci. 127(2):55-66.

Ma PC, Kim J, Tang BZ. 2006. Functionalization of carbon nanotubes using a silane coupling agent. Carbon 44(15):3232-8.

Maillard J, Hartemann P. 2013. Silver as an antimicrobial: facts and gaps in knowledge. Crit.Rev.Microbiol. 39(4):373-83.

Makamba H, Hsieh Y, Sung W, Chen S. 2005. Stable permanently hydrophilic protein-resistant thin-film coatings on poly(dimethylsiloxane) substrates by electrostatic self-assembly and chemical cross-linking. Anal.Chem. 77(13):3971-8.

Mallory G, Hajdu J. 1990. Electroless plating fundamentals and applications. Orlando, FL: AESF ; Noyes Publications/William Andrew Pub. 539 p.

Mansilla AY, Albertengo L, Rodriguez MS, Debbaudt A, Zuniga A, Casalongue CA. 2013. Evidence on antimicrobial properties and mode of action of a chitosan obtained from crustacean exoskeletons on *Pseudomonas syringae* pv. tomato DC3000. Appl.Microbiol.Biotechnol. 97(15):6957-66.

Marambio-Jones C, Hoek EMV. 2010. A review of the antibacterial effects of silver nanomaterials and potential implications for human health and the environment. J.Nanopart.Res. 12(5):1531-51.

Marques SC, Oliveira Silva Rezende,Jaine das Gracas, de Freitas Alves LA, Silva BC, Alves E, de Abreu LR, Piccoli RH. 2007. Formation of biofilms by *Staphylococcus aureus* on stainless steel and glass surfaces and its resistance to some selected chemical sanitizers. Brazilian J.Microbiol. 38(3):538-43.

Martin J, Mancheno J, Arche R. 1993. Inactivation of Penicillin Acylase from *Kluyvera citrophila* by N-Ethoxycarbonyl-2-Ethoxy-1,2-Dihydroquinoline - a Case of Time-Dependent Noncovalent Enzyme-Inhibition. Biochem.J. 291(3):907-14.

Martin TP, Kooi SE, Chang SH, Sedransk KL, Gleason KK. 2007. Initiated chemical vapor deposition of antimicrobial polymer coatings. Biomaterials 28(6):909-15.

Matoba T, Shiono T, Kito M. 1985. Cross-Linking of $\alpha_{s\text{-}1}$ Casein by Sodium Hypochlorite. J.Food Sci. 50(6):1738.

Maukonen J, Matto J, Wirtanen G, Raaska L, Mattila-Sandholm T, Saarela M. 2003. Methodologies for the characterization of microbes in industrial environments: a review. J.Ind.Microbiol.Biotechnol. 30(6):327-56.

Mauter MS, Wang Y, Okemgbo KC, Osuji CO, Giannelis EP, Elimelech M. 2011. Antifouling Ultrafiltration Membranes via Post-Fabrication Grafting of Biocidal Nanomaterials. ACS Appl.Mater.Interfaces 3(8):2861-8.

McKenna S, Davies K. 1988. The Inhibition of Bacterial-Growth by Hypochlorous Acid - Possible Role in the Bactericidal Activity of Phagocytes. Biochem.J. 254(3):685-92.

McLandsborough L, Rodriguez A, Perez-Conesa D, Weiss J. 2006. Biofilms: At the interface between biophysics and microbiology. Food Biophys. 1(2):94-114.

Mead P, Slutsker L, Dietz V, McCaig L, Bresee J, Shapiro C, Griffin P, Tauxe R. 2000. Food-related illness and death in the United States (Reprinted from Emerging Infectious Diseases). J.Environ.Health 62(7):9-18.

Milovic N, Wang J, Lewis K, Klibanov A. 2005. Immobilized N-alkylated polyethylenimine avidly kills bacteria by rupturing cell membranes with no resistance developed. Biotechnol.Bioeng. 90(6):715-22.

Møretrø T, Langsrud S. 2011. Effects of Materials Containing Antimicrobial Compounds on Food Hygiene. J.Food Prot. 74(7):1200-11.

Müller A, Schmidt H, Alstädt V. 2010. Complex macromolecular systems II. Berlin, Germany: Springer-Verlag. 220 p.

Munro IC, Haighton LA, Lynch BS, Tafazoli S. 2009. Technological challenges of addressing new and more complex migrating products from novel food packaging materials. Food Addit.Contam.Part A-Chem. 26(12):1534-46.

Murata H, Koepsel RR, Matyjaszewski K, Russell AJ. 2007. Permanent, non-leaching antibacterial surfaces - 2: How high density cationic surfaces kill bacterial cells. Biomaterials 28(32):4870-9.

Niinomi M. 2008. Metallic biomaterials. J.Artif.Organs 11(3):105-10.

Noimark S, Dunnill CW, Parkin IP. 2013a. Shining light on materials - A self-sterilising revolution. Adv.Drug Deliv.Rev. 65(4):570-80.

Noimark S, Bovis M, MacRobert AJ, Correia A, Allan E, Wilson M, Parkin IP. 2013b. Photobactericidal polymers; the incorporation of crystal violet and nanogold into medical grade silicone. RSC Adv. 3(40):18383-94.

Noimark S, Dunnill CW, Kay CWM, Perni S, Prokopovich P, Ismail S, Wilson M, Parkin IP. 2012. Incorporation of methylene blue and nanogold into polyvinyl chloride catheters; a new approach for light-activated disinfection of surfaces. J.Mater.Chem. 22(30):15388-96.

Noyce JO, Michels H, Keevil CW. 2006. Use of copper cast alloys to control*Escherichia coli*O157 cross-contamination during food processing. Appl.Environ.Microbiol. 72(6):4239-44.

Onnis-Hayden A, Hsu BB, Klibanov AM, Gu AZ. 2011. An antimicrobial polycationic sand filter for water disinfection. Water Sci.Technol. 63(9):1997-2003.

Oulahal N, Brice W, Martial A, Degraeve P. 2008. Quantitative analysis of survival of *Staphylococcus aureus* or *Listeria innocua* on two types of surfaces: Polypropylene and stainless steel in contact with three different dairy products. Food Control 19(2):178-85.

Oussalah M, Caillet S, Salmieri S, Saucier L, Lacroix M. 2004. Antimicrobial and antioxidant effects of milk protein-based film containing essential oils for the preservation of whole beef muscle. J.Agric.Food Chem. 52(18):5598-605.

Park J, Sudarshan T. 2001. Chemical vapor deposition. Materials Park, Ohio: ASM International. 481 p.

Parkar S, Flint S, Brooks J. 2004. Evaluation of the effect of cleaning regimes on biofilms of thermophilic *bacilli* on stainless steel. J.Appl.Microbiol. 96(1):110-6.

Peleg M. 2003. Calculation of the non-isothermal inactivation patterns of microbes having sigmoidal isothermal semi-logarithmic survival curves. Crit.Rev.Food Sci.Nutr. 43(6):645-58.

Peleg M. 2006. Advanced quantitative microbiology for foods and biosystems : models for predicting growth and inactivation. Boca Raton: Taylor & Francis.

Penna T, Moraes D. 2002. The influence of nisin on the thermal resistance of *Bacillus cereus*. J.Food Prot. 65(2):415-8.

Perez Espitia P, Ferreira Soares N, dos Reis Coimbra J, de Andrade N, Cruz R, Alves Medeiros E. 2012. Bioactive Peptides: Synthesis, Properties, and Applications in the Packaging and Preservation of Food. Compr.Rev.Food.Sci.Food Saf. 11(2):187-204.

Periolatto M, Ferrero F, Vineis C. 2012. Antimicrobial chitosan finish of cotton and silk fabrics by UV-curing with 2-hydroxy-2-methylphenylpropane-1-one. Carbohydr.Polym. 88(1):201-5.

Perni S, Piccirillo C, Pratten J, Prokopovich P, Chrzanowski W, Parkin IP, Wilson M. 2009. The antimicrobial properties of light-activated polymers containing methylene blue and gold nanoparticles. Biomaterials 30(1):89-93.

Pierson H. 1999. Handbook of Chemical Vapor Deposition Principles, Technology, and Applications. Materials Science and Process Technology Series. 2nd ed. Norwich, NY: Noyes Publications. 482 p.

Plagge A, Adler H, Jaehne E, Paliwoda G, Rohwerder M, Stratmann M, Eichhorn K. 2007. Single and double polymer layer arrangements of acid groups containing cellulose and basic groups containing polyethyleneimine on steel. Macromol.Mater.Eng. 292(12):1245-55.

Pollock N, Fowler G, Twyman LJ, McArthur SL. 2007. Synthesis and characterization of immobilized PAMAM dendrons. Chemical Communications (24):2482-4.

Qian L, Sun G. 2003. Durable and regenerable antimicrobial textiles: Synthesis and applications of 3-methylol-2,2,5,5-tetramethylimidazolidin-4-one (MTMIO). J Appl Polym Sci 89(9):2418-25.

Rai M, Yadav A, Gade A. 2009. Silver nanoparticles as a new generation of antimicrobials. Biotechnol.Adv. 27(1):76-83.

Ratner B. 2004. Biomaterials science : an introduction to materials in medicine. 2nd ed. Amsterdam; Boston: Elsevier Academic Press. 851 p.

Ratner B. 1995. Surface Modification of Polymers - Chemical, Biological and Surface Analytical Challenges. Biosens.Bioelectron. 10(9-10):797-804.

Raynor JE, Capadona JR, Collard DM, Petrie TA, Garcia AJ. 2009. Polymer brushes and self-assembled monolayers: Versatile platforms to control cell adhesion to biomaterials (Review). Biointerphases 4(2):FA3-FA16.

Ren X, Kocer HB, Worley SD, Broughton RM, Huang TS. 2013. Biocidal Nanofibers via Electrospinning. J Appl Polym Sci 127(4):3192-7.

Rodriguez A, Autio WR, Mclandsborough LA. 2007. Effect of Biofilm dryness on the transfer of *Listeria monocytogenes* Biofilms grown on stainless steel to Bologna and hard salami. J.Food Prot. 70(11):2480-4.

Roman MJ, Tian F, Decker EA, Goddard JM. 2014. Iron Chelating Polypropylene Films: Manipulating Photoinitiated Graft Polymerization to Tailor Chelating Activity. J Appl Polym Sci 131(4):39948.

Rutala W, Weber D. 2008. Guideline for Disinfection and Sterilization in Healthcare Facilities, 2008. Washington, DC: Centers for Disease Control (U.S.). 158 p.

Saad NY, Muller CD, Lobstein A. 2013. Major bioactivities and mechanism of action of essential oils and their components. Flavour Fragrance J. 28(5):269-79.

Schafer R, Kressler J, Neuber R, Mulhaupt R. 1995. FTIR Spectroscopy and Microscopy on the Interfacial Reaction and Interdiffusion of Styrene/maleic Anhydride Copolymer and Bis(amine)-Terminated Poly(tetrahydrofuran). Macromolecules 28(14):5037-42.

Scott C, Macosko C. 1994. Model Experiments for the Interfacial Reaction between Polymers during Reactive Polymer Blending. J.Polym.Sci.Pt.B-Polym.Phys. 32(2):205-13.

Seow YX, Yeo CR, Chung HL, Yuk H. 2014. Plant Essential Oils as Active Antimicrobial Agents. Crit.Rev.Food Sci.Nutr. 54(5):625-44.

Sgolastra F, Deronde BM, Sarapas JM, Som A, Tew GN. 2013. Designing Mimics of Membrane Active Proteins. Acc.Chem.Res. 46(12):2977-87.

Sharma M, Ryu J, Beuchat L. 2005. Inactivation of *Escherichia coli* O157 : H7 in biofilm on stainless steel by treatment with an alkaline cleaner and a bacteriophage. J.Appl.Microbiol. 99(3):449-59.

Sidhu M, Langsrud S, Holck A. 2001. Disinfectant and antibiotic resistance of lactic acid bacteria isolated from the food industry. Microbial Drug Resistance-Mechanisms Epidemiology and Disease 7(1):73-83.

Silva S, Teixeira P, Oliveira R, Azeredo J. 2008. Adhesion to and viability of *Listeria monocytogenes* on food contact surfaces. J.Food Prot. 71(7):1379-85.

Simões M, Simões LC, Vieira MJ. 2010. A review of current and emergent biofilm control strategies. Lwt-Food Science and Technology 43(4):573-83.

Smith B. 1999. Infrared spectral interpretation: a systematic approach. Boca Raton, FL: CRC Press. 265 p.

Smith R, Hansen D. 1998. The pH-rate profile for the hydrolysis of a peptide bond. J.Am.Chem.Soc. 120(35):8910-3.

Song Z, Baker W. 1992. Chemical-Reactions and Reactivity of Primary, Secondary, and Tertiary Diamines with Acid Functionalized Polymers. J.Polym.Sci.Pol.Chem. 30(8):1589-600.

Stockton W, Rubner M. 1997. Molecular-level processing of conjugated polymers .4. Layer-by-layer manipulation of polyaniline via hydrogen-bonding interactions. Macromolecules 30(9):2717-25.

Stranak V, Wulff H, Ksirova P, Zietz C, Drache S, Cada M, Hubicka Z, Bader R, Tichy M, Helm CA, Hippler R. 2014. Ionized vapor deposition of antimicrobial Ti-Cu films with controlled copper release. Thin Solid Films 550:389-94.

Sun G, Hong KH. 2013. Photo-induced antimicrobial and decontaminating agents: recent progresses in polymer and textile applications. Text.Res.J. 83(5):532-42.

Sun Y, Sun G. 2002. Durable and regenerable antimicrobial textile materials prepared by a continuous grafting process. J Appl Polym Sci 84(8):1592-9.

Sun Y, Sun G. 2003. Novel refreshable N-halamine polymeric biocides: Grafting hydantoin-containing monomers onto high performance fibers by a continuous process. J Appl Polym Sci 88(4):1032-9.

Sun Y, Sun G. 2001. Novel regenerable N-halamine polymeric biocides. III. Grafting hydantoin-containing monomers onto synthetic fabrics. J Appl Polym Sci 81(6):1517-25.

Sun Y, Chen T, Worley S, Sun G. 2001. Novel refreshable N-halamine polymeric biocides containing imidazolidin-4-one derivatives. Journal of Polymer Science Part A-Polymer Chemistry 39(18):3073-84.

Suppakul P, Sonneveld K, Bigger SW, Miltz J. 2011. Loss of AM additives from antimicrobial films during storage. J.Food Eng. 105(2):270-6.

Tan K, Obendorf SK. 2007. Fabrication and evaluation of electrospun nanofibrous antimicrobial nylon 6 membranes. J.Membr.Sci. 305(1-2):287-98.

Tan K, Obendorf SK. 2007. Fabrication and evaluation of electrospun nanofibrous antimicrobial nylon 6 membranes. J.Membr.Sci. 305(1-2):287-98.

Tian F, Decker EA, Goddard JM. 2013. Controlling Lipid Oxidation via a Biomimetic Iron Chelating Active Packaging Material. J.Agric.Food Chem. 61(50):12397-404.

Tiller JC. 2011. Antimicrobial Surfaces. Adv.Polym.Sci. 240:193-217.

Tsukruk V, Bliznyuk V, Visser D, Campbell A, Bunning T, Adams W. 1997. Electrostatic deposition of polyionic monolayers on charged surfaces. Macromolecules 30(21):6615-25.

Tsutsui K, Iwata A, Ikeda S. 1989. Plasma Surface-Treatment of Polypropylene-Containing Plastics. J.Coatings Technol. 61(776):65-72.

Uchida E, Uyama Y, Ikada Y. 1993. Sorption of Low-Molecular-Weight Anions into Thin Polycation Layers Grafted Onto a Film. Langmuir 9(4):1121-4.

Van Boeijen IKH, Moezelaar R, Abee T, Zwietering MH. 2008. Inactivation Kinetics of Three *Listeria monocytogenes* Strains under High Hydrostatic Pressure. J.Food Prot. 71(10):2007-13.

Van der Maaden K, Sliedregt K, Kros A, Jiskoot W, Bouwstra J. 2012. Fluorescent Nanoparticle Adhesion Assay: a Novel Method for Surface pK_a Determination of Self-Assembled Monolayers on Silicon Surfaces. Langmuir 28(7):3403-11.

Van Houdt R, Michiels CW. 2010. Biofilm formation and the food industry, a focus on the bacterial outer surface. J.Appl.Microbiol. 109(4):1117-31.

Verran J, Airey P, Packer A, Whitehead KA. 2008. Microbial retention on open food contact surfaces and implications for food contamination. Adv.Appl.Microbiol. 64:223-46.

Vezenov D, Noy A, Rozsnyai L, Lieber C. 1997. Force titrations and ionization state sensitive imaging of functional groups in aqueous solutions by chemical force microscopy. J.Am.Chem.Soc. 119(8):2006-15.

Vignesh G, Arunachalam S, Vignesh S, James RA. 2012. BSA binding and antimicrobial studies of branched polyethyleneimine-copper(II)bipyridine/phenanthroline complexes. Spectroc.Acta Pt.A-Molec.Biomolec.Spectr. 96:108-16.

Vorst K, Todd E, Ryser E. 2006. Transfer of *Listeria monocytogenes* during mechanical slicing of turkey breast, bologna, and salami. J.Food Prot. 69(3):619-26.

Wang Q, Gao X, Fan X, Yuan J. 2010. Immobilization of Lysozyme on Wool Surface via Layer-by-layer Electrostatic Self-assembly and Its Antibacterial Property. Acta Chim.Sin. 68(20):2099-103.

Wang B, Navath RS, Menjoge AR, Balakrishnan B, Bellair R, Dai H, Romero R, Kannan S, Kannan RM. 2010. Inhibition of bacterial growth and intramniotic infection in a guinea pig model of chorioamnionitis using PAMAM dendrimers. Int.J.Pharm. 395(1-2):298-308.

Wang L, Chen J, Shi L, Shi Z, Ren L, Wang Y. 2014. The promotion of antimicrobial activity on silicon substrates using a "click" immobilized short peptide. Chem.Commun. 50(8):975-7.

Wang Q, Uzunoglu E, Wu Y, Libera M. 2012. Self-Assembled Poly(ethylene glycol)-*co*-Acrylic Acid Microgels to Inhibit Bacterial Colonization of Synthetic Surfaces. ACS Appl.Mater.Interfaces 4(5):2498-506.

Wang Z, von dem Bussche A, Kabadi PK, Kane AB, Hurt RH. 2013. Biological and Environmental Transformations of Copper-Based Nanomaterials. ACS Nano 7(10):8715-27.

Wilks SA, MichelS HT, Keevil CW. 2006. Survival of *Listeria monocytogenes* Scott A on metal surfaces: Implications for cross-contamination. Int.J.Food Microbiol. 111(2):93-8.

Williams D, Elder E, Worley S. 1988. Is Free Halogen Necessary for Disinfection? Appl.Environ.Microbiol. 54(10):2583-5.

Williams D, Swango L, Wilt G, Worley S. 1991. Effect of Organic N-Halamines on Selected Membrane Functions in Intact *Staphylococcus aureus* Cells. Appl.Environ.Microbiol. 57(4):1121-7.

Williams D, Worley S, Barnela S, Swango L. 1987. Bactericidal Activities of Selected Organic N-Halamines. Appl.Environ.Microbiol. 53(9):2082-9.

Williams J, Suess J, Santiago J, Chen Y, Wang J, Wu R, Worley S. 2005. Antimicrobial properties of novel N-halamine siloxane coatings. Surface Coatings International Part B-Coatings Transactions 88(1):35-9.

Worley B, Wheatley W, Lauten S, Williams D, Mora E, Worley S. 1992. Inactivation of *Salmonella enteritidis* on Shell Eggs by Novel N-Halamine Biocidal Compounds. J.Ind.Microbiol. 11(1):37-42.

Worley S, Sun G. 1996. Biocidal polymers. Trends in Polymer Science 4(11):364-70.

Worley S, Williams D. 1988. Halamine Water Disinfectants. Crc Critical Reviews in Environmental Control 18(2):133-75.

Worley S, Li F, Wu R, Kim J, Wei C, Williams J, Owens J, Wander J, Bargmeyer A, Shirtliff M. 2003. A novel N-halamine monomer for preparing biocidal polyurethane coatings. Surf.Coat.Int.Pt.B-Coat.Trans. 86(4):273-7.

Xia B, Dong C, Lu Y, Rong M, Lv Y, Shi J. 2011. Preparation and characterization of chemically-crosslinked polyethyleneimine films on hydroxylated surfaces for stable bactericidal coatings. Thin Solid Films 520(3):1120-4.

Yang M, Lin W. 2002. The grafting of chitosan oligomer to polysulfone membrane via ozone-treatment and its effect on anti-bacterial activity. J.Polym.Res.-Taiwan 9(2):135-40.

Yu J, Ho W, Lin J, Yip K, Wong P. 2003. Photocatalytic activity, antibacterial effect, and photoinduced hydrophilicity of TiO_2 films coated on a stainless steel substrate. Environ.Sci.Technol. 37(10):2296-301.

Yu K, Huang Y, Yang S. 2013. The antifungal efficacy of nano-metals supported TiO_2 and ozone on the resistant*Aspergillus niger*spore. J.Hazard.Mater. 261155-62.

Yudovin-Farber I, Golenser J, Beyth N, Weiss E, Domb A. 2010. Quaternary Ammonium Polyethyleneimine: Antibacterial Activity. J.Nanomater. (826343):1-11.

Yun H, Kim JD, Choi HC, Lee CW. 2013. Antibacterial Activity of CNT-Ag and GO-Ag Nanocomposites Against Gram-negative and Gram-positive Bacteria. Bull.Korean Chem.Soc. 34(11):3261-4.

Zasadzinski J, Viswanathan R, Madsen L, Garnaes J, Schwartz D. 1994. Langmuir-Blodgett-Films. Science 263(5154):1726-33.

Zhang W, Shi X, Huang J, Zhang Y, Wu Z, Xian Y. 2012. Bacitracin-Conjugated Superparamagnetic Iron Oxide Nanoparticles: Synthesis, Characterization and Antibacterial Activity. ChemPhysChem 13(14):3388-96.

Zhao B, Brittain W. 2000. Polymer brushes: surface-immobilized macromolecules. Prog.Polym.Sci. 25(5):677-710.

Zhao X, Pan F, Lu JR. 2005. Adsorption of polyethyleneimine characterized by spectroscopic ellipsometry RID A-1690-2011. Progress in Natural Science 15:56-9.

Zhao Z, Sakagami Y, Osaka T. 1998. Toxicity of hydrogen peroxide produced by electroplated coatings to pathogenic bacteria. Can.J.Microbiol. 44(5):441-7.

Zisman W. 1964. Contact angle, wettability, and adhesion: the Kendall Award Symposium honoring W. A. Zisman ... Los Angeles, 2-3 April 1963. American Chemical Society Division of Colloid and Surface Chemistry(Kendall Award Symposium):Los Angeles, CA.